

Appendix H

Industrial Site Fault Study

**FAULT STUDY
PROPOSED WAREHOUSE DEVELOPMENT**

NEC Todd Avenue and 10th Street

Azusa, California

for

Overton Moore Properties



**SOUTHERN
CALIFORNIA
GEOTECHNICAL**

A California Corporation

June 28, 2022

Overton Moore Properties
19700 South Vermont Avenue, Suite 101
Torrance, California 90502



**SOUTHERN
CALIFORNIA
GEOTECHNICAL**
A California Corporation

Attention: Ms. Montana Kanen
Analyst

Project No.: **22G144-2**

Subject: **Fault Study**
Proposed Warehouse Development
NEC Todd Avenue and 10th Street
Azusa, California

Ms. Kanen:

In accordance with your request, we have conducted a fault study at the subject site. We are pleased to present this report summarizing the conclusions and recommendations developed from our investigation.

We sincerely appreciate the opportunity to be of service on this project. We look forward to providing additional consulting services during the course of the project. If we may be of further assistance in any manner, please contact our office.

Respectfully Submitted,

SOUTHERN CALIFORNIA GEOTECHNICAL, INC.

Jamie Hayward
Staff Geologist

Daryl Kas, CEG 2467
Senior Geologist

Robert G. Trazo, CE 2655
Principal Engineer



Distribution: (1) Addressee

TABLE OF CONTENTS

1.0 INTRODUCTION	1
1.1 Purpose and Scope	1
1.2 Site Description	1
1.3 Proposed Development	2
2.0 GEOLOGIC TIME SCALE AND FAULT ACTIVITY	3
2.1 Geologic Time Scale	3
2.2 Fault Activity	3
3.0 BACKGROUND REVIEW	4
3.1 Previous Investigations by Others (Off-Site)	4
3.2 Previous Investigations by Others (On-Site)	6
3.3 Concurrent Study	7
4.0 HISTORICAL AERIAL PHOTOGRAPH REVIEW	8
5.0 SUBSURFACE INVESTIGATION	9
5.1 Fault Trenching and Logging	9
5.2 Ground-Penetrating Radar (GPR)	9
5.3 Seismic Refraction Survey	10
5.4 Seismic Reflection Survey	10
5.5 Backfilling of Fault Trench	10
6.0 SUMMARY OF GEOLOGIC CONDITIONS	12
6.1 Regional Geology	12
6.2 Regional Faulting	12
6.4 Sediment Age	15
6.5 On-Site Faulting	15
7.0 CONCLUSIONS AND RECOMMENDATIONS	17
8.0 GENERAL COMMENTS	18
9.0 REFERENCES	19

APPENDICES

- A Plate 1: Site Location Map
 - Plate 2: Fault Trench Location Plan
 - Plate 3: Geologic Map (Dibblee, 1998)
 - Plate 4: Earthquake Zone of Required Investigation Map
 - Plate 5: Ground Penetrating Radar
- B Trench Logs
- C Historical Aerial Photographs
- D Plate 6: Density Test Location Plan
 - Table 3: Summary of Field Density Tests
 - Table 4: Summary of Moisture Density Relationships
- E Geophysical Survey (Ground Penetrating Radar and Seismic Refraction)
- F Seismic Reflection Survey

1.0 INTRODUCTION

1.1 Purpose and Scope

The subject site is located within an Alquist-Priolo Earthquake Fault Zone (APEFZ). Therefore, a fault study was required to be performed within the area of the proposed development. This report presents the results of our fault study for the proposed warehouse development in Azusa, California. The purpose of our study was to evaluate the possible presence of on-site faulting and to provide conclusions and appropriate recommendations. Our scope of services included:

- Review of pertinent available geologic and geotechnical literature, maps, and aerial photographs.
- Observing the excavation and performing the logging of two (2) fault trenches across the proposed development area within the APEFZ to depths of 18 to 22± feet below existing site grade. The trenches extended 280 to 368± feet north of West 10th Street in a direction perpendicular to the mapped trace of the Upper Duarte Fault (UDF). The UDF is a parallel fault strand of the Sierra Madre Fault Zone (SMFZ).
- Collection of subsurface data using geophysical methods including seismic reflection, seismic refraction, and ground penetrating radar.
- Geologic review and analysis of the collected data.
- Preparation of this report presenting our fault investigation findings and conclusions.

1.2 Site Description

The subject site is located in the southwestern portion of the Azusa Greens Country Club, which includes an 18-hole golf course. The subject site is located at the northeast corner of North Todd Avenue and West 10th Street in Azusa, California. The general location of the site is illustrated on the Site Location Map, included as Plate 1 of this report.

The subject site consists of an L-shaped parcel, 19.33± acres in size. The site is presently developed as a golf course. The site consists of several fairways and greens, a restroom building and concrete pathways. Ground surface cover consists of turf grass, exposed soil, sand traps and large trees. A stockpile, consisting of soil, cobbles, boulders, and decaying tree branches and leaves, is located in the southwest area of the subject site. Three (3) stockpiles, consisting of soil, cobbles, and boulders are located in the eastern area of the east-west trending portion of the subject site.

Based on elevation data obtained from a site plan prepared by Thienes Engineering, the overall site topography generally slopes downward to the south at a gradient of 1± percent. Minor localized undulations and/or hills are present across the fairways and sand traps. The stockpile

located in the southwest area of the subject site is 5 to 10± feet higher in elevation than the surrounding topography. The stockpiles located in the eastern area of the southern portion of the subject site are 2 to 8± feet higher in elevation than the surrounding topography. The minimum site elevation is 631± feet mean sea level (msl) in the southwestern corner of the subject site. The maximum site elevation is 645± feet msl in the eastern area of the southern portion of the subject site.

1.3 Proposed Development

Based on a conceptual site plan, prepared by Thienes Engineering, Inc., the subject site will be developed with five (5) new commercial/industrial buildings, ranging in size from 31,007 to 105,863± ft² in size, located in the northern and eastern areas of the site. Dock-high doors will be constructed along portions of one building wall of each building. We expect that the buildings will be surrounded by asphaltic concrete (AC) pavements in the parking and drive areas, Portland cement concrete (PCC) pavements in the loading dock areas, and limited areas of landscape planters throughout. Additionally, the southwestern area of the site will be developed as a PCC or AC parking lot.

Detailed structural information has not been provided. It is assumed that the new buildings will be single-story structures of tilt-up concrete construction, supported on conventional shallow foundation systems with a concrete slab-on-grade floors. Based on the assumed construction, maximum column and wall loads are expected to be on the order of 80 to 100 kips and 4 to 7 kips per linear foot, respectively.

Grading plans for the proposed development were not available at the time of this report. No significant amounts of below-grade construction such as basements or crawl spaces are expected to be included in the proposed development. Based on the assumed topography, cuts and fills of 4 to 6± feet are expected to be necessary to achieve the proposed site grades.

2.0 GEOLOGIC TIME SCALE AND FAULT ACTIVITY

2.1 Geologic Time Scale

The age of the geologic events discussed in this report occurred during the Quaternary Period. The Quaternary Period is subdivided into the Holocene and Pleistocene Epochs. The name and associated time interval designations utilized in this report include ka, thousand years ago and Ma, million years ago.

TABLE 1

Period	Epoch	Time Period
Quaternary	Holocene Latest Holocene (Historical) Late Holocene Mid-Holocene Early Holocene	~past 200 years 4 ka to 200 years ago 8 to 4 ka 11.7 ka to 8 ka
	Pleistocene Latest Pleistocene Late Pleistocene Middle Pleistocene Early Pleistocene	~15 to 12 ka 125 to 15 ka 670 to 125 ka ~2.6 Ma to 670 ka

2.2 Fault Activity

California Geologic Survey (CGS) defines a Holocene-active fault (i.e. active fault) as a fault that has had surface displacement within Holocene time (within the last 11,700 years; CGS SP42, Revised 2018). A fault is considered to be "sufficiently active" if there is evidence of Holocene-age surface displacement along one or more of its segments or branches. A fault can be considered Pre-Holocene (i.e., inactive fault) if there is positive evidence that indicates that the fault has not ruptured within the last 11,700 years.

The age of fault activity is estimated by establishing the age of the youngest materials (soil or rock) displaced by the fault. This is established using either carbon dating or relative age dating. If organic material, such as charcoal, is present within the soil layers, a numerical age can be obtained using carbon dating. If no organic material is found within the soil layers, then only a relative age can be assigned to the movement of the fault based on qualitative interpretation.

Faults must also be well defined to be included in an APEFZ. A fault is considered to be well defined if the fault or fault trace is detectable by a trained geologist as a physical feature at or below the ground surface. The fault may be identified by direct observation or by indirect methods. The fault or fault trace needs to be located with sufficient precision and confidence in the field to be considered for inclusion in the APEFZ.

3.0 BACKGROUND REVIEW

3.1 Previous Investigations by Others (Off-Site)

We reviewed relevant reports from fault investigations and research publications within the vicinity of the site. The reports reviewed are listed below in Table 2.

TABLE 2

Author, Year	Property Address	Title
Crook, et al., 1987	Mouth of Big Tujunga Canyon to mouth of San Gabriel Canyon (40km segment)	Quaternary Geology and Seismic Hazard of the Sierra Madre and Associated Faults, Western San Gabriel Mountains in recent reverse faulting in the Transverse Ranges, California: U.S. Geological Survey Professional Paper 1339.
TGR Geotechnical, 2013	NWC Todd Ave and 10 th Street, City of Azusa	Geotechnical Investigation Report, 1001 North Todd Avenue, Azusa, California, Project No. 12-4026, May 16, 2013.
Jerome A. Treiman, 2013	The Sierra Madre Fault Zone in the Azusa Quadrangle	California Geological Survey, Fault Evaluation Report FER-249, The Sierra Madre Fault Zone in the Azusa Quadrangle, Los Angeles County, California, by Jerome A. Treiman, December 20, 2013.
City of Azusa, CA, 2014	NWC Todd Ave and 10 th Street, City of Azusa	Environmental Impact Report, Tenth Street Center Industrial Park (Public Review Draft), May 2014.

Summaries of the reports in Table 2 and their relevant findings are presented below.

1. Quaternary Geology and Seismic Hazard of the Sierra Madre and Associated Faults, Western San Gabriel Mountains, by Richard Crook, Jr., Allen, Barclay Kamb, C.M. Payne, and R.J. Proctor, 1987.

The study was conducted in an effort to better understand the seismic hazard posed by the Sierra Madre fault system of the San Gabriel Mountains along a 40 km segment which includes the Azusa area. Methods of the investigation included delineating fault traces via trenching, surface inspection and review of aerial photographs, and determination of subsurface fault locations using groundwater and geophysical data. In the Azusa area, the authors inferred the location of three separate fault traces of the Sierra Madre fault using groundwater level discrepancy, seismic-refraction, and magnetometer surveys. The three faults were named as the Sierra Madre fault, the Upper Duarte fault and the Duarte fault. Without any Carbon-14 (C^{14}) dating or visual observations of subsurface soils, the age of the faulting could only be inferred using relative age dating methods. The elevations of the groundwater levels and the groundwater discrepancy suggests Holocene-age faulting,

according to the authors.

2. Geotechnical Investigation Report, 1001 North Todd Avenue, Azusa, California, Project No. 12-4026, May 16, 2013, prepared for Xebec Realty Partners by TGR Geotechnical (TGR).

This investigation evaluated the on-site subsurface conditions for the development of four (4) proposed buildings, located at the NWC of Todd Avenue and W. 10th Street, in Azusa, California (westerly adjacent to the subject site, across Todd Avenue). The study included a seismic review of potential on-site faulting as a result of the mapped Upper Duarte fault trace on the site. The seismic review included a review of onsite and adjacent site groundwater data and performance and evaluation of six (6) resistivity (Sting) lines across the southern area of the site. A groundwater discrepancy of 70 to 90 feet between the northern and southern areas of the site was reported. The results of the Sting lines indicate the presence of a fault related feature that is consistent with the groundwater data and mapped upper Duarte fault location. TGR recommended a 50-foot setback line from the surface projection of the inferred fault location.

3. California Geological Survey, Fault Evaluation Report FER-249, The Sierra Madre Fault Zone in the Azusa Quadrangle, Los Angeles County, California, by Jerome A. Treiman, December 20, 2013.

This report evaluated potential Holocene-age displacement of sediments along traces of the Sierra Madre fault zone within the Azusa Quadrangle. Relevant studies performed within the Azusa Quadrangle were compiled and reviewed to determine the displacement potential. The Upper Duarte Fault (UDF) was first inferred by groundwater elevation discrepancies by California Department of Water Resources (CDWR) in 1966. The CDWR interpreted the UDF to have at least 100 feet of vertical displacement within the young alluvial fan of the San Gabriel River. Crook et al. (1987) further defined the location of the UDF reviewing the same groundwater data in addition to anomalies in geophysical data collected by private consulting firms. This paper also included a reference for a slope stability study performed by Amec for the Reliance Quarry (located southeast of the subject site). Based on groundwater discrepancies and seismic reflection profiles, Amec interpreted the fault to be located immediately north of the quarry. The fault trace was interpreted by Amec to be a steeply north-dipping with a vertical displacement of up to 200 feet. Amec reported that this displacement extended into the visible wall of the quarry. However, it was not determined if the fault displaced sediment within the upper 50± feet of the alluvial fan. Amec interpreted the upper 50± feet of the fan to be Holocene-age. In contrast, the CGS's mineral program personal estimated that the Holocene section of the San Gabriel River fan to be several hundreds of feet thick.

4. Tenth Street Center Industrial Park Project, Environmental Impact Report, Public Review Draft, May 2014, prepared for City of Azusa by RBF Consulting (RBF).

This report assessed the potential environmental impacts associated with the proposed development on the NWC of Todd Avenue and West 10th Street (westerly adjacent to the subject site, across Todd Avenue). This report summarizes the findings of other investigations that took place on the site. The reviewed investigation required a 50-foot

setback from the Duarte Fault trace to mitigate the substantial adverse effects if a rupture on the fault were to occur.

3.2 Previous Investigations by Others (On-Site)

A preliminary engineering geologic investigation was prepared at the subject site, referenced below:

Preliminary Engineering Geologic Findings, Proposed Multi-Unit Residential Development, California Grand Village at Azuza [sic] Greens Golf Course, Northeast Corner of N. Todd Ave. and W. 10th St., City of Azuza [sic], California, prepared by Land Phases Inc. (LPI), prepared for CGVA Partners, LLC, LPI Project No. LP1261, dated July 5, 2016.

As part of this investigation, LPI reviewed available geologic publications concerning the subject site and surrounding area, performed an analysis of aerial photographs, performed geologic field mapping, excavation and logging of 10 backhoe-excavated test pits, 38 Cone Penetrometer Tests (CPT), and 3 deep borings. LPI reported that the subsurface soils consist of a thick layer of artificial fill soils over a thick accumulation of natural alluvial deposits consisting of sand and gravel. It should be noted that LPI did not report any of the data from the 38 CPTs due to poor data recover from the CPT borings. None of these borings were advanced below 10± feet due to the presence of cobbles and boulders. LPI drilled 3 deep borings up to depths of 220 feet below the existing site grades. LPI reported that the groundwater at Boring Nos. B-1 and B-2 were at a depth of 134 to 138± feet below the existing grades and groundwater at Boring No. B-3 was at a depth of 216± feet below the existing grades. LPI indicated that there was an 80±-foot vertical groundwater offset between Boring Nos. B-2 and B-3. LPI indicated that the exact location of the fault was uncertain, a fault is estimated to be located in the southern portion of the site with a general east-west trend. LPI indicated that limitations in determining the age of the underlying sediments and the age of the faulted horizons, LPI recommended that the fault be considered "active" for planning purposes. LPI recommended additional borings to determine the location of the faulting in the southern portion of the site.

A second engineering geologic investigation was performed at the subject site, referenced below:

Report of Engineering Geologic Study, Proposed Multi-Unit Senior Living Residential Development – California Grand Village at Azuza [sic] Greens, Southeast Corner of N. Todd Ave. and W. Sierra Madre Avenue, City of Azuza [sic], California, prepared by LPI, prepared for CGVA Partners, LLC, LPI Project No. LP1261, dated November 11, 2016 (revised January 19, 2017).

The purpose of the study was to assess the site conditions for a proposed multi-level senior housing development. This report used the data from the previous investigation to complete the engineering geologic study. LPI reported that alluvium was encountered at all of the exploration locations beneath the fill soils or at the ground surface. The alluvium consisted of interlayered mixtures of sand and gravel with cobbles and boulders extending to the maximum depth explored of 219± feet. LPI reported that a groundwater discrepancy of 82± feet was encountered between two borings located in the southwest area of the parcel. LPI indicated that the groundwater discrepancy could be due to the possible presence of the Upper Duarte Fault which is mapped through the southwest corner of the site.

3.3 Concurrent Study

SCG concurrently conducted a feasibility study for the subject site. This report is identified as follows:

Geotechnical Feasibility Investigation, Proposed Warehouse Development, NEC Todd Avenue and 10th Street, Azusa, California, prepared by Southern California Geotechnical, Inc. (SCG), prepared for Overton Moore Properties, SCG Project No. 22G144-1 dated June 24, 2022.

As part of this study, a total of eight (8) trenches were excavated to depths of 3 to 9± feet below the existing site grades. Turf grass/topsoil was encountered at the ground surface of each trench location, except Trench No. T-3, extending to depths of 3 to 9± inches below ground surface. The turf grass is 2± inches in thickness. Beneath the turf grass, the topsoil generally consists of loose silty fine sands and silty fine to coarse sands with little to extensive fine root fibers and roots. Artificial fill soils were encountered at the ground surface at Trench No. T-3 and below the turf grass/topsoil at the remaining trench locations, extending to depths of 1¼ to 5½± feet below ground surface. The fill soils generally consist of loose to dense silty fine to coarse sands, fine to coarse sands, gravelly fine to coarse sands and fine sands. Native alluvium was encountered beneath the fill of each trench location, extending to at least the maximum depth explored of 9± feet below ground surface. The alluvial soils generally consist of medium dense to very dense gravelly fine to coarse sands with little cobbles and boulders.

Free water was not encountered during the excavation of any of the trenches. Based on the lack of any water within the trenches, and the moisture contents of the recovered soil samples, the static groundwater table is considered to have existed at a depth in excess of 9± feet at the time of the subsurface exploration.

The SCG geotechnical feasibility study presented preliminary grading, foundation, and floor slab design recommendations based on the conditions encountered at the boring locations.

4.0 HISTORICAL AERIAL PHOTOGRAPH REVIEW

Historical aerial photographs were obtained from the Fairchild Aerial Surveys (FAS) collection housed at the UC Santa Barbara library https://mil.library.ucsb.edu/ap_indexes/FrameFinder/. The stereographic aerial photographs were reviewed to characterize site geomorphology and topography and surrounding vicinity prior to urbanization. Relative topographic expression can be interpreted using stereo aerial photographs.

Photographs from the FAS collection, within the vicinity of the subject site, from the following years were available for review: 1930, 1934, and 1949. Copies of the 1930, 1934, and 1949 aerial photographs are provided in Appendix C of this report. A brief summary of these aerial photographs reviewed is presented below.

The site appears to be vacant and undeveloped, except for a paved road, trending east-west transects a portion of the site since at least 1930. Stream channels and alluvial fan outwash of the San Gabriel River appear to be the dominate features at the subject site.

We also performed an analysis of these stereo-paired historical aerial photographs (1930, 1934, and 1949) using a stereoscope. The stereoscope is a tool that creates an exaggerated three-dimensional image from aerial photographs taken at slightly different angles. Lineaments can be an indication of geologically recent ground deformation, including the presence of potentially active faulting. This is useful in identifying potential geologically related linear features (lineaments). Topographic linear features (lineaments), such as fault scarps, fault-line scarps, stream channel offsets, were not visible within the subject site or the surrounding areas in any of the three photographs reviewed.

5.0 SUBSURFACE INVESTIGATION

The major purpose of the subsurface investigation was to determine if any faults are present at the site and; if so, what is their relative activity (time of last offset). Accordingly, two (2) trenches were excavated at the site to depths of 18 to 22± feet. The two exploratory trenches were excavated and logged in detail by staff geologists and a certified engineering geologist from our firm to evaluate the possible presence of on-site faulting. Organic plant material discovered within the soils near the bottom of the exploratory trenches allowed for radiocarbon dating.

5.1 Fault Trenching and Logging

The two trenches were excavated across the proposed development as follows:

Trench No.	Length (feet)	Depth (feet)	Orientation	Elevation (feet)
FT-1	368	18 to 21	N 09° E	634 to 636
FT-2	280	20 to 22	N 10° E	632 to 637

The trenches were excavated in an orientation that is roughly perpendicular to the projection of the Upper Duarte Fault, a parallel strand of the Sierra Madre Fault Zone system. This section of the Upper Duarte Fault is inferred to extend into or near the southwestern portion of the subject site (<https://usgs.maps.arcgis.com>). The approximate locations of the fault trenches are presented on the Trench Location Plan (Plate 2). This allowed for a thorough assessment of the proposed development with regard to possible faults that may cross the proposed development. Cross-sections of the trenches are presented in the enclosed Fault Investigation Trenches (Plate B-1 and B-2).

The trenches were excavated using track-mounted excavators equipped with a 48-inch-wide bucket. The trenches were excavated with approximately 4-foot-wide benches on each side of the trench every 4± vertical feet to allow for SCG personnel to safely log the trench. The trenches were flagged with stations at 10-foot horizontal intervals.

The trench walls were scraped using picks and shovels to remove smears, gouge marks and slough material left by the excavator. To prepare a graphic log of the trench, we used the horizontal stations as a reference to scale the trench walls and the geologic features exposed at a 1 inch to 5-foot scale log. The trench locations were surveyed by the project civil engineer, Thienes Engineering.

5.2 Ground-Penetrating Radar (GPR)

As a part of this investigation, SCG contracted Terra GeoSciences to perform a GPR survey. The results of this survey are presented in a separate report, included as Appendix E of this report. The GPR survey consisted of one survey traverse along the bottom of Fault Trench No. FT-1, identified as GPR-1 and one survey travers along the bottom of Fault Trench No. FT-2, identified as GPR-2. The results of the GPR survey indicate that the soils encountered at the bottom of the trench consist of relatively planar and slightly undulating stratigraphic alluvial sedimentation

extending to depths of 8 to 10± feet below the bottom of the trench (approximately 30± feet below the existing site grades). One to two anomalous features suggestive of thrust-type faulting were observed. These anomalous features dip to the north at a low-angle. These features also appear to be locally continuous and are observed within Fault Trench Nos. FT-1 and FT-2.

5.3 Seismic Refraction Survey

A Seismic Refraction Survey was performed by Terra GeoSciences at the bottom of Fault Trench No. FT-1. The results of this survey are presented in a separate report, included as Appendix E of this report. The purpose of this survey was to identify if there is offset stratigraphy or lateral velocity contrasts that would be suggestive of structural discontinuities and/or faulting at depth below the trench. The seismic survey line is identified as TG S-1. The location of TG S-1 is depicted on Plate 2 of this report. Both the Layer Velocity Model and the Refraction Tomographic Model were used for the analysis that was performed for TG S-1.

The seismic refraction survey using the Layer Velocity Method indicated that there were three distinct velocity layers (V1 through V3). V1 is considered to be comprised of recent (late to middle Holocene age) unconsolidated alluvial fan deposits. The middle V2 velocity layer is considered to be comprised of denser and more indurated, probably older alluvial deposits likely associated with the early Holocene sediments. The deeper V-3 velocity layer appears to be very well-consolidated and undurated, consistent with Pleistocene-age deposits. The seismic refraction survey using the Refraction Tomographic Model revealed two generally parallel anomalous features suggestive of faulting. These features have a relatively low angle and dip to the north.

5.4 Seismic Reflection Survey

Additionally, SCG contracted GeoVision to perform a Seismic Reflection Survey near the western property line. The seismic reflection line is identified as GV S-1. The result of this survey is presented in a separate report included as Appendix F of this report. The purpose of this survey was to screen the area beneath the seismic line for a fault which may act as a groundwater barrier. The results of the Seismic Reflection Survey indicate that GeoVision was unable to definitively interpret any features observed in the data set as being caused by a shallow fault.

5.5 Backfilling of Fault Trench

After the trenches were logged, both of the trenches were backfilled and compacted. Backfilling operations occurred between May 11, 2022 and May 16, 2022 for Fault Trench No. T-1 and between May 4, 2022 and May 11, 2022 for Fault Trench No. T-2. The trenches were backfilled with the previously excavated on-site soils. The soil was moisture conditioned as necessary and compacted using a loader and a vibratory roller in 12± inch lifts. Moisture-density tests indicate that the fill soils were compacted to at least 90 percent of the ASTM D-1557 maximum dry density. In place density testing of the structural fill was performed using the Nuclear test method (ASTM D-2922-81), referenced to the maximum dry density values obtained by the Modified Proctor method (ASTM D-1557-91). The density test locations are shown on the enclosed Density Test Location Plan, Plate 7 in Appendix D of this report. Moisture density test results are presented on

Table 1, enclosed in Appendix D. In addition, data regarding the soil types used as structural fill are presented on Table 2 in Appendix D.

6.0 SUMMARY OF GEOLOGIC CONDITIONS

6.1 Regional Geology

The site is located within the Transverse Ranges physiographic provinces of California. The Transverse Ranges province is characterized by several anomalous east-west trending mountain ranges that truncate the northwesterly-trending Peninsular Ranges to the southeast and grades into the northwesterly-trending Coastal Ranges to the northwest. The eastern Transverse Ranges are bounded to the south by the San Andres fault and bounded to the north by a thrust fault system. The central and western Transverse Ranges are bounded to the north by the San Andres Fault and to the south by several thrust fault systems. The site is located in the San Gabriel Mountains, which is considered the central Transverse Ranges. The San Gabriel Mountains are bounded to the north by the San Andres Fault Zone and to the south by the Sierra Madre Fault Zone.

The bedrock geology that dominates the elevated areas of the central Transverse Ranges (San Gabriel mountains) consists of high-grade metamorphic Precambrian rocks intruded by Paleozoic to Cretaceous plutons. During the Cretaceous, extensive mountain building occurred during the emplacement of the southern California batholith. The central Transverse Ranges have been significantly disrupted and uplifted by Tertiary and Quaternary strike-slip faulting along the San Andres fault and thrust faulting along the north dipping Sierra Madre fault. This tectonic activity has resulted in the present terrain. Several deep alluvial fans are present at the southern base of the San Gabriel mountains.

The regional geologic conditions were obtained from a portion of the Geologic Map of the Mount Wilson and Azusa Quadrangles, Los Angeles County, California, by Thomas W. Dibblee Jr., 1998, presented as Plate 3 of this report. The map indicates that the site is underlain by Holocene surficial sediments (Map Symbol Qg). These deposits are described as gravel and sand of stream channels, and alluvial fan out-wash from major canyons. A buried segment of the Sierra Madre fault is mapped 4,000± feet to the north of the site. Additionally, a buried segment of the Duarte Fault is mapped 3,250± feet to the south of the site.

6.2 Regional Faulting

There are three main structural geologic features on or near the subject site, the Sierra Madre Fault Zone (SMFZ), the Duarte Fault and the Upper Duarte Fault. The SMFZ, located north of the subject site, extends from Tujunga, California to San Bernardino, California. The SMFZ is a roughly east-west trending, thrust fault system. Information presented on the Southern California Earthquake Data Center (SCEDC) website operated by Caltech has assigned the following parameters to the Sierra Madre Fault Zone:

- Length: 75 kilometers
- Slip Rate: 0.36 to 4 millimeters per year
- Probable Magnitudes (M_w): 6.0 to 7.0

- Recurrence Interval: Several thousand years

Several of the large segments of the SMFZ have individual identities. One of the central segments of the SMFZ is identified as the Sierra Madre D section. This segment of the SMFZ is nearest the subject site. This section of the fault is a thrust fault that trends N 76° W with a dip less than or equal to 55 degrees to the north. The slip rate is between 1 and 5 millimeters per year. The recurrence interval is unknown (<https://earthquake.usgs.gov>).

The SCEDC highlights that the Duarte fault is a strand of Segment D of the SMFZ. No other information was listed for the Duarte fault specifically. The Duarte fault is located south of the subject site. The Upper Duarte fault, located between the Duarte fault and the SMFZ, encompasses a portion of the subject site. No information or mention of the Upper Duarte Fault was listed on the SCEDC website.

6.3 Site Specific Geology

The subject site is located within the alluvial fan of the San Gabriel River. The San Gabriel River extends from the eastern San Gabriel mountains, trending northeast-southwest to north-south, towards the Pacific Ocean. Based on our subsurface exploration, and review of pertinent geologic and geotechnical literature, the site is underlain by a surficial layer of artificial fill and alluvial soils characteristic of stream channels and alluvial fan outwash deposits. A description of the units is presented below.

Pavements

Portland cement concrete (PCC) was encountered at the ground surface of Fault Trench No. FT-1, from 340 to 348± feet. The PCC is ½± foot in thickness with no discernable underlying aggregate base.

Turf Grass/Topsoil

Turf grass was encountered at the ground surface of both fault trench locations. The turf grass is 2± inches in thickness. The turf grass grades in to topsoil that extends to depth of ½ to 1± feet below ground surface. The topsoil generally consists of loose silty fine to coarse sand and silty fine sand with little medium to coarse sand and trace fine to coarse gravel. The topsoil possesses abundant to extensive fine root fibers from the turf grass.

Artificial Fill

Artificial fill was encountered beneath the topsoil of both fault trench locations extending to depths of 1 to 5± feet below ground surface. The artificial fill consists of loose to medium dense, mottled, fine sands, fine to coarse sands, silty fine to medium sands and gravelly fine to coarse sands. The fill soils possess trace to some cobbles and occasional boulders. Some layers possess debris including roots, trash, and concrete fragments.

Older Topsoil

An older topsoil layer was encountered beneath the fill at both fault trench locations. This older topsoil layer is presumably the previous ground surface prior to grading activities to facilitate the

construction of the existing golf course. The older topsoil, ½ to 1± feet in thickness, consists of loose to medium dense silty fine sand with trace to little amounts of medium to coarse sand, fine to coarse gravel and cobbles. The older topsoil in Trench No. FT-1 possesses little to some fine root fibers and roots.

Alluvium

Native alluvium was encountered beneath the artificial fill at both fault trench locations, extending to at least the maximum depth explored of 22± feet below ground surface. The alluvium consists of interbedded loose to medium dense fine sands to silty fine sands in the upper 10 to 15± feet. The alluvium consists of interbedded dense gravelly fine to coarse sands and cobbly fine to coarse sands in the upper 13 to 15± feet. Occasional layers of dense fine sand were encountered in the upper 13 to 15± feet. The deeper alluvial soils generally consist of dense cobbly fine to coarse sands, gravelly fine to coarse sands, fine to coarse sands and fine sands. The alluvial soils occasionally possess layers with boulders. Slight cementation was observed in the layers that possess trace amounts of silt. Small amounts of calcium deposits were observed on the bottom side of cobbles at depth. In addition, grussification (granular disintegration of rock), was observed on several of the mafic cobbles at depth.

The near surface alluvium generally consists of unbroken sediments and the deeper alluvium generally consists of sand, gravelly sand and cobbly sand layers that pinch out horizontally which is characteristic of channel deposits. It should be noted that three (3) organic plant samples were collected within the deeper alluvial soils at Trench Nos. FT-1 and FT-2.

Groundwater

Free water was not encountered during the excavation of the two fault trenches of this study. As previously stated, groundwater was encountered by LPI during the drilling of the borings of the previous geologic study. LPI encountered groundwater in the southwest area of the subject site between depths of 134 to 216± feet below the ground surface. LPI noted a groundwater discrepancy of 82± feet in this area of the site, indicating the presence of a groundwater barrier which could be caused by faulting. The static groundwater was considered to have existed at depths of 134 to 216± feet below ground surface at the time of the previous subsurface exploration.

As part of our research for the feasibility study, we reviewed readily available groundwater data in order to determine recent regional groundwater depths. The primary reference used to determine the groundwater depths in the subject site area is the California Department of Water Resources website, <http://www.water.ca.gov/waterdatalibrary/>. One monitoring well is located approximately 1,354 feet northeast from the site. Water level readings within this monitoring well indicates a high groundwater level of 61 feet below the ground surface in July 2021. A second monitoring well is located 4,220± feet southwest of the site. Water level readings within this monitoring well indicates a high ground water level 352± feet below ground surface in August 2021.

6.4 Sediment Age

A total of three (3) organic plant samples were collected from Fault Trench Nos. FT-1 and FT-2. These samples were submitted to DirectAMS, a radiocarbon dating service. The results of the testing is below:

Sample	Radiocarbon Age (before present)
FT-1 @ 18 feet	308
FT-1 @ 18.5 feet	874
FT-2 @ 17 feet	189

Based on the results of the radiocarbon dating, the deeper alluvial soils have an average radiocarbon age of 457 years before present. Therefore, the deeper soils are considered to be late Holocene-age sediments.

6.5 On-Site Faulting

Based on our review of the Earthquake Zones of Required Investigation Azusa Quadrangle, California, published by the CGS, the subject site is located within a designated earthquake fault zone as defined by the Alquist-Priolo Earthquake Fault Zoning Act. In accordance with the provisions of the Act, all new construction of habitable structures within the Fault Rupture Hazard Zone will be preceded by a fault trenching investigation to determine the presence of on-site strands of any active or potentially active fault and to determine the need for a structural setback. The general location of the site relative to the Upper Duarte Fault Zone is illustrated on the Earthquake Zones of Required Investigation Map, included as Plate 4 of this report.

Approximately 18 to 22± feet of alluvial sediments were exposed at Fault Trench Nos. FT-1 and FT-2. The upper 13 to 15± feet generally consisted of unbroken sediments. The deeper alluvial soils were characteristic of channel deposits with interbedded sand, gravelly sand and cobbly sand layers that pinch out horizontally. The cobbles and boulders were generally rounded and sub-rounded. None of the deeper alluvial channel deposits were offset.

The channel deposits were observed with fining upward alluvial sequences that span 3 to 4 layers (1 to 4± feet) at a time. A fining upward sequence describes a depositional event where a large volume of fast-moving water deposits coarser material at the bottom of a channel and gradually deposits less coarse material as the volume and velocity of the water decreases. The sequences observed indicate that the area has experienced several high volume and high velocity depositional events in the past that deposited several feet vertically of material during one event. This observation is consistent with the relatively young ages of the soil measured by radiocarbon dating. As previously stated, the sediments exposed near the bottom of the trenches were deposited less than 1,000 years before present within the late Holocene. In addition, the slight grussification of the mafic cobbles and the slightly developed calcium deposits on the bottom of the cobbles also indicate a relatively young age.

Based on the GPR data collected by Terra Geosciences, relatively planar and slightly undulating stratigraphic alluvial sedimentation extending to 8 to 10± feet below the bottom of the trench (approximately 30± feet below the existing site grades) was observed at both trench locations.

These horizontal discontinuous layers are considered to be caused by channel deposits. Two anomalous features were identified approximately 8 to 10± feet below the bottom of both trenches. The anomalous features were encountered at Station 2+54 and 3+15 at Fault Trench No. FT-1 and at Station 0+91 and 1+58 at Fault Trench No. FT-2. These two anomalous features dip between 13 to 19 degrees downward to the north. These two anomalous features are suggestive of low-angle thrust faulting. In addition, the sediments north of the anomalous features appear to dip slightly to the north, which is an opposite direction to the expected deposition of the upper alluvial fan deposits in this area. The north-dipping layers are likely due to back-tilting of the alluvium associated with the low-angle thrust faulting. The two anomalous features are approximately 60 feet apart in each trench. It appears that the anomalous features are related due to the similar apparent structure and the similar distance apart. When the two anomalous features are connected between both fault trenches, the resulting line is nearly parallel to the mapped Upper Duarte Fault trace to the south of the site. Therefore, SCG considers these anomalous features to likely be low-angle thrust faults associated with the Upper Duarte Fault which is mapped to the south of the site. A copy of the Ground Penetrating Radar results is available on Plate 5 of this report.

Terra Geosciences also performed a seismic refraction survey at the bottom of Fault Trench No. FT-1. The results of the seismic refraction line identified two anomalous features that dip downward to the north at relatively low angles. The southern anomalous feature was encountered at Station 0+75 at a depth of 30± feet below the bottom of the trench (approximately 50± feet below the existing site grades). The northern anomalous feature was encountered at Station 2+30, near the bottom of the trench (approximately 20± feet below the existing site grades). The southern anomalous feature would project beyond the property line to the south. This anomalous feature could possibly be the fault trace of the mapped Upper Duarte fault to the south of the site. Additionally, the anomalous feature could be the cause of the groundwater discrepancy observed between B-2 and B-3 which was reported in the previous LPI study. The northern anomalous feature is likely the same anomalous feature discussed in the GPR study above. Both anomalous features are located in a similar location within Fault Trench No. FT-1 with a similar north-dipping low angle. The two anomalous features defined in the seismic refraction survey are considered to be north-dipping, low-angle thrust-faulting.

The seismic reflection survey, performed by GeoVision, was performed to the west of Fault Trench No. FT-1, adjacent to North Todd Avenue. The survey was inconclusive due to space limitations, the noise of street traffic and a lack of knowledge of the potential fault location at the time of the survey. Additionally, the reflection data was only viable at 100± feet and below, eliminating the potential to confirm the location of the two possible faults.

7.0 CONCLUSIONS AND RECOMMENDATIONS

7.1 Conclusions

We have reviewed readily available reports, maps, and performed a subsurface fault study of the subject site to evaluate the potential for surface faulting at the site. There is positive evidence that potentially active faults transect the subject site. This conclusion is based on the following factors:

- The groundwater discrepancy observed by LPI during the drilling of their borings indicates the presence of a groundwater barrier, likely a fault. An anomaly observed in the seismic refraction survey correlates with this discrepancy.
- Geophysical surveys indicate the presence of two anomalous features within both fault trenches at a depth of $30\pm$ feet below ground surface. The anomalous features are considered to be north-dipping, low-angle thrust-faults. The projection of the anomalous features is parallel to the Upper Duarte Fault trace mapped to the south of the site. Therefore, these two faults are considered to be associated with the Upper Duarte Fault.
- Radiocarbon dating on samples taken at the bottom of both fault trenches indicates that the average age of the sediment is $457\pm$ years old at a depth of 18 to $18\frac{1}{2}\pm$ below ground surface. Thick, fining-upward sequences were observed in both trenches indicating the site has experienced rapid depositional events possibly depositing several feet or more during each depositional event. Extrapolating the age of the sediment to depths of approximately $30\pm$ feet below the ground surface, the depth the likely faults were encountered during the GPR survey, indicates that the sediment could possibly be 1,500 to $2,000\pm$ years old. Therefore, the broken sediments at a depth of $30\pm$ feet are considered to be late Holocene-age. Therefore, these two faults are considered to be active.
- Reports from nearby investigations indicate that at least the upper $50\pm$ feet of the alluvial fan deposits are Holocene age.

7.2 Recommendations

Based on the results of this fault study, positive evidence indicates that active faults occur at the subject site. Therefore, SCG recommends a 50-foot habitable structure setback “no build zone” from the surface projection of the two buried, north-dipping, low-angle faults associated with the Upper Duarte Fault for any proposed structures. The location of the habitable structure setback is depicted on Plate 2 of this report.

8.0 GENERAL COMMENTS

This report has been prepared for use by the client, in order to aid in the evaluation of this property and to assist the architects and engineers in the design and preparation of the project plans and specifications. This report may be provided to the contractor(s) and other design consultants to disclose information relative to the project. However, this report is not intended to be utilized as a specification in and of itself, without appropriate interpretation by the project architect, civil engineer, and/or structural engineer. The reproduction and distribution of this report must be authorized by the client and Southern California Geotechnical, Inc. Furthermore, any reliance on this report by an unauthorized third party is at such party's sole risk, and we accept no responsibility for damage or loss which may occur.

The analysis of this site was based on a subsurface profile interpolated from limited discrete soil samples. While the materials encountered in the project area are considered to be representative of the total area, some variations should be expected between boring and trench locations and sample depths. If the conditions encountered during construction vary significantly from those detailed herein, we should be contacted immediately to determine if the conditions alter the recommendations contained herein.

This report has been based on assumed or provided characteristics of the proposed development. It is recommended that the owner, client, architect, structural engineer, and civil engineer carefully review these assumptions to ensure that they are consistent with the characteristics of the proposed development. If discrepancies exist, they should be brought to our attention to verify that they do not affect the conclusions and recommendations contained herein. We also recommend that the project plans and specifications be submitted to our office for review to verify that our recommendations have been correctly interpreted.

The analysis, conclusions, and recommendations contained within this report have been promulgated in accordance with generally accepted professional geological and geotechnical engineering practice. No other warranty is implied or expressed.

9.0 REFERENCES

- Amec Geomatrix, Inc., 2010, Slope stability evaluation for north slope & Duarte Fault for Reliance 1 quarry, Project No. 10168.011.3, October 29, 2010.
- City of Azusa, CA, 2014, Environmental Impact Report, Tenth Street Center Industrial Park (Public Review Draft), May 2014.
- Crook, R., Jr., Allen, C.R., Kamb, B., Payne, C.M., and Proctor, R.J., 1987, Quaternary geology and seismic hazard of the Sierra Madre and associated faults, western San Gabriel Mountains *in* Recent reverse faulting in the Transverse Ranges, California: U.S. Geological Survey Professional Paper 1339, p. 27-63, plates 1:24,000.
- Dibblee, T.W., Jr., 1998, Geologic map of the Mt. Wilson and Azusa quadrangles, Los Angeles County, California: Dibblee Geological Foundation, Map DF-67, 1:24,000.
- Earthquake Zones of Required Investigation, Azusa 7.5 Minute Quadrangle, California Geological Survey, Scale 1:24,000.
- Land Phases, Inc., 2017, Report of Engineering Geologic Study, Proposed Multi-Unit Senior Living Residential Development-California Grand Village at Azusa Greens, Southeast Corner of N. Todd Avenue and W. Sierra Madre Avenue, City of Azusa, California, Prepared for: CGVA Partners, LLC, November 11, 2016 (revised Jan. 19, 2017), Project No.: LP1261.
- Quaternary Fault and Fold Database of the United States, <https://earthquake.usgs.gov/>, maintained by USGS.
- Southern California Earthquake Data Center, www.data.scec.org, Sierra Madre Fault.
- Southern California Geotechnical, Inc. (SCG), 2022, Geotechnical Feasibility Study, Proposed Warehouse Development, NEC Todd Avenue and 10th Street, Azusa, California, prepared for Overton Moore Properties, SCG Project No. 22G144-1, dated May 27, 2022.
- TGR Geotechnical, 2013, Geotechnical Investigation Report, 1001 North Todd Avenue, Azusa, California, Project No. 12-4026, May 16, 2013.
- Treiman, Jerome A., 2013, The Sierra Madre Fault Zone in the Azusa Quadrangle, Los Angeles County, California: California Geological Survey Fault Evaluation Report FER-249.

APPENDIX A



GEOTECHNICAL LEGEND

APPROXIMATE FAULT TRENCH LOCATION

APPROXIMATE TRENCH LOCATION
(SCG PROJECT NO. 22G144-1)

PREVIOUS BORING LOCATION
(LAND PHASES INC., 2017)

PROJECTED FAULT TRACE TO SURFACE
QUERIED WHERE UNCERTAIN

GROUND PENETRATING RADAR (GPR-1 AND GPR-2)

SEISMIC REFRACTION LINE (TG S-1)

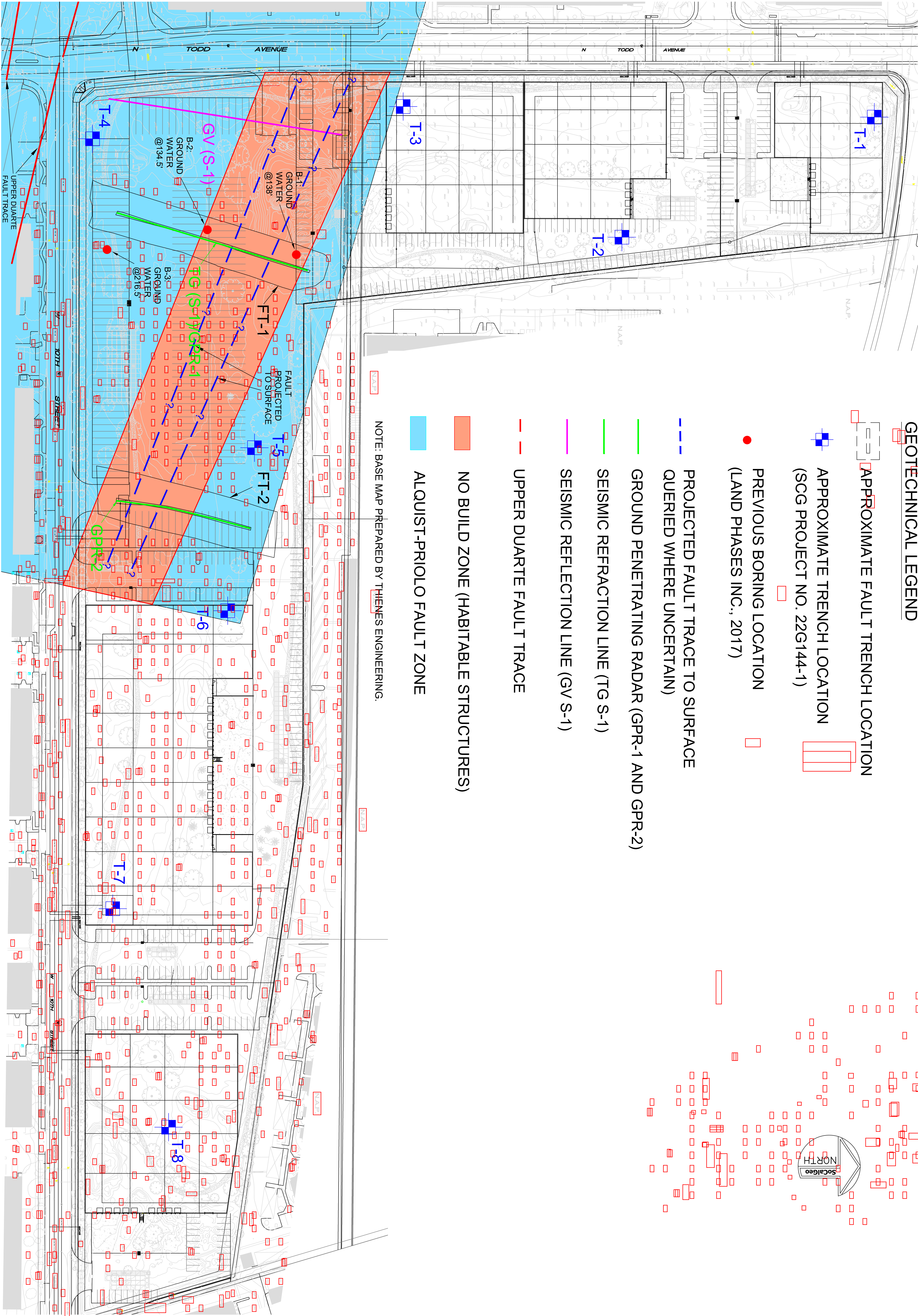
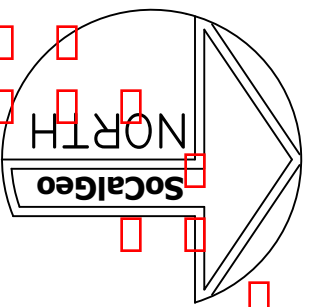
SEISMIC REFLECTION LINE (GV S-1)

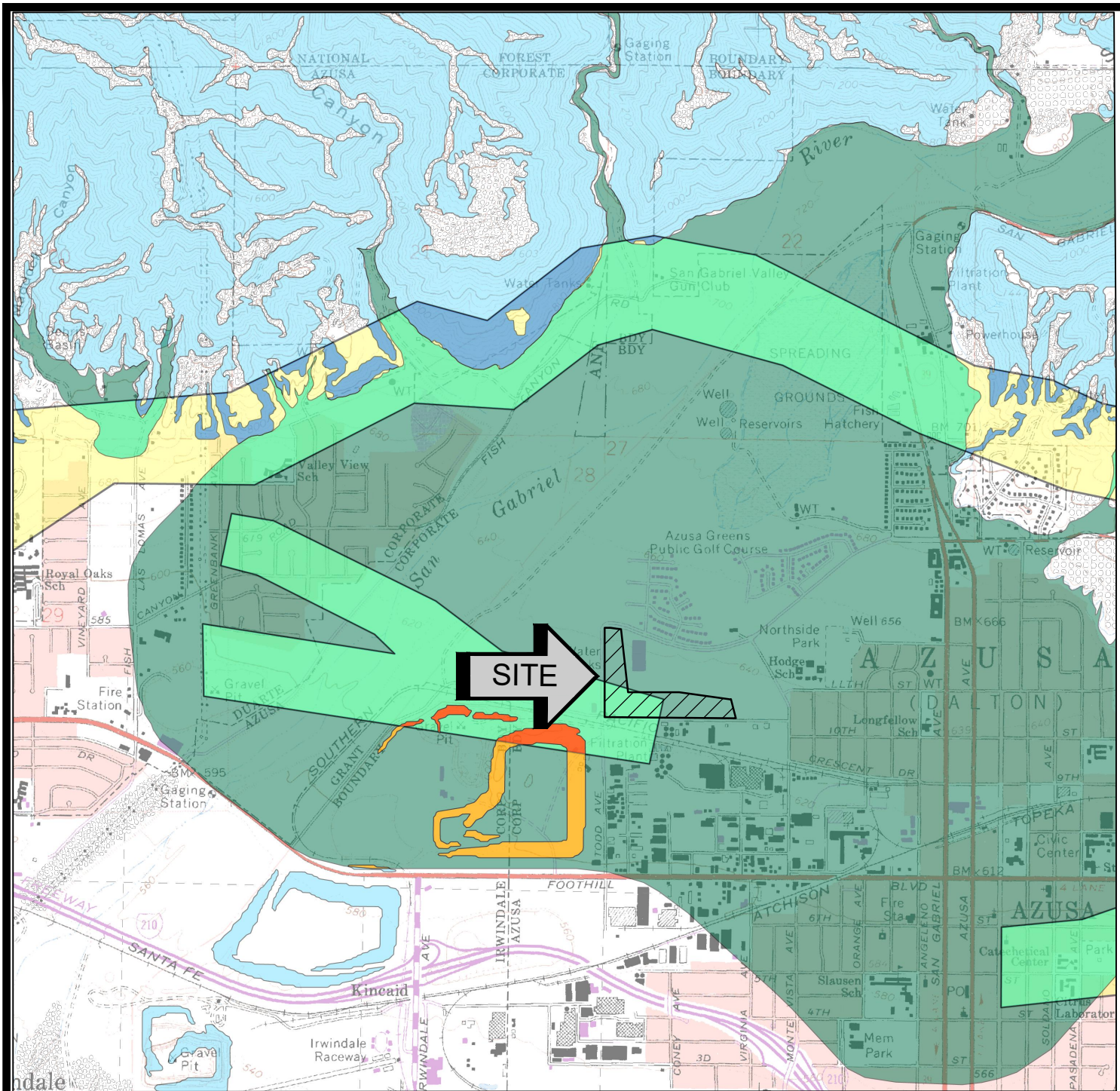
UPPER DUARTE FAULT TRACE

NO BUILD ZONE (HABITABLE STRUCTURES)

ALQUIST-PRIOLO FAULT ZONE

NOTE: BASE MAP PREPARED BY THIENES ENGINEERING.





SEISMIC HAZARD ZONES



Liquefaction Zones
Areas where historical occurrence of liquefaction, or local geological, geotechnical and ground water conditions indicate a potential for permanent ground displacements such that mitigation as defined in Public Resources Code Section 2693(c) would be required.



Earthquake-Induced Landslide Zones
Areas where previous occurrence of landslide movement, or local topographic, geological, geotechnical and subsurface water conditions indicate a potential for permanent ground displacements such that mitigation as defined in Public Resources Code Section 2693(c) would be required.



Overlapping Liquefaction and Earthquake-Induced Landslide Zones
Areas that lie within zones of required investigation for both liquefaction and earthquake-induced landslides.

OVERLAPPING EARTHQUAKE FAULT AND SEISMIC HAZARD ZONES



Overlap of Earthquake Fault Zone and Liquefaction Zone
Areas that are covered by both Earthquake Fault Zone and Liquefaction Zone.



Overlap of Earthquake Fault Zone and Earthquake-Induced Landslide Zone
Areas that are covered by both Earthquake Fault Zone and Earthquake-Induced Landslide Zone.



Overlap of Earthquake Fault Zone and Seismic Hazard Zones
Areas that are covered by Earthquake Fault Zone, Liquefaction Zones and Earthquake-Induced Landslide Zone.

Note: Mitigation methods differ for each zone – AP Act only allows avoidance; Seismic Hazard Mapping Act allows mitigation by engineering/geotechnical design as well as avoidance.

Earthquake Fault Zones

Zone boundaries are delineated by straight-line segments; the boundaries define the zone encompassing active faults that constitute a potential hazard to structures from surface faulting or fault creep such that avoidance as described in Public Resources Code Section 2621.5(a) would be required.

Active Fault Traces

Faults considered to have been active during Holocene time and to have potential for surface rupture: Solid Line in Black or Red where Accurately Located; Long Dash in Black or Solid Line in Purple where Approximately Located; Short Dash in Black or Solid Line in Orange where Inferred; Dotted Line in Black or Solid Line in Rose where Concealed; Query (?) indicates additional uncertainty. Evidence of historic offset indicated by year of earthquake-associated event or C for displacement caused by fault creep.



SOURCE: EARTHQUAKE ZONES OF REQUIRED INVESTIGATION AZUSA QUADRANGLE, CALIFORNIA GEOLOGICAL SURVEY (BOTH ALIQUIST-PRIOLO EARTHQUAKE FAULT ZONE AND SEISMIC HAZARD ZONES ISSUED FOR THE AZUSA QUADRANGLE), NOVEMBER 6TH, 2014.

EARTHQUAKE ZONE OF REQUIRED INVESTIGATION MAP PROPOSED WAREHOUSE DEVELOPMENT AZUSA, CALIFORNIA

SCALE: 1" = 2,000'

DRAWN: JAH

CHKD: DK

SCG PROJECT
22G144-2

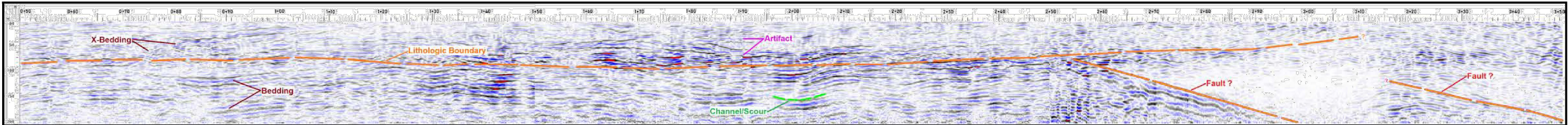
PLATE 4



**SOUTHERN
CALIFORNIA
GEOTECHNICAL**

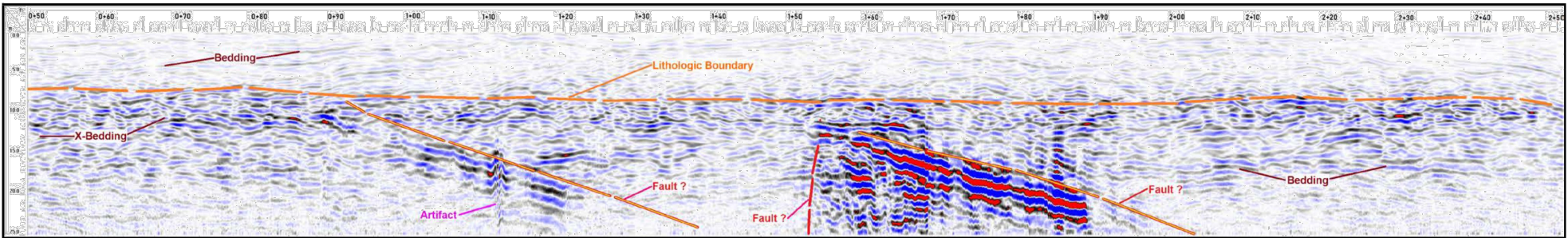
SURVEY LINE GPR-1

< South – North >




SURVEY LINE GPR-2

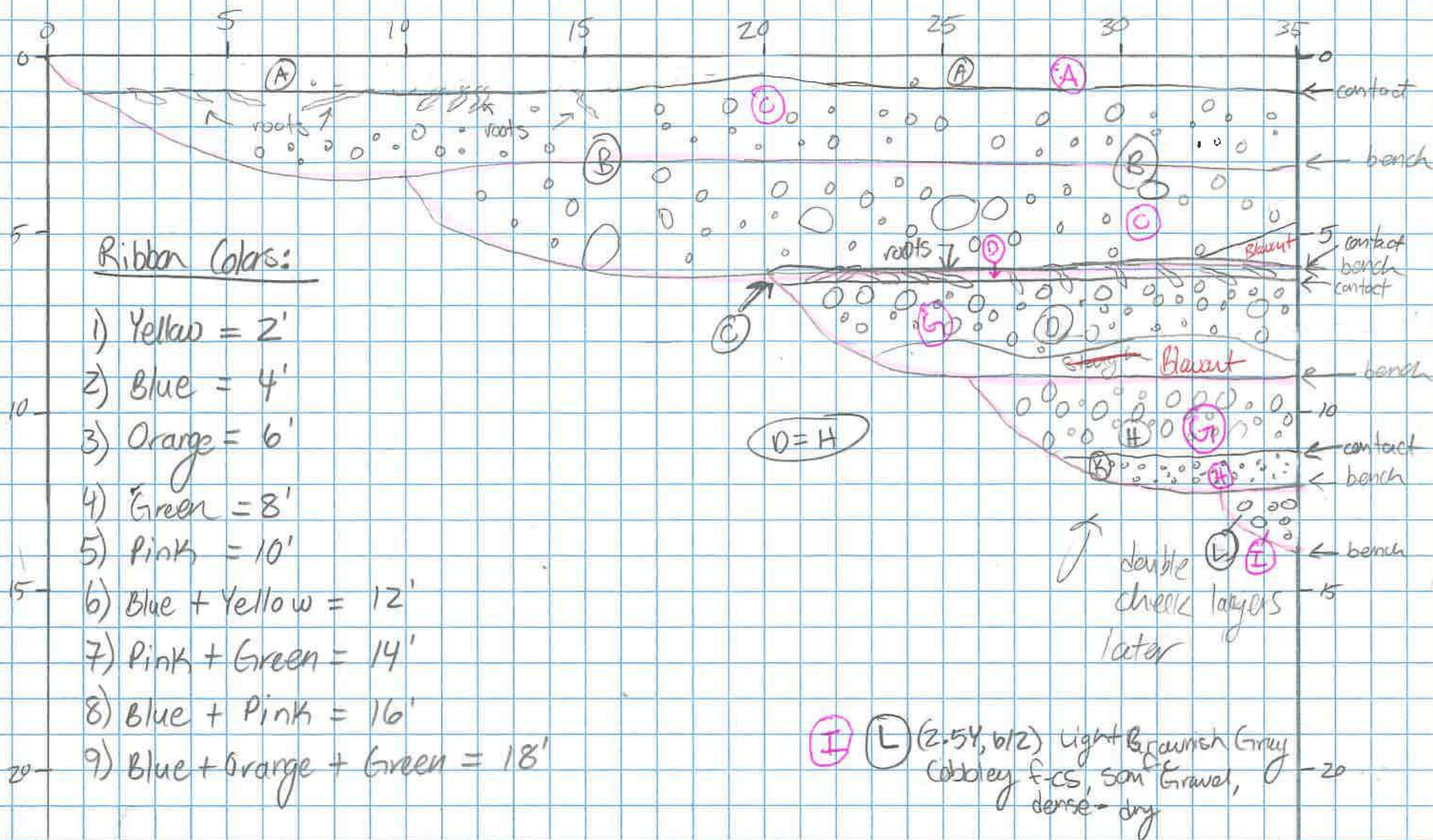
< South – North >



SOURCE: GEOPHYSICAL SURVEY, PROPOSED WAREHOUSE DEVELOPMENT PROJECT, SEC TODD AND DIERRA MADRE AVENUE, CITY OF AZUSA, CALIFORNIA, PREPARED BY TERRA GEOSCIENCES, PREPARED FOR SCG, PROJECT NO. 223808-1, DATED MAY 11, 2022

GROUND PENETRATING RADAR	
PROPOSED INDUSTRIAL DEVELOPMENT	
AZUSA, CALIFORNIA	
SCALE: 1" = 20'	 SOUTHERN CALIFORNIA GEOTECHNICAL
DRAWN: DRK CHKD: RGT	
SCG PROJECT 22G144-2	
PLATE 5	

APPENDIX B



(A) (A) Top soil: Turf grass + Grayish Brown f-cs, some frf, loose - damp

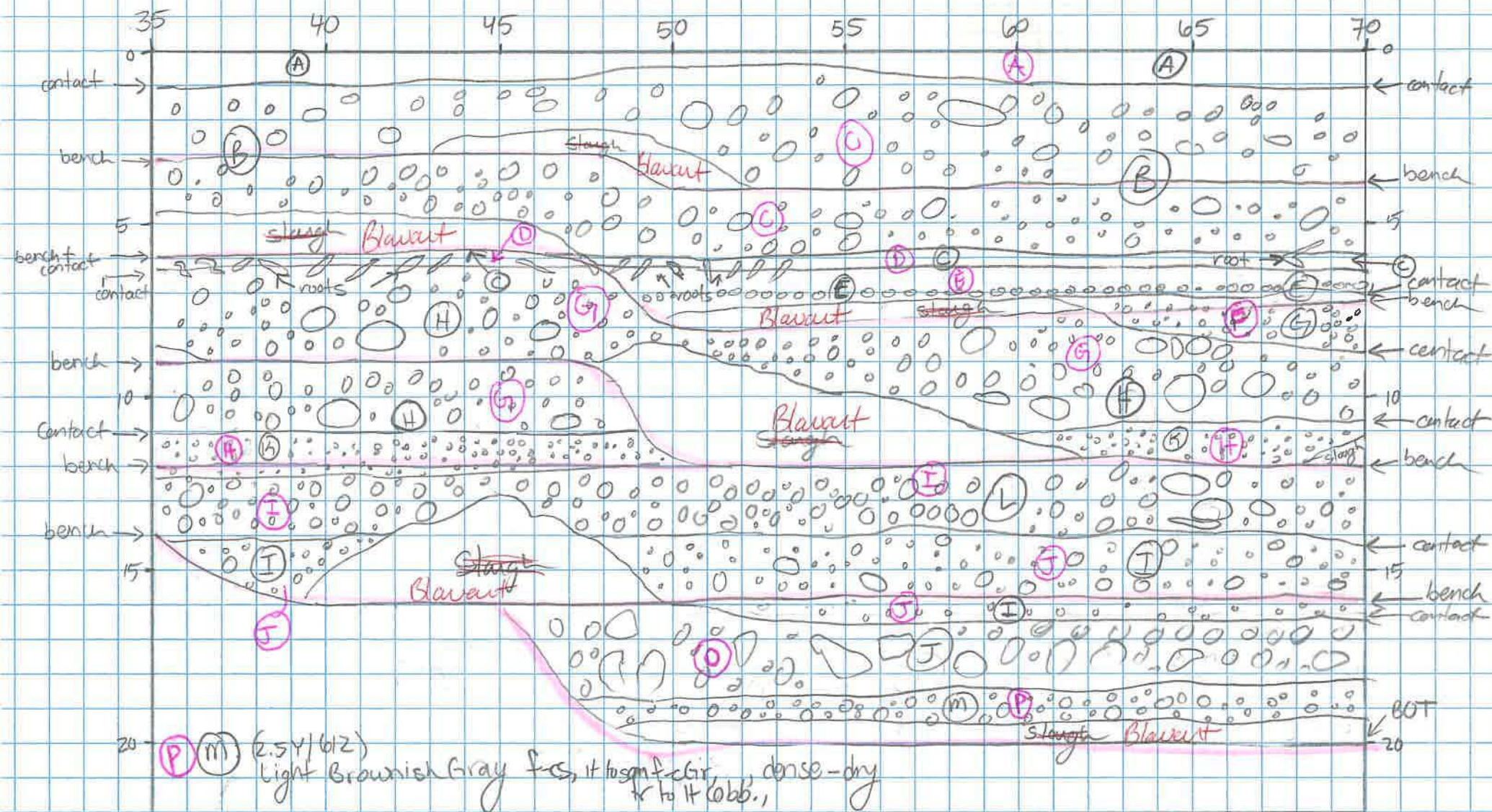
(C) (B) Fill: Light Brownish Gray f-cs, to h H, some cobb, occ boulder, m dense - damp

(D) (C) Bal: (old top soil?) Very Dark Grayish Brown f-cs, H to some f-cs, it to some Cobb, H to some frf + roots, loose to m. dense - damp to m.

(G) (D) (2.5Y, 6/2) Light Brownish Gray f-cs, some cobb., occ bult., dense - dry

(H) (B) (5Y, 6/2) Gr f-cs, occ cobb., dense - damp

(I) (L) (2.5Y, 6/2) Light Brownish Gray Cobbles f-cs, some Gravel, dense - dry



- (E) (2.5Y 6/2) Light Brownish Gray fcs, tr to m-cs, 2-inch Gravel lense in layer, accobb. dense-damp
- (G) (2.5Y 6/2) Light Grayish Brown Grv fcs, sam cobb., tr boulder, dense-dry
- (J) (2.5Y 6/2) Light Brownish Gray Grv fcs, tr to m-cs, 2-inch Gravel lense in layer, accobb. dense-damp
- (O) (2.5Y 6/2) Light Brownish Gray Grv fcs, tr to m-cs, 2-inch Gravel lense in layer, accobb. dense-damp
- (S) (2.5Y 6/2) Light Brownish Gray Grv fcs, tr to m-cs, 2-inch Gravel lense in layer, accobb. dense-damp
- (T) (2.5Y 6/2) Light Brownish Gray Grv fcs, tr to m-cs, 2-inch Gravel lense in layer, accobb. dense-damp
- (U) (2.5Y 6/2) Light Brownish Gray Grv fcs, tr to m-cs, 2-inch Gravel lense in layer, accobb. dense-damp
- (V) (2.5Y 6/2) Light Brownish Gray Grv fcs, tr to m-cs, 2-inch Gravel lense in layer, accobb. dense-damp
- (W) (2.5Y 6/2) Light Brownish Gray Grv fcs, tr to m-cs, 2-inch Gravel lense in layer, accobb. dense-damp
- (X) (2.5Y 6/2) Light Brownish Gray Grv fcs, tr to m-cs, 2-inch Gravel lense in layer, accobb. dense-damp
- (Y) (2.5Y 6/2) Light Brownish Gray Grv fcs, tr to m-cs, 2-inch Gravel lense in layer, accobb. dense-damp
- (Z) (2.5Y 6/2) Light Brownish Gray Grv fcs, tr to m-cs, 2-inch Gravel lense in layer, accobb. dense-damp

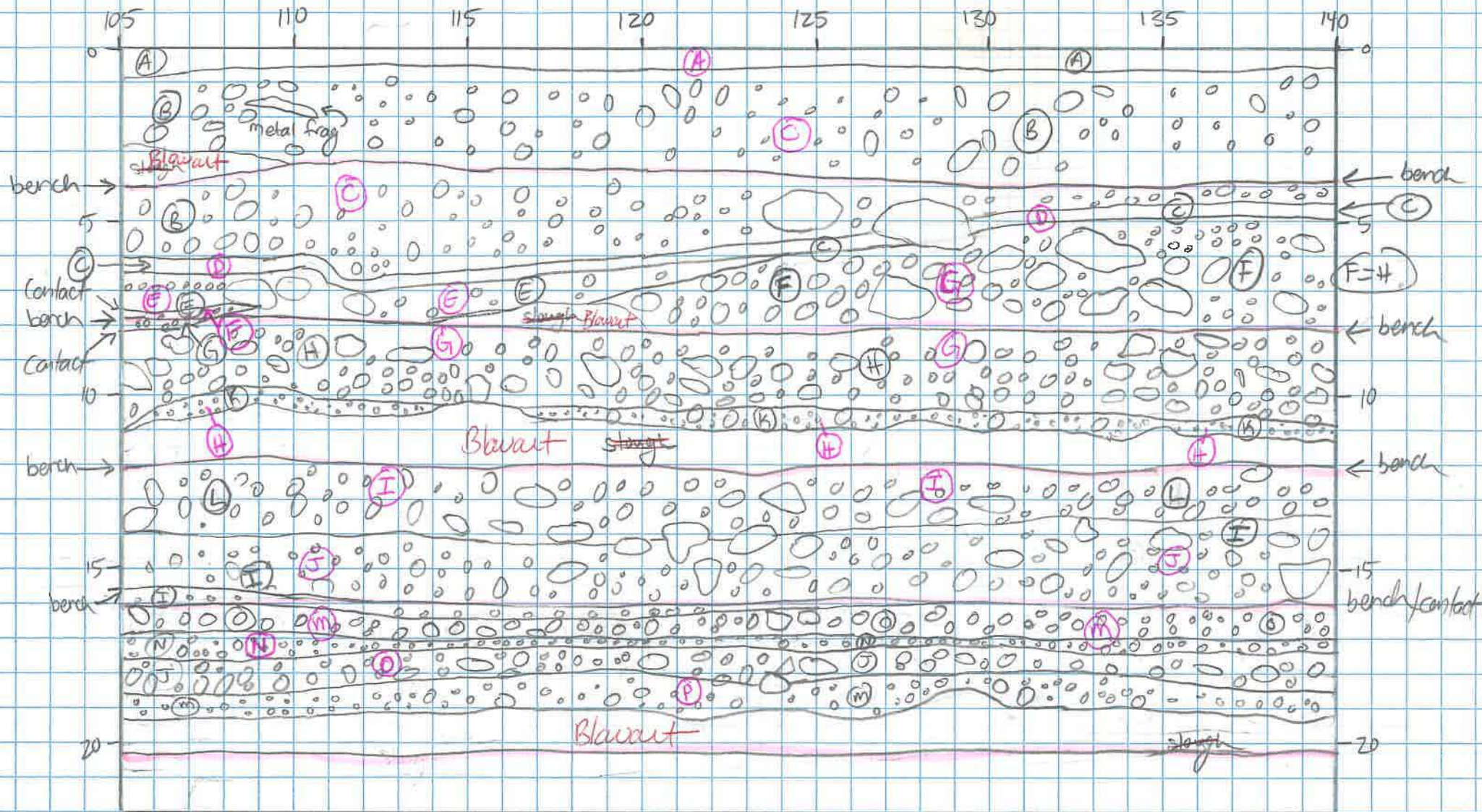


(m) (0) (2.5Y, 6/2) light brownish gray abby fcs, dense-dry

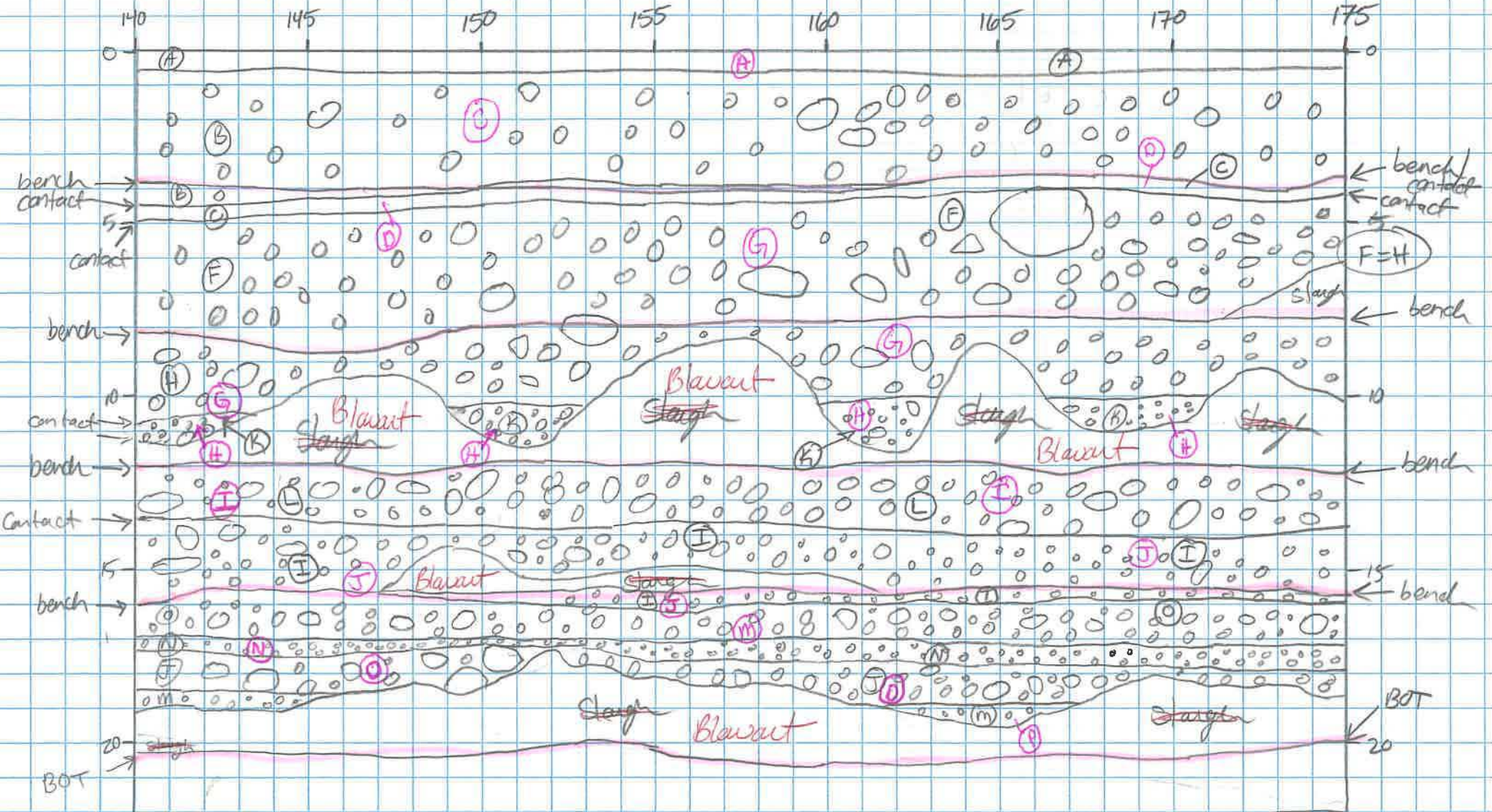
226144

FT-1

pg 4
of 11

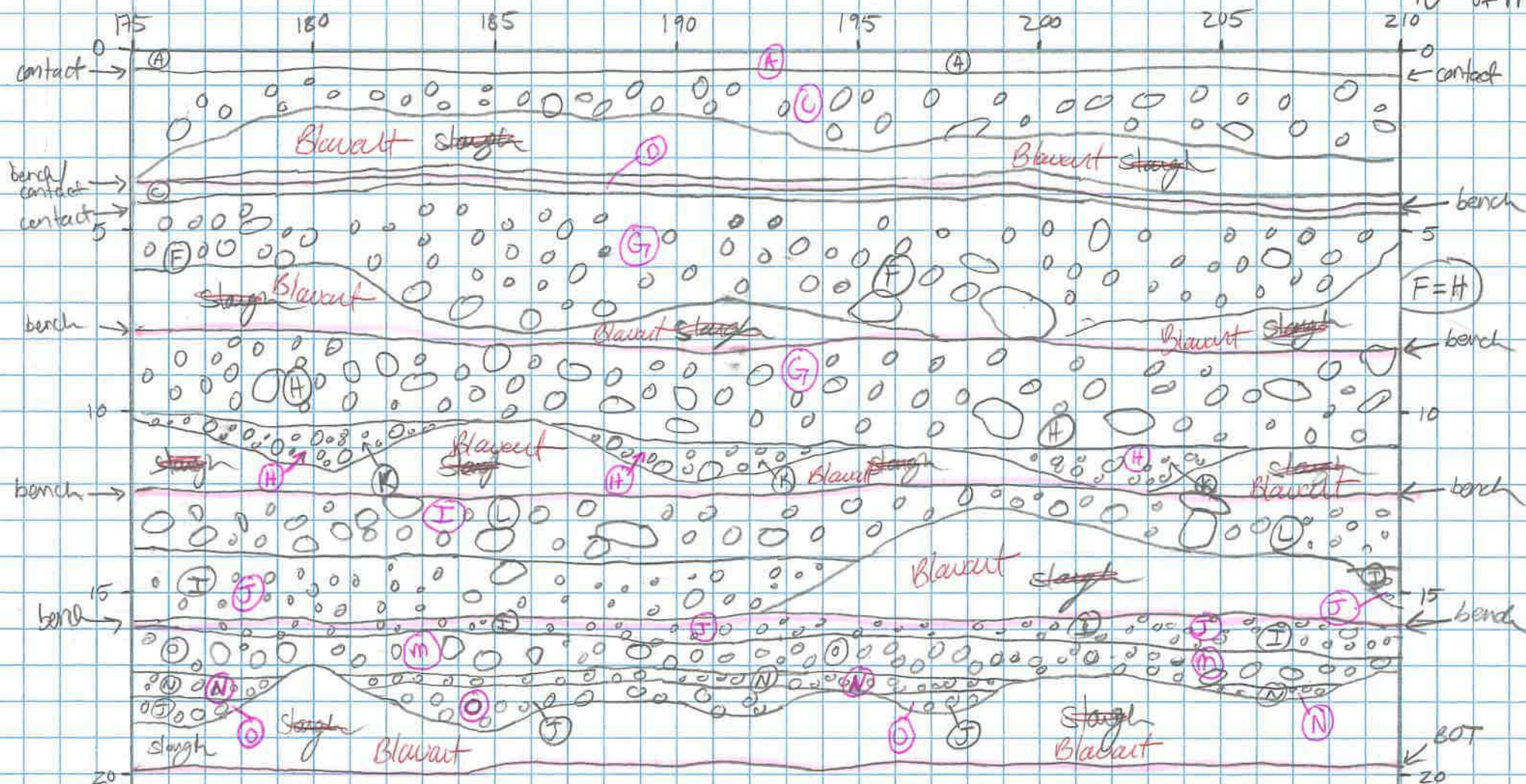


(G) (F) ~~very~~ Grv f-cs, som cobb., H boulder, dense-damp
 L \rightarrow (25Y, 6/2) light Brownish Gray



FT-1

pg. 6
of 11

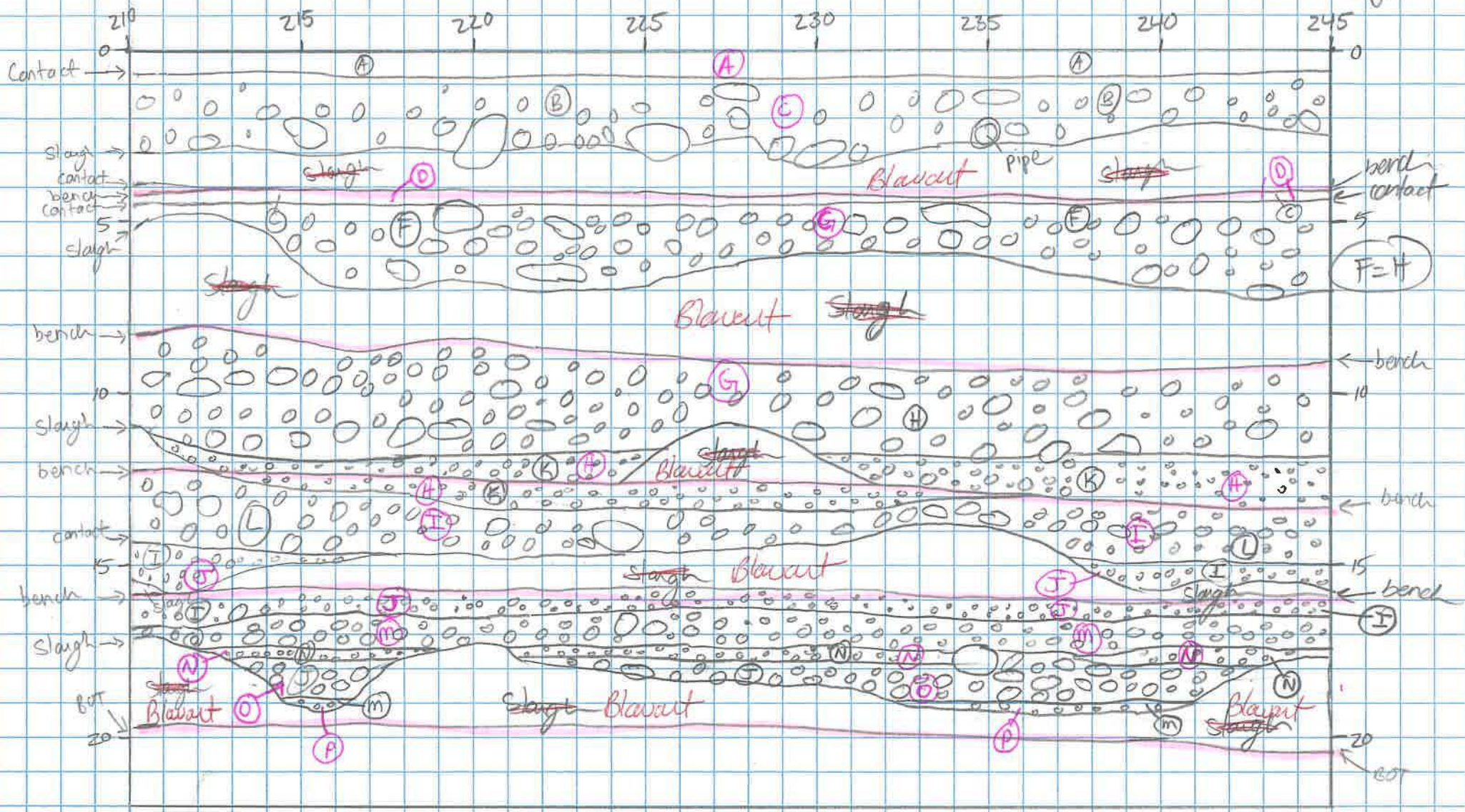


226144

FT-1

4/6/22

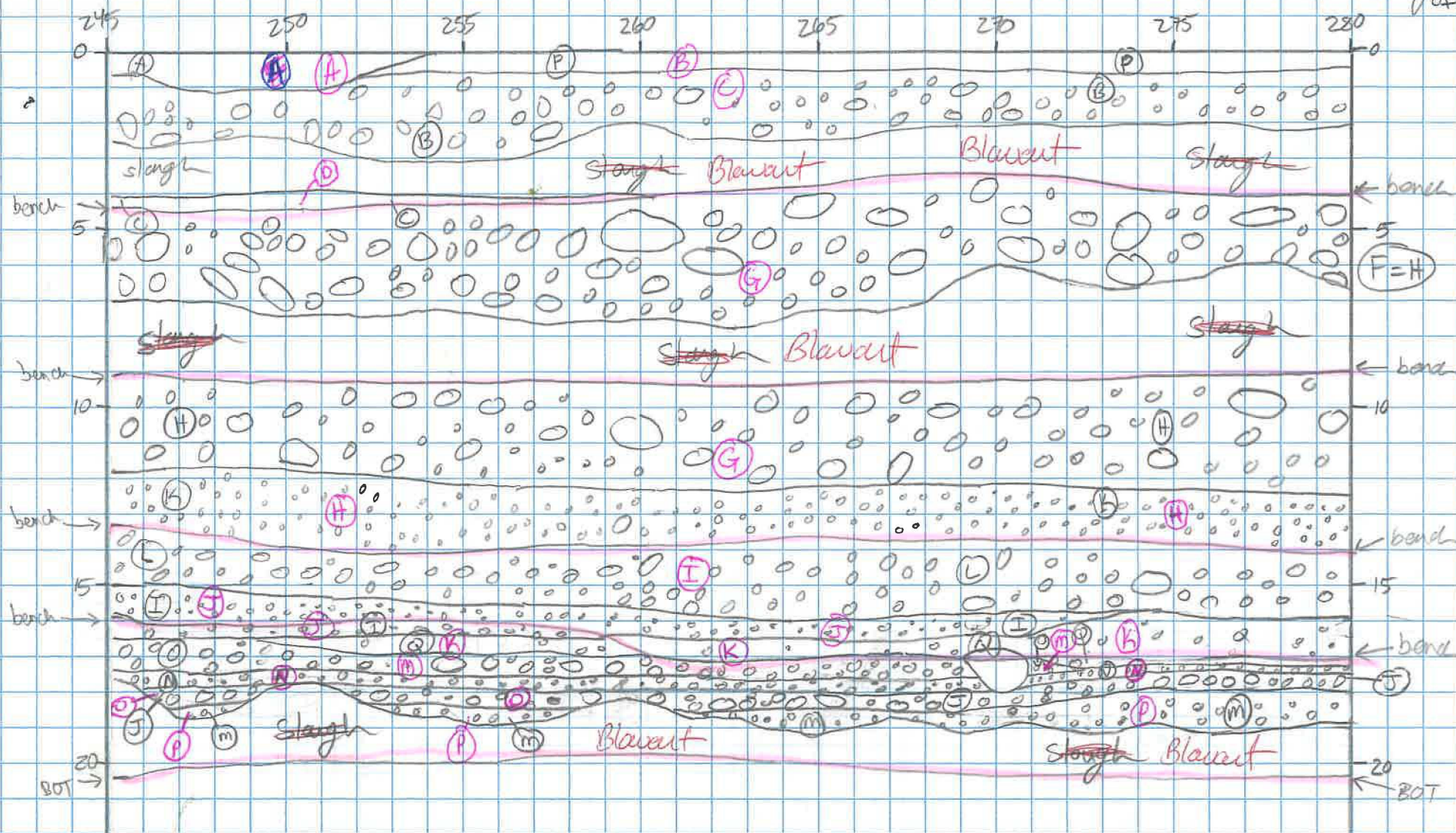
pg. 7 of 11



226144

FT-1

4/6/22

pg. 8
of 11

tr fbr, tr, bolt fbr, matted

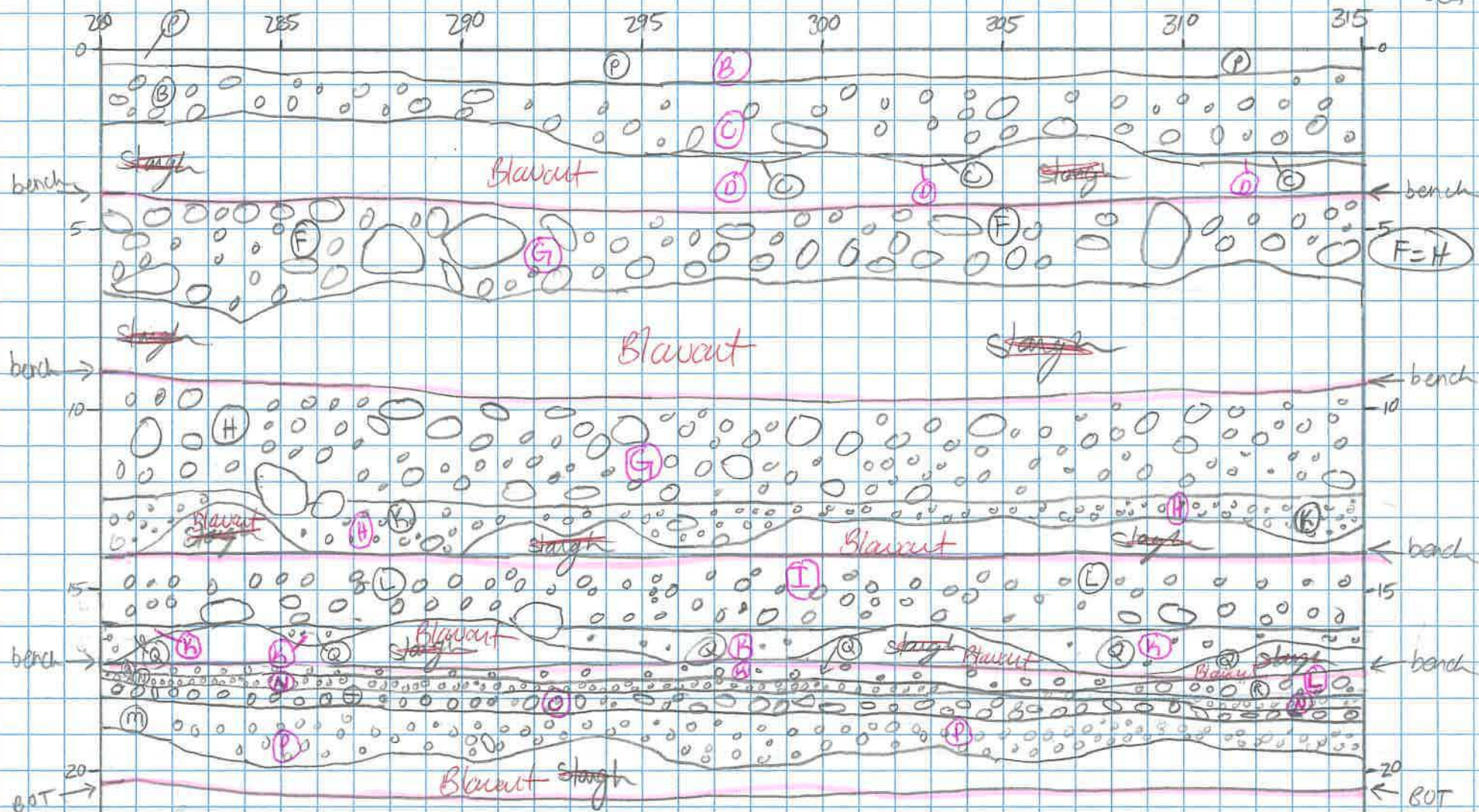
(P) FILL: (Z.54 5/2) Grayish Brown s.f.m.s, lcs, lt Fe_2O_3 st. cemented, m. dense-dry

(K) (Z.54 6/2) Light Brownish Gray fs, lt mcs, tr to lt cobb., m. dense-dry to damp

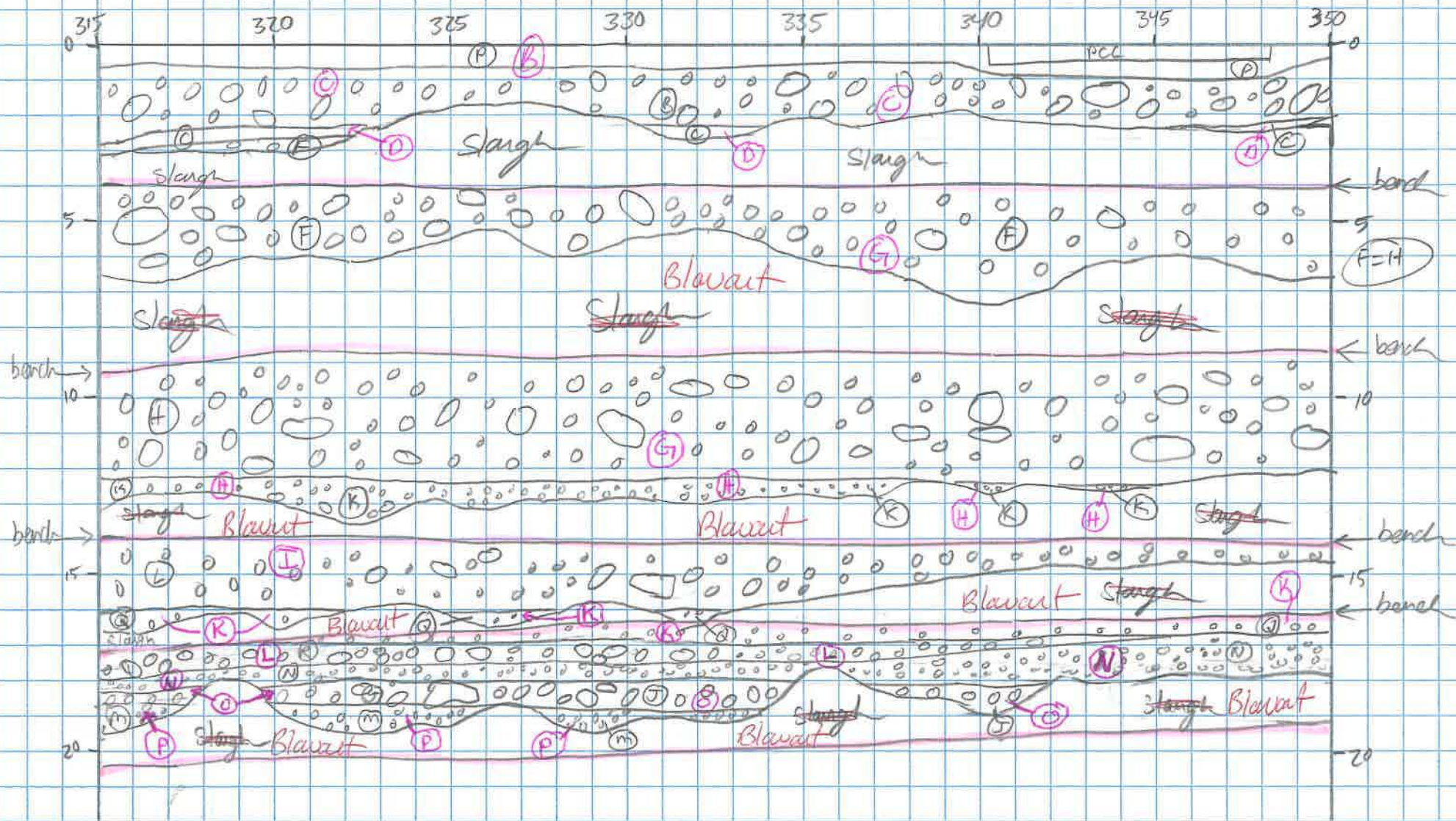
2267144

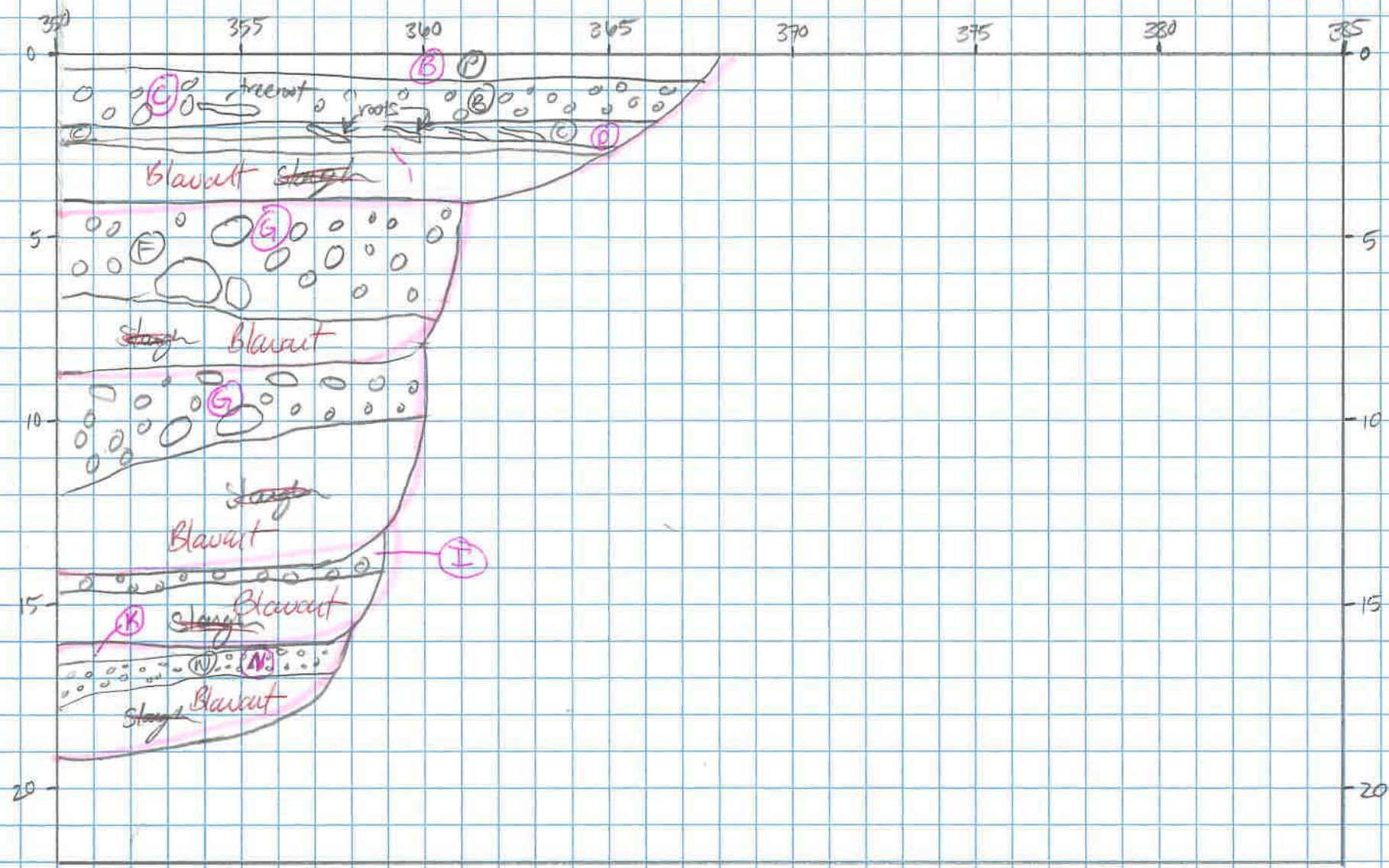
FT-1

4/6/22

pg 9
of 11

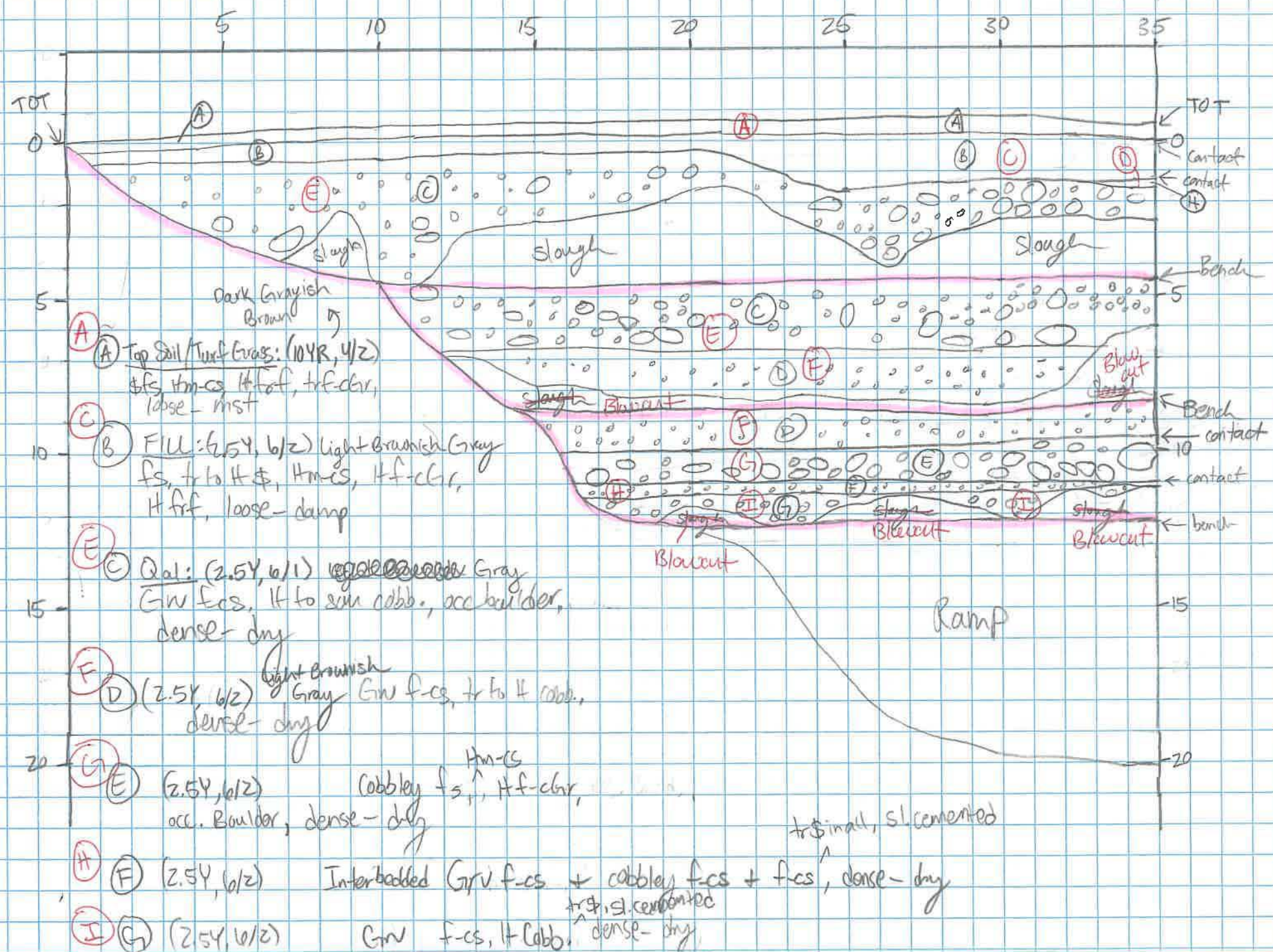
(L) (R) (2.5Y 6/2) light Brownish Gray Gv f. cs, lt rob., dense-dry

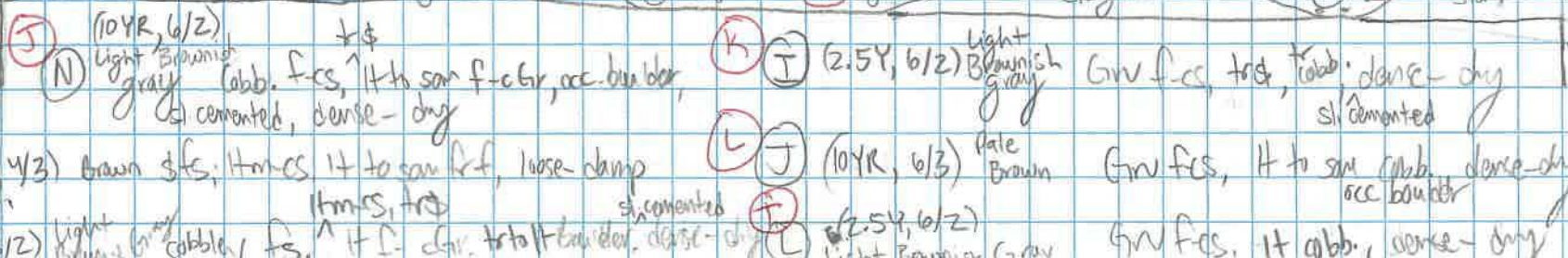


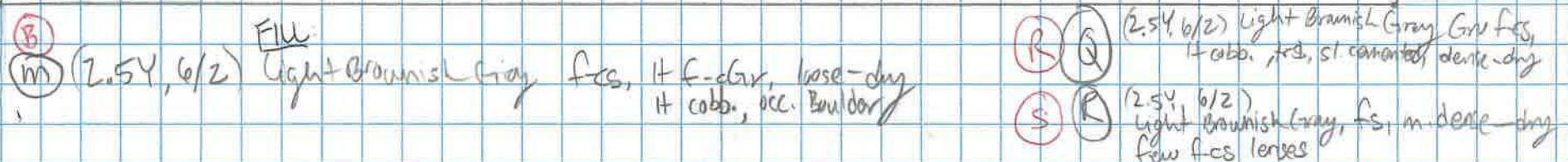


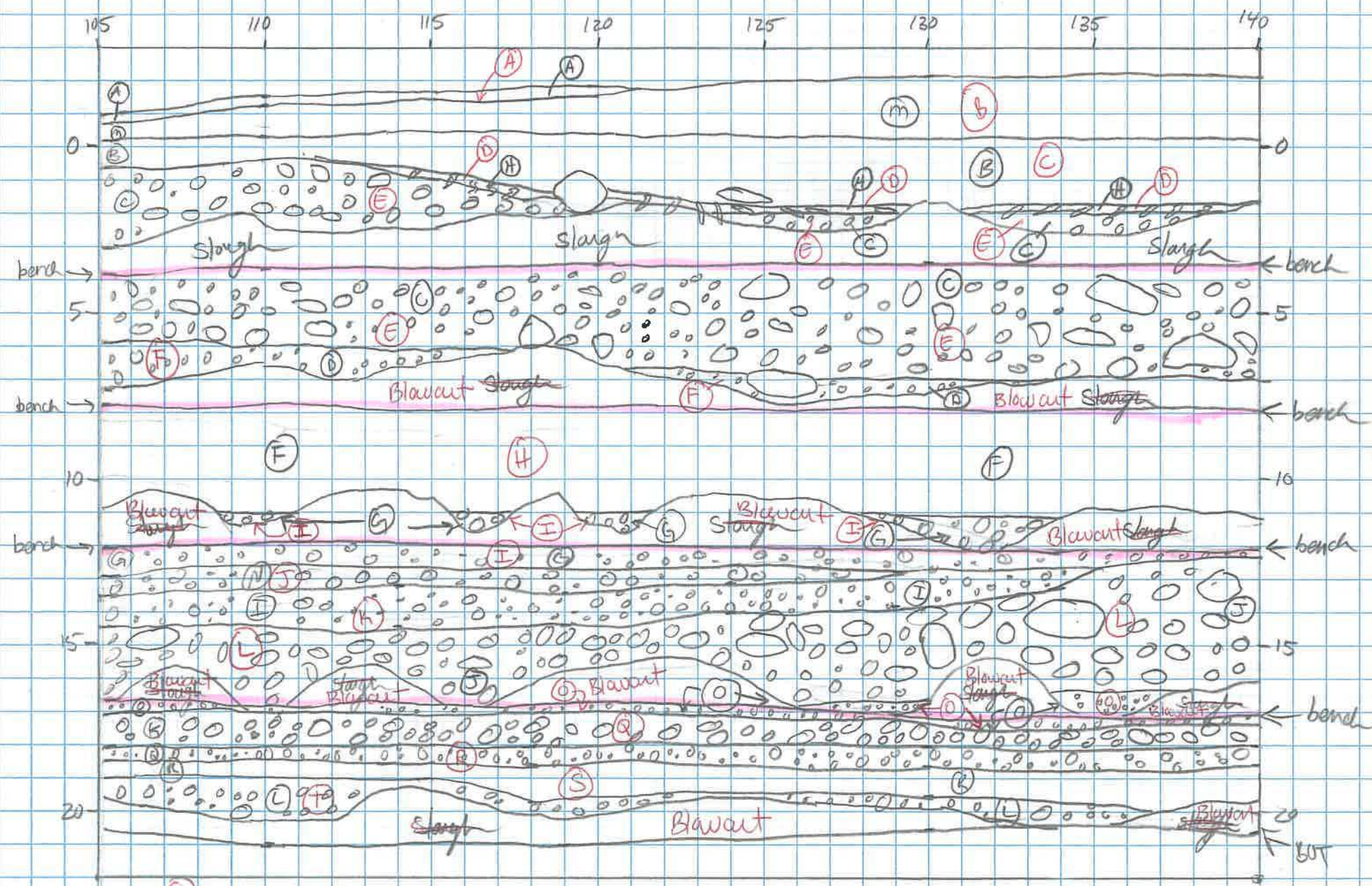
- (A) Top Soil / Turf Grass: (2.5Y, 5/2): Grayish Brown \$f\$-cs, som frf, loose-mst
- (B) FILL: (2.5Y, 5/2) Grayish Brown \$f\$-ms, Hcs, tr fGr, tr to lt frf, lt Fe₂O₃st., mottled, cemented, m. dense - dry
- (C) FILL: (2.5Y, 6/2) Light Brownish Gray Gr f-cs, tr to H\$, som. cobb., occ boulder, m. dense - dry
- (D) Qal: (2.5Y, 3/2) Very Dark Grayish Brown, \$fs\$, lt to som f-clr, lt to som cobb., lt to som frf, tr roots, loose to m. dense - damp
- (E) (2.5Y, 6/1) Gray fs, tr to lt m-cs, 2-inch Gravel lense, occ. cobb., dense - damp
- (F) (2.5Y, 6/1) Gray Gr f-cs, lt. cobb., dense - dry
- (G) (2.5Y, 6/2) Light Brownish Gray Gravelly f-cs, lt to som cobb., occ Boulder, dense - dry
- (H) (2.5Y, 6/2) ^{Light Brownish Gray} Grv f-cs, occ. cobb., dense - dry
- (I) (2.5Y, 6/2) Light Brownish Gray Cobb. f-cs, som f-clr, dense - dry
- (J) (2.5Y, 6/2) Light Brownish Gray Grv f-cs, tr to lt cobb., dense - dry
- (K) (2.5Y, 6/2) Light Brownish Gray fs, Hm-cs, tr to lt cobb., m. dense - dry to damp
- (L) (2.5Y, 6/2) Light Brownish Gray Grv f-cs, lt cobb., dense - dry
- (M) (2.5Y, 6/2) Light Brownish Gray Cobbley f-cs, dense - dry
- (N) (2.5Y, 6/2) Grv f-cs, tr to lt cobb., dense - dry
- (O) (2.5Y, 6/2) Light Brownish Gray Cobb. f-cs, som f-clr, occ. Boulder, sl. cemented, dense - dry
- (P) (2.5Y, 6/2) Light Brownish Gray f-cs, lt to som f-clr, tr to lt cobb., dense - dry

FT-1









(2.5Y, 6/2) Light brownish Gray, Grv F-cs, dense-dry

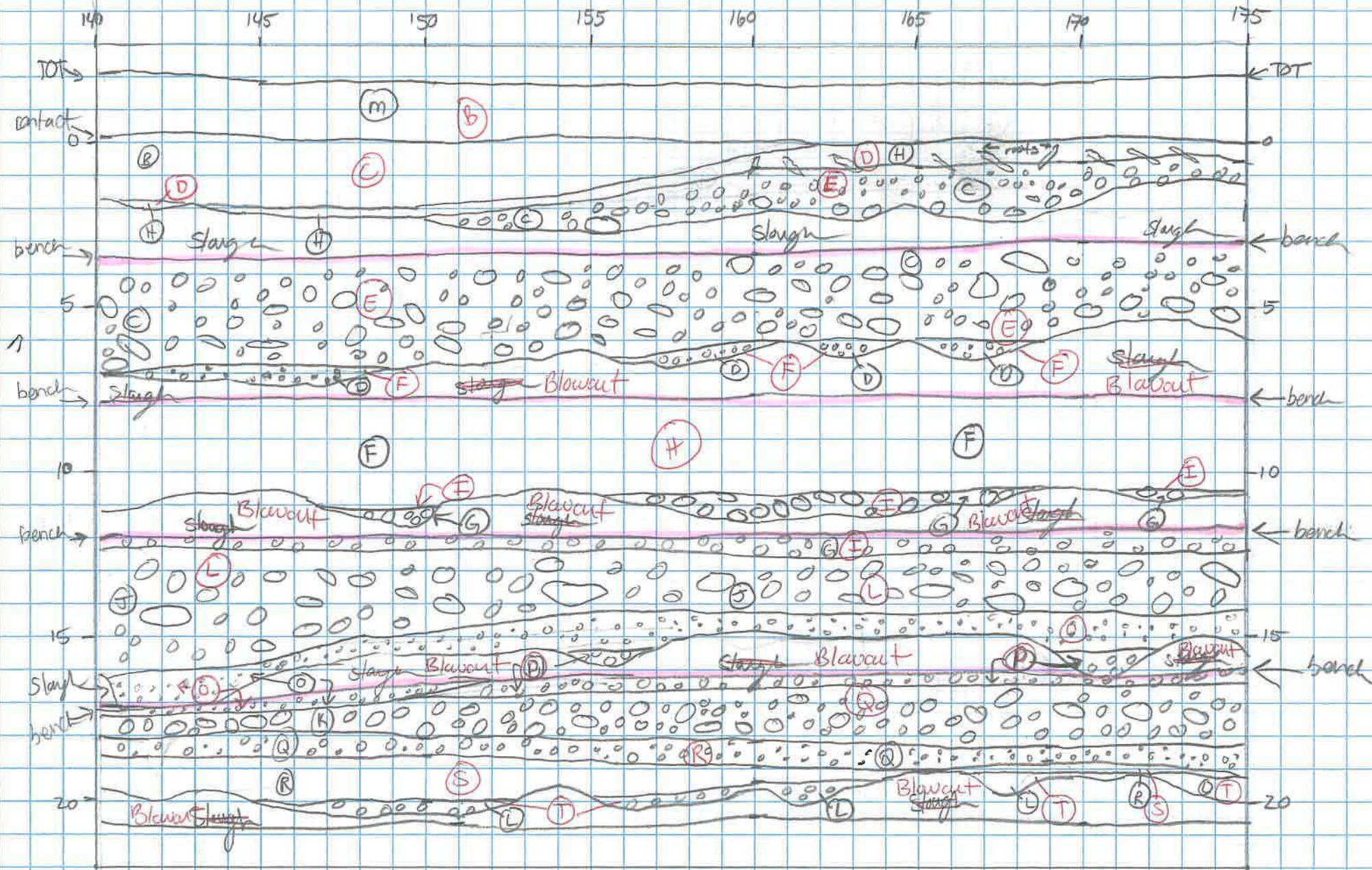
22G1144

FT-2

4/10/22

West Face

pg. 5 of 8



(P) (2.5, 6/2) Light Brownish Gray Grv fcs, 1 to 10 cbb. ^{trd} sl. cemented, dense-dry

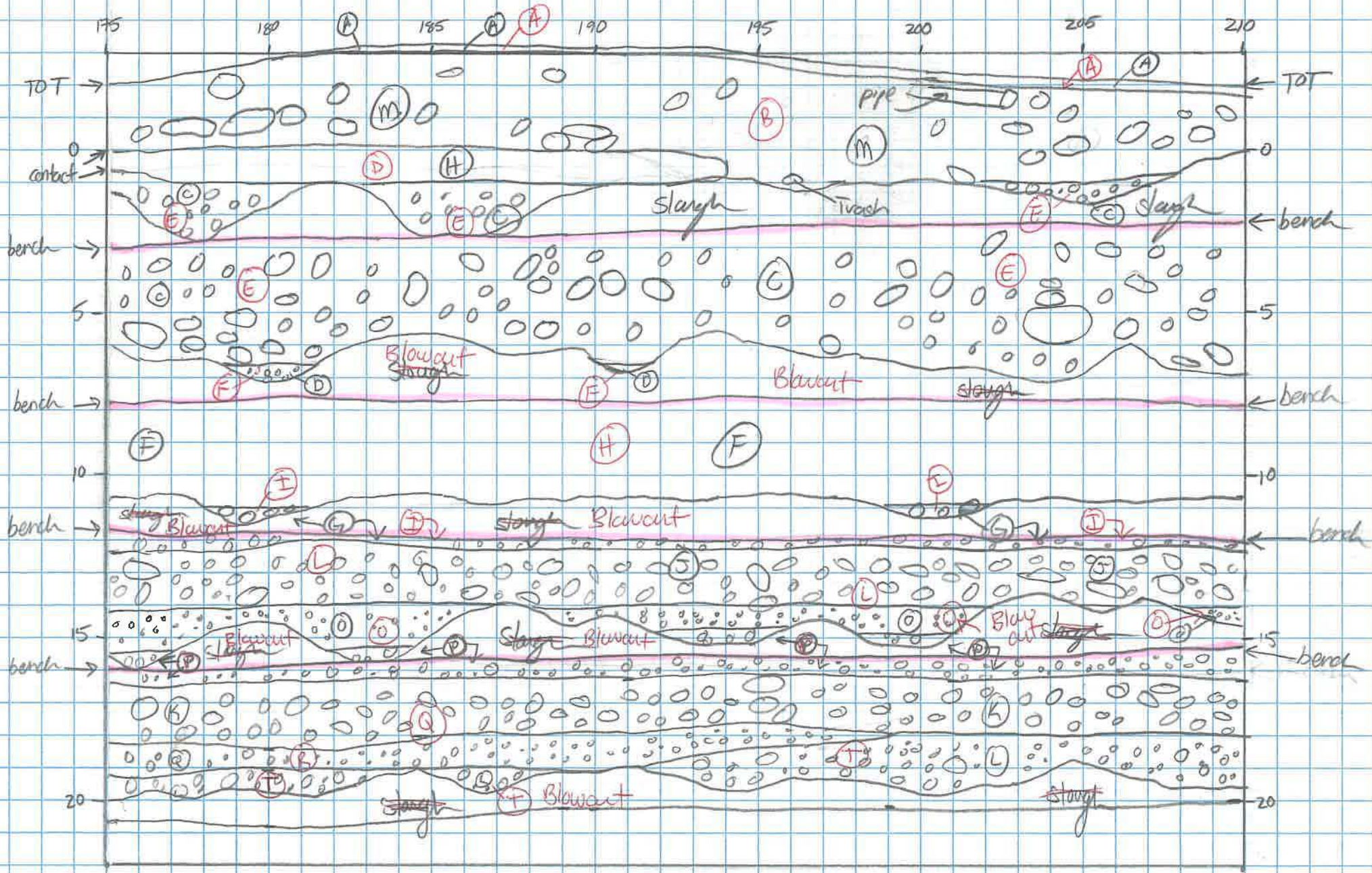
2267144

FT-2

4/12/22

West Face

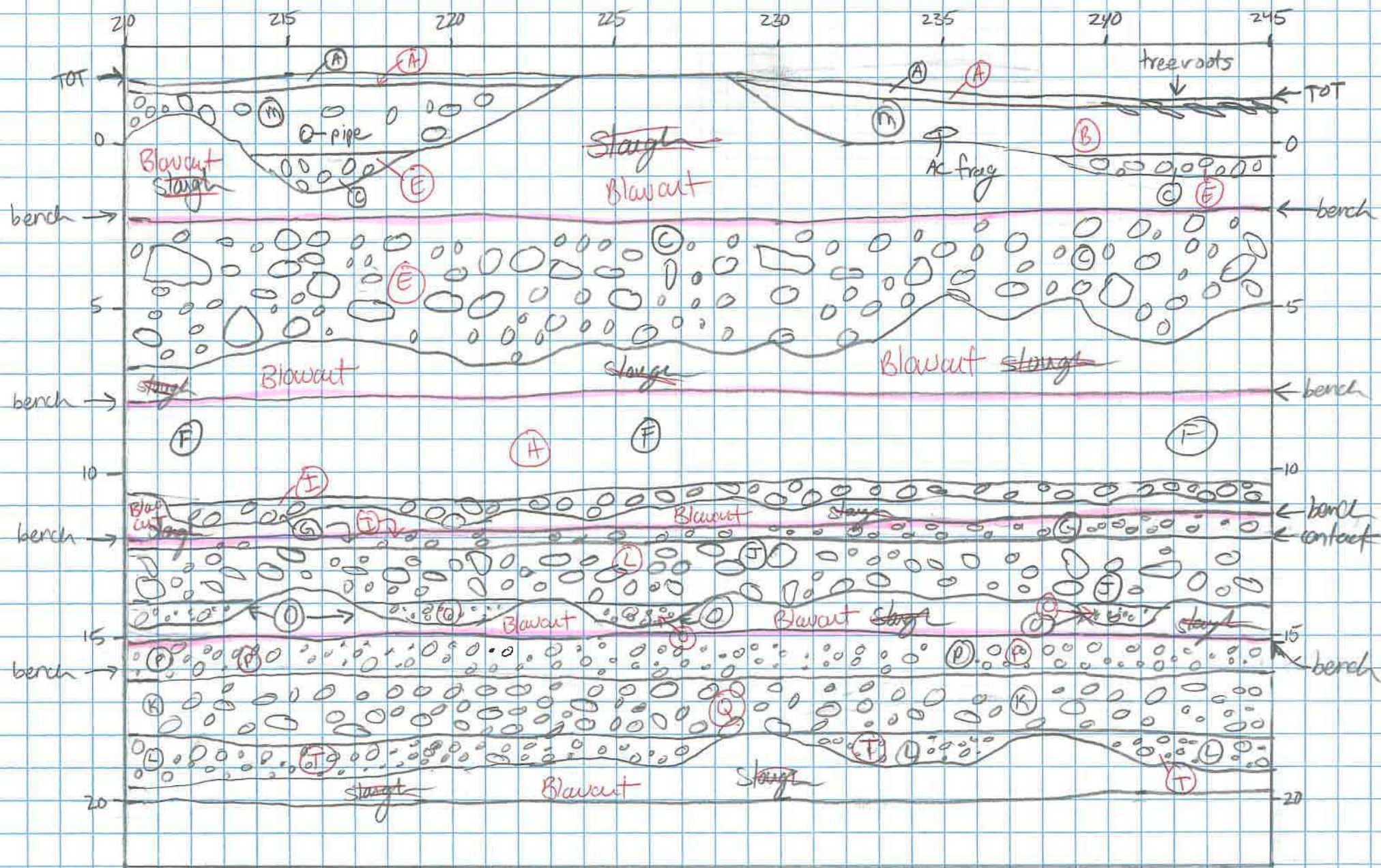
pg. 6 of 8



226144

FT-2

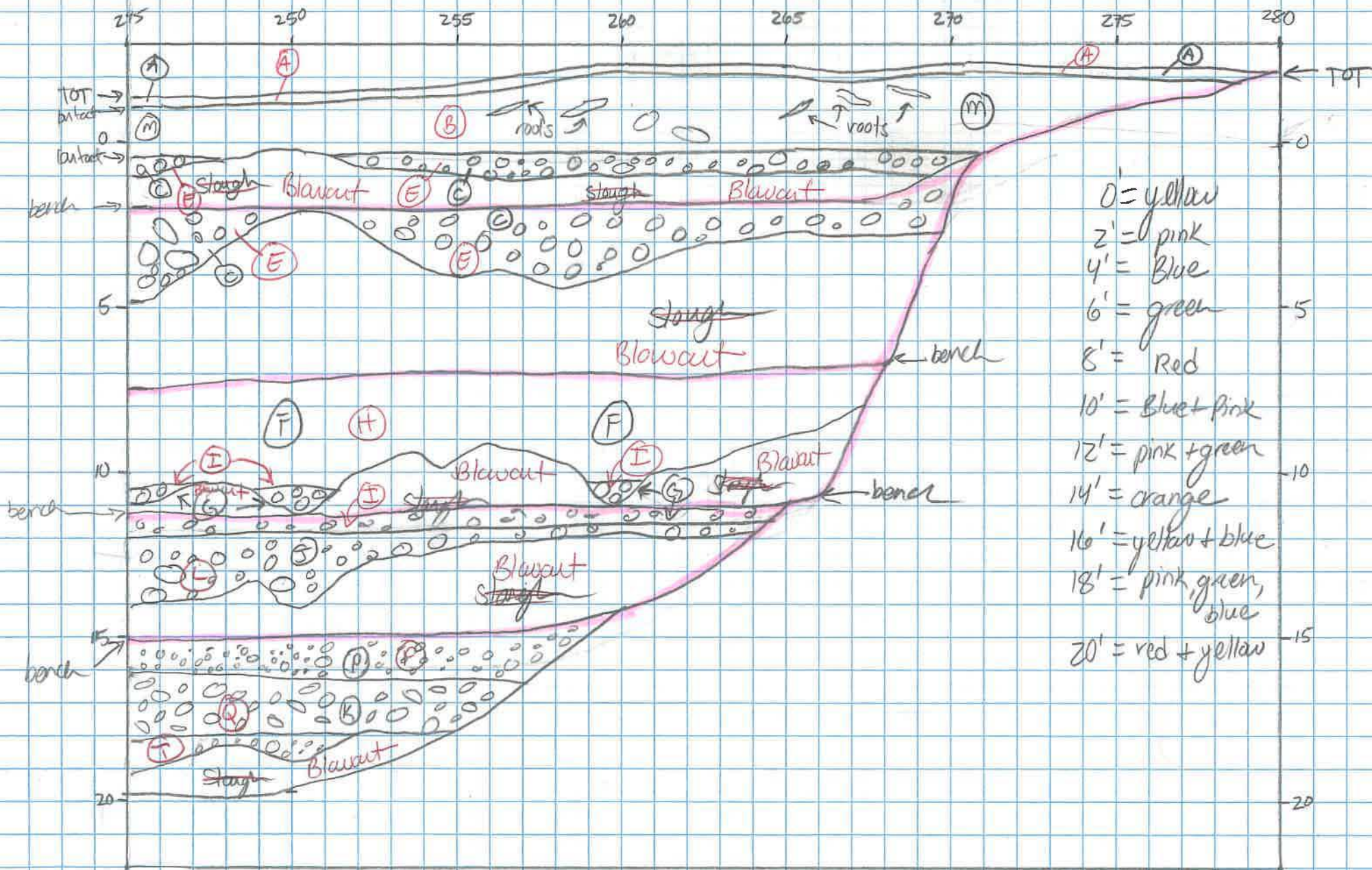
pg. 7 of 8

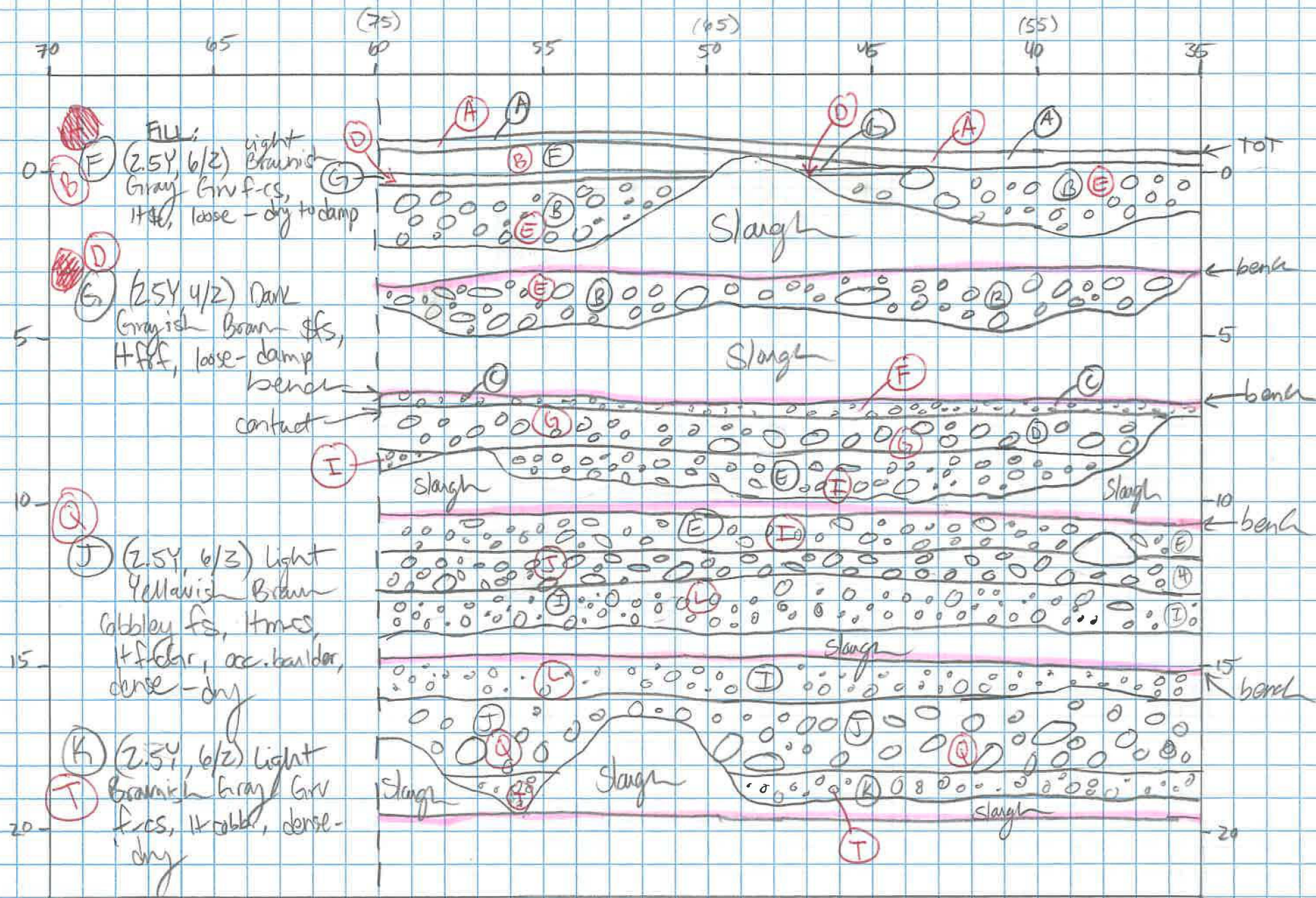


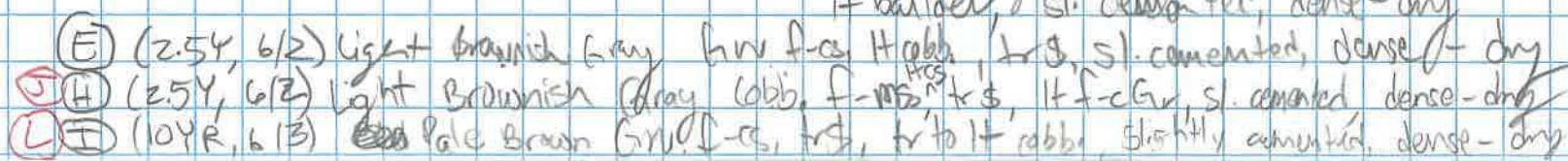
226144

FT-2 West Face

pg. 8 of 8







FT-2

- (A) Topsoil / Turf Grass: (10YR, 4/2) Dark Grayish Brown sfs, lt m-cs, tr f-clr, ext. ~~lt f-clr~~, loose-mst to trash, mottled
- (B) Fill: (2.5Y, 6/2) Light Brownish Gray f-cs, lt f-clr, lt cobb., occ. Boulder, loose-dry
- (C) Fill: (2.5Y, 6/2) Light Brownish Gray fs, tr to lt s, lt m-cs, lt f-clr, lt f-clr, loose-damp
- (D) Qal: (10YR, 4/3) Brown sfs, lt m-cs, lt to som f-clr, loose-damp
- (E) (2.5Y, 6/1) Gray Grv f-cs, lt to som cobb., occ. Boulder, dense-dry
- (F) (2.5Y, 6/2) Light Brownish Gray Grv f-cs, tr to lt cobb., dense-dry
- (G) (2.5Y, 6/2) Light Brownish Gray Cobb. fs, lt m-cs, lt f-clr, occ. Boulder, dense-dry
- (H) (2.5Y, 6/2) Interbedded Grv f-cs, Cobb. f-cs, and f-cs, tr s, sl. cemented, dense-dry
- (I) (2.5Y, 6/2) ~~Cobb.~~ Grv f-cs, ~~lt cobb.~~ tr s, sl. cemented, dense-dry
- (J) (10YR, 6/2) Light Brownish Gray Cobb. f-cs, tr s, lt to som f-clr, occ. Boulder, sl. cemented, dense-dry
- (K) (2.5Y, 6/2) Light Brownish Gray Grv f-cs, tr s, tr cobb., sl. cemented, dense-dry
- (L) (10YR, 6/3) Pale Brown Grv f-cs, lt to som Cobb., occ. Boulder, dense-dry
- (O) (2.5Y, 6/2) Light Brownish Gray Grv f-cs, dense-dry
- (P) (2.5Y, 6/2) Light Brownish Gray Grv f-cs, tr to lt cobb., tr s, sl. cemented, dense-dry
- (Q) (2.5Y, 6/2) Light Brownish Gray cobbly fs, ^{tr s} lt m-cs, lt f-clr, tr to lt Boulder, sl. cemented, dense-dry
- (R) (2.5Y, 6/2) Light Brownish Gray Grv f-cs, ^{tr s} lt Cobb., sl. cemented, dense-dry
- (S) (2.5Y, 6/2) Light Brownish Gray fs, tr m-cs, few f-cs lenses, dense-dry
- (T) (2.5Y, 6/2) Light Brownish Gray Grv f-cs, lt Cobb., dense-dry

APPENDIX



HISTORICAL PHOTOGRAPH - 1930	
PROPOSED WAREHOUSE DEVELOPMENT	
AZUSA, CALIFORNIA	
1" = 750'	 SOUTHERN CALIFORNIA GEOTECHNICAL
DRAWN: DRK	
CHKD: RGT	
SCG PROJECT 22G144-2	
PLATE C-1	



HISTORICAL PHOTOGRAPH - 1934	
PROPOSED WAREHOUSE DEVELOPMENT	
AZUSA, CALIFORNIA	
1" = 750'	 SOUTHERN CALIFORNIA GEOTECHNICAL
DRAWN: DRK	
CHKD: RGT	
SCG PROJECT 22G144-2	
PLATE C-2	



HISTORICAL PHOTOGRAPH - 1949

PROPOSED WAREHOUSE DEVELOPMENT

AZUSA, CALIFORNIA

1" = 1500'

DRAWN: DRK
CHKD: RGT

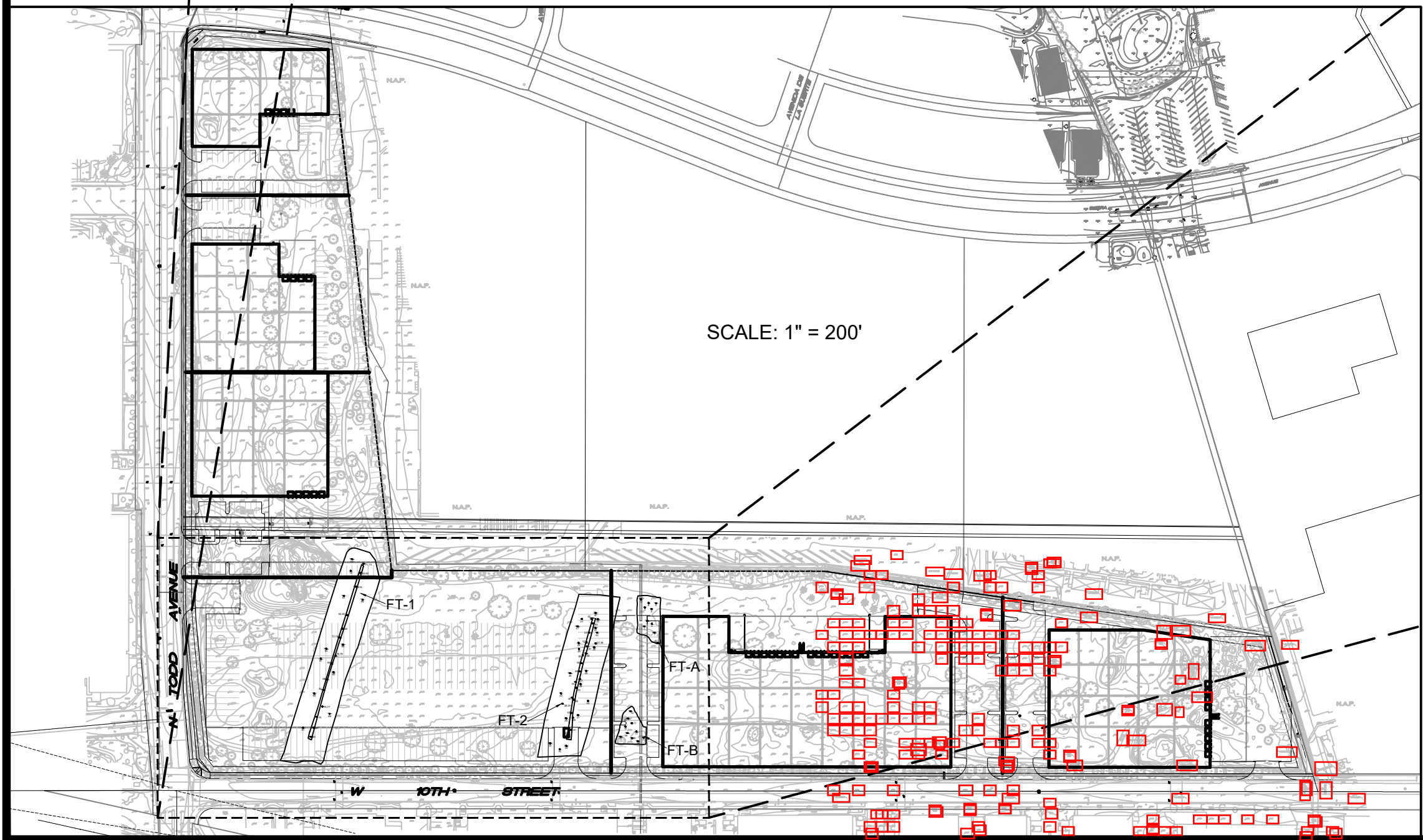
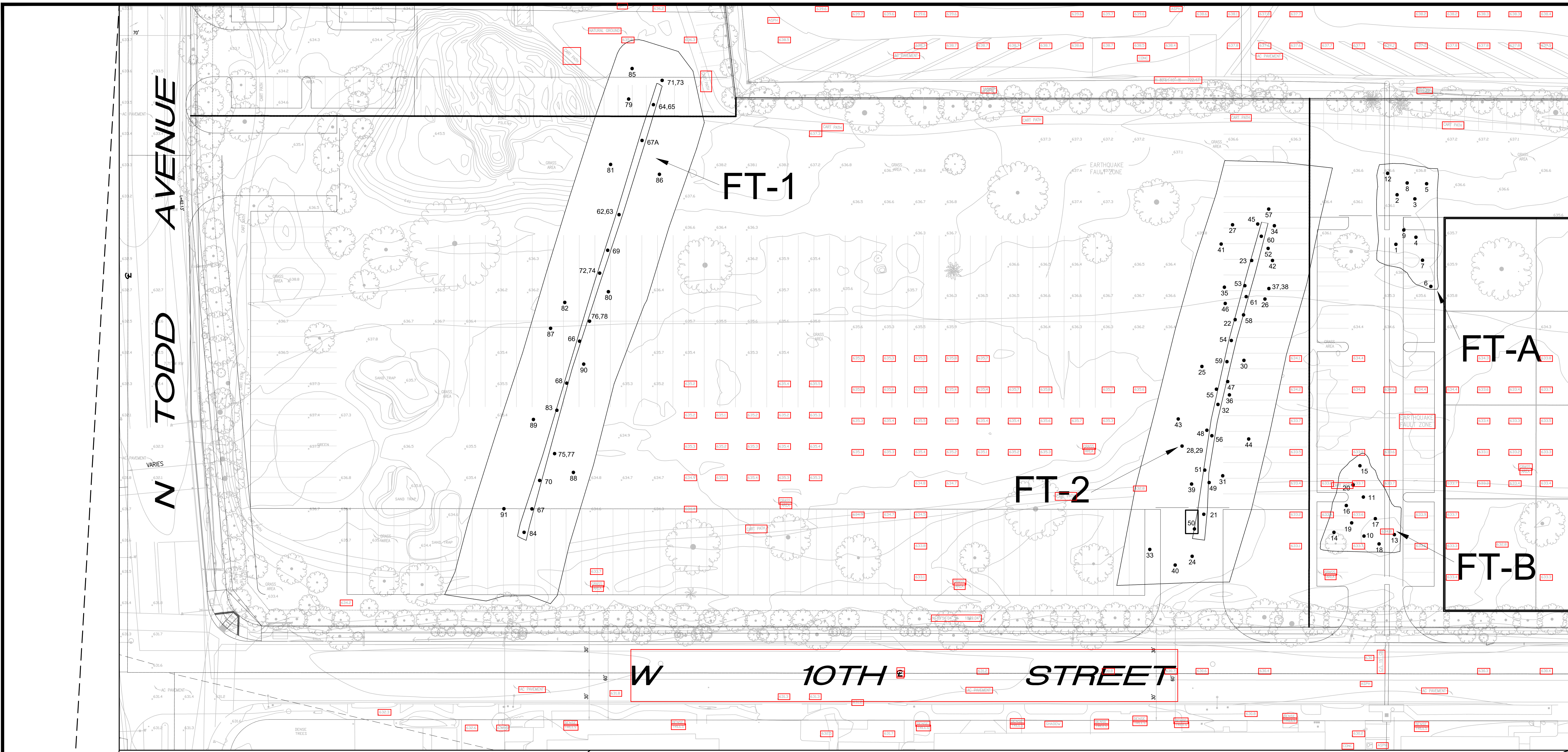
SCG PROJECT
22G144-2

PLATE C-3



**SOUTHERN
CALIFORNIA
GEOTECHNICAL**

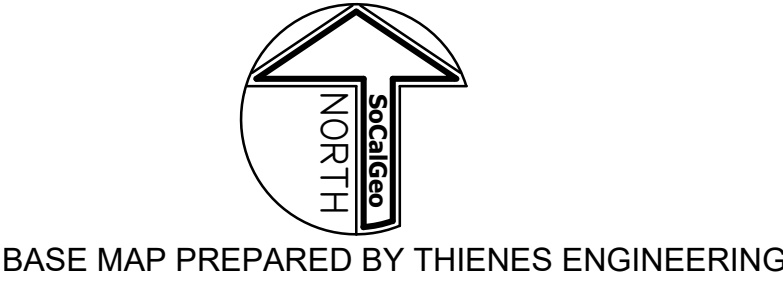
APPENDIX



GEOTECHNICAL LEGEND

● 100 APPROXIMATE LOCATION OF IN-PLACE DENSITY TEST

— APPROXIMATE FAULT TRENCH LOCATION



DENSITY TEST LOCATION PLAN
PROPOSED WAREHOUSE DEVELOPMENT
AZUSA, CALIFORNIA

PLATE

6

SCALE: 1" = 30'
DRAWN: JAH
CHKD: DK
SCG PROJECT
22G1442



SOUTHERN
CALIFORNIA
GEOTECHNICAL
A California Corporation

22885 Savi Ranch Parkway
Suite E
Yorba Linda, CA 92887
Phone: (714) 685-1115
Fax: (714) 685-1118
www.socalgeo.com

**TABLE 3
SUMMARY OF FIELD DENSITY TESTS**

Test No.	Date	Elev. (ft)	Test Location	Soil Type	Moisture Content (%)	Dry Density (pcf)	Relative Compaction (%)	Comments
1	03-May-22	-10.0	FT-A	A	10.8	122.6	90	
2	03-May-22	-8.0	FT-A	A	10.9	122.8	90	
3	03-May-22	-8.0	FT-A	A	10.7	123.9	91	
4	03-May-22	-6.0	FT-A	A	10.8	122.9	90	
5	03-May-22	-6.0	FT-A	A	10.6	124.3	91	SC
6	03-May-22	-4.0	FT-A	A	10.9	123.1	91	
7	03-May-22	-4.0	FT-A	A	10.7	122.8	90	
8	03-May-22	-2.0	FT-A	A	10.9	124.4	91	
9	03-May-22	-1.0	FT-A	A	10.8	124.2	91	
10	03-May-22	-10.0	FT-B	A	10.8	123.1	91	
11	03-May-22	-8.0	FT-B	A	10.7	123.4	91	
12	04-May-22	-1.0	FT-A	A	10.8	122.7	90	
13	04-May-22	-1.0	FT-A	B	8.7	129.5	91	
14	04-May-22	-1.0	FT-A	B	8.5	129.9	91	
15	04-May-22	-6.0	FT-B	B	8.8	128.3	90	
16	04-May-22	-6.0	FT-B	B	8.6	127.9	90	
17	04-May-22	-4.0	FT-B	B	8.9	128.1	90	SC
18	04-May-22	-2.0	FT-B	B	8.8	130.1	92	
19	04-May-22	-2.0	FT-B	B	8.6	127.9	90	
20	04-May-22	-1.0	FT-B	B	8.5	128.3	90	
21	04-May-22	-18.0	FT-2	B	8.7	128.1	90	
22	04-May-22	-18.0	FT-2	B	8.6	127.9	90	
23	05-May-22	-18.0	FT-2	B	8.7	128.1	90	
24	05-May-22	-16.0	FT-2	B	8.6	129.4	91	
25	05-May-22	-16.0	FT-2	B	8.9	128.2	90	SC
26	05-May-22	-16.0	FT-2	B	8.7	127.8	90	
27	05-May-22	-14.0	FT-2	B	8.8	129.6	91	
28	05-May-22	-14.0	FT-2	A	10.1	119.7	88	Fail: 90% Required
29	05-May-22	-14.0	FT-2	A	10.7	122.4	90	Retest #28
30	05-May-22	-14.0	FT-2	A	10.8	122.6	90	
31	05-May-22	-14.0	FT-2	B	8.8	127.8	90	
32	05-May-22	-12.0	FT-2	B	8.6	128.3	90	SC
33	05-May-22	-12.0	FT-2	B	8.9	128.1	90	
34	06-May-22	-12.0	FT-2	B	8.6	128.2	90	
35	06-May-22	-12.0	FT-2	B	8.6	128.1	90	
36	06-May-22	-10.0	FT-2	B	8.7	128.2	90	
37	06-May-22	-10.0	FT-2	A	8.9	121.1	89	Fail: 90% Required
38	06-May-22	-10.0	FT-2	A	9.7	122.3	90	Retest #37

**TABLE 3
SUMMARY OF FIELD DENSITY TESTS**

Test No.	Date	Elev. (ft)	Test Location	Soil Type	Moisture Content (%)	Dry Density (pcf)	Relative Compaction (%)	Comments
39	06-May-22	-10.0	FT-2	A	10.1	122.4	90	
40	06-May-22	-10.0	FT-2	A	10.4	123.9	91	SC
41	06-May-22	-8.0	FT-2	B	8.9	127.9	90	
42	06-May-22	-8.0	FT-2	B	8.7	129.4	91	
43	06-May-22	-8.0	FT-2	B	8.7	128.1	90	
44	06-May-22	-8.0	FT-2	B	8.8	128.2	90	
45	09-May-22	-7.0	FT-2	B	8.6	127.9	90	
46	09-May-22	-6.0	FT-2	B	8.9	128.3	90	
47	09-May-22	-5.0	FT-2	B	8.1	128.0	90	
48	09-May-22	-4.0	FT-2	A	9.6	122.5	90	SC
49	09-May-22	-3.0	FT-2	A	9.8	122.9	90	
50	09-May-22	-2.0	FT-2	A	10.3	122.6	90	
51	09-May-22	-3.0	FT-2	A	9.7	122.7	90	
52	10-May-22	-5.0	FT-2	B	8.6	128.1	90	
53	10-May-22	-4.0	FT-2	B	8.1	127.9	90	
54	10-May-22	-3.0	FT-2	B	8.2	128.0	90	
55	10-May-22	-2.0	FT-2	B	8.5	128.2	90	
56	10-May-22	-1.0	FT-2	B	8.8	127.9	90	
57	10-May-22	-3.0	FT-2	B	8.2	128.0	90	
58	10-May-22	-2.0	FT-2	A	9.9	122.7	90	SC
59	10-May-22	-1.0	FT-2	A	10.3	123.0	90	
60	11-May-22	-2.0	FT-2	A	9.6	122.9	90	
61	11-May-22	-1.0	FT-2	A	10.1	122.6	90	
62	11-May-22	-14.0	FT-1	A	9.7	120.1	88	Fail: 90% Required
63	11-May-22	-14.0	FT-1	A	9.8	122.3	90	Retest #62
64	11-May-22	-13.0	FT-1	B	5.0	120.3	85	Fail: 90% Required
65	11-May-22	-13.0	FT-1	B	7.9	128.3	90	Retest #64
66	11-May-22	-13.0	FT-1	B	7.8	128.4	90	
67	11-May-22	-14.0	FT-1	A	10.2	122.0	90	
67A	12-May-22	-12.0	FT-1	B	8.6	127.9	90	
68	12-May-22	-12.0	FT-1	B	8.9	128.5	90	SC
69	12-May-22	-10.0	FT-1	B	8.1	128.2	90	
70	12-May-22	-10.0	FT-1	B	8.5	127.8	90	
71	12-May-22	-8.0	FT-1	B	6.6	125.1	88	Fail: 90% Required
72	12-May-22	-8.0	FT-1	B	8.5	125.5	88	Fail: 90% Required
73	12-May-22	-8.0	FT-1	B	8.1	128.0	90	Retest #71
74	12-May-22	-8.0	FT-1	B	8.3	128.4	90	Retest #72
75	13-May-22	-8.0	FT-1	B	8.6	125.1	88	Fail: 90% Required

**TABLE 3
SUMMARY OF FIELD DENSITY TESTS**

Test No.	Date	Elev. (ft)	Test Location	Soil Type	Moisture Content (%)	Dry Density (pcf)	Relative Compaction (%)	Comments
76	13-May-22	-8.0	FT-1	B	8.1	125.4	88	Fail: 90% Required
77	13-May-22	-8.0	FT-1	B	7.9	128.1	90	Retest #75
78	13-May-22	-8.0	FT-1	B	7.8	127.8	90	Retest #76
79	13-May-22	-6.0	FT-1	A	9.6	123.1	91	
80	13-May-22	-6.0	FT-1	A	9.1	122.4	90	
81	13-May-22	-4.0	FT-1	A	9.4	122.9	90	
82	13-May-22	-2.0	FT-1	B	7.7	127.8	90	
83	13-May-22	-6.0	FT-1	B	7.5	128.5	90	SC
84	13-May-22	-5.0	FT-1	B	7.2	128.0	90	
85	16-May-22	-1.0	FT-1	B	7.6	127.1	90	
86	16-May-22	-2.0	FT-1	B	7.1	127.5	90	
87	16-May-22	-4.0	FT-1	B	7.5	127.2	90	
88	16-May-22	-4.0	FT-1	B	7.4	127.9	90	
89	16-May-22	-3.0	FT-1	B	7.9	128.2	90	
90	16-May-22	-2.0	FT-1	B	7.2	127.6	90	SC
91	16-May-22	-1.0	FT-1	B	7.9	127.3	90	

NOTES: Elevations Referenced To GPS Data Provided By Others
 Negative Elevations Referenced to SG
 SG = Finished Subgrade Elevation
 Retests Performed After Recomaction
 All Tests Performed By Nuclear Test Method (ASTM D-6938) Unless Otherwise Noted
 SC = Sand Cone Test Method (ASTM D-1556)

TABLE 4
SUMMARY OF MOISTURE-DENSITY RELATIONSHIPS

Soil Type	Soil Description	Maximum Dry Density (pcf)	Optimum Moisture (%)
A	Dark Brown Silty fine Sand, trace fine Gravel, extensive Cobbles	136.0	7.0
B	Brown Gravelly fine to coarse Sand, little to some Cobbles, occasional Boulders	142.0	5.0

Note: All Moisture-Density Relationships determined per ASTM D-1557 (Modified Proctor)

APPENDIX



GEOPHYSICAL SURVEY
PROPOSE WAREHOUSE DEVELOPMENT PROJECT
SEC TODD AND SIERRA MADRE AVENUES
CITY OF AZUSA, CALIFORNIA

Project No. 223808-1

May 11, 2022

Prepared for:

Southern California Geotechnical, Inc.
22885 E. Savi Ranch Parkway
Suite E
Yorba Linda, CA 92887

Southern California Geotechnical, Inc.
22885 E. Savi Ranch Parkway, Suite E
Yorba Linda, CA 92887

Attention: Mr. Daryl R. Kas, Project Geologist

Regarding: Geophysical Survey
Proposed Warehouse Development Project
SEC Todd and Sierra Madre Avenues
City of Azusa, California
SCG Project No. 22G144

INTRODUCTION

In accordance with your request, we have completed a geophysical survey using the seismic refraction and ground-penetrating radar methods within the above referenced site. We understand that since the site is located within the limits of a designated Earthquake Fault Zone associated with the Sierra Madre Fault Zone, non-invasive geophysical methods have been deemed appropriate to aid in evaluating the deeper subsurface lithologic characteristics and geological structure. This report will describe in detail the seismic refraction methodology, field procedures used, data processing of the various seismic modeling programs utilized, and the results of this survey, along with the representative seismic models being presented within Appendices A and B for visual and reference purposes. As authorized by you, the following services were performed during this study:

- **Review of available pertinent published and unpublished geologic and geophysical data in our files pertaining to the site, along with a field reconnaissance.**
- **Conducting a geophysical survey using the ground-penetrating radar (GPR) and seismic refraction methods, that were performed by a licensed State of California Professional Geophysicist.**
- **Preparation of representative geophysical profiles for both survey methods displaying the modeled subsurface geologic structure.**
- **Preparation of this report, presenting the results of our interpretation of the geophysical data with respect to any possible anomalous structural feature(s) that may be suggestive of subsurface faulting at depth.**

Accompanying Maps, Illustrations, and Appendices

- Plate 1 - Google™ Earth Imagery Map
- Plate 2 - Geophysical Survey Map
- Plates 3 & 4 - Survey Line Photographs
- Appendix A - Seismic Refraction Survey
- Appendix B - Ground-Penetrating Radar Survey
- Appendix C - References

PROJECT SUMMARY

As requested, we have performed geophysical surveys along selected portions of the subject property, which is located at the northeast corner of Todd Avenue and 10th Street, in the City of Azusa, California. The subject site is an “L” shaped parcel comprising 19.22± acres in size and is proposed for construction of six warehouse buildings that range from 33,560 to 114,540± square feet in dimension. Locally, the proposed development occupies a portion of the golf course associated with the Azusa Greens County Club. At the time of our field survey there were two exploratory trenches open, which were approximately 20± feet deep each. The purpose of this geophysical study was to provide both a qualitative and quantified geophysical analysis of the subsurface geologic structure, in order to discern and any anomalous geologic structures that may be related to faulting beneath the subject site locally.

The location of our geophysical survey lines were performed along the bottom of both existing exploratory trenches (SCG Trench Nos. FT-1 and FT-2), as shown on Plates 1 and 2. Representative photographs of these lines are presented on Plates 3 and 4 for visual and reference purposes. From a geologic standpoint, the subject site has been mapped by Morton (1973) to be superficially mantled by Holocene age alluvium of the San Gabriel River Fan, in turn underlain by progressively older aged alluvial deposits.

GEOPHYSICAL SURVEYS

To aid in evaluating subsurface lithology and structure, geophysical surveys were performed using the seismic refraction and ground-penetrating radar (GPR) methods. The purpose of these surveys was to aid in obtaining deeper subsurface information that was not able to be conventionally observed by trenching. While the use of geophysical methods alone cannot determine the presence or absence of faulting, it does provide supporting data that can be used for analysis and interpretation. Both of these geophysical methods are summarized below with a more detailed description of the methodology, field procedures, and data reduction for both the seismic refraction and GPR surveys, being provided within Appendix A and B respectively, along with the accompanying pertinent survey data.

Seismic Refraction Survey

The primary purpose of the seismic refraction survey was to identify if there is offset stratigraphy or lateral velocity contrasts that would be suggestive of structural discontinuities and/or faulting at depth. This survey line was performed along the bottom of your Fault Trench FT-1, at a depth of 20± feet below the existing ground surface (bgs), corresponding to your trench stationing of 0+50 to 3+50. The seismic refraction method is well suited to identify these types of subsurface structural features. The raw field data was considered to be of good quality with little ambient “noise” being introduced during our survey. Analysis of the data and selection of the primary “P”-wave arrivals was therefore performed with very little difficulty.

Two methods of analysis were performed for the seismic survey. The first method uses the traditional approach of creating velocity layers (Layer Velocity Model, see Appendix A). This method allows for identification of boundary contacts, which are typically identifiable between varying lithologic and/or geologic units, including saturated sediments. The layer velocities also provide an estimation of the relative sediment ages and earth material types. The second method involved using tomographic imaging (Refraction Tomographic Model, See Appendix A) to visualize the relative structure and velocity distribution of the subsurface sediments. This method is sensitive to both vertical and lateral velocity differentials (such as would be expected with faulting at depth) and does not identify layer boundaries due to the gradient nature of the inversion software.

The “Layer Velocity Model” for Seismic Line S-1 indicated the presence of three distinct velocity layers. The upper lower velocity layer V1 (2,551 feet/second) appears to be comprised of recent (late to middle Holocene age) unconsolidated alluvial fan deposits, such as exposed along the bottom of the exploratory trench excavation. This velocity is typical for near surface, younger unconsolidated to slightly-consolidated alluvial sediments. The middle V2 velocity layer appears to be comprised of denser and more indurated, probable older alluvial fan deposits. This somewhat higher velocity of 3,632 feet/second is most likely associated with early Holocene to late Pleistocene age sediments. The deeper V3 velocity layer, with a velocity of 5,249 feet/second, appears to be very well-consolidated and indurated, consistent with that of Pleistocene age earth materials.

The Refraction Tomographic Model for Seismic Line S-1 revealed two generally parallel anomalous features suggestive of faulting, both of which appear to dip towards the north at relatively low angles. The possible fault anomaly shown on the lower left-hand portion of the model would project beyond the site boundaries to the south. The anomaly in the upper right-hand portion of the model projects upwards towards Station 2+30± along the bottom of the trench. Due to the anomaly being close to the northern end of the trench, the imaging is not able to capture much detail in this area at depth due to the ray-path waves that diverge towards the middle of the survey line, creating an overall “U”-shaped model, with minimal data at the survey line ends. However, there is some observable evidence to suggest that thrust faulting may be present locally, which includes the relatively higher velocity material near the surface of the profile on the north (upper) side, along with the lower velocity zone at the base of the northerly dipping anomaly (approximately around Station 3+30 at a relative depth of -15 feet).

Ground-Penetrating Radar Survey

The GPR survey consisted of performing one survey traverse along the bottom of each of the exploratory trenches FT-1 and FT-2, which were scanned at a depth of 20± feet below the existing ground surface (see Survey Line Photographs, Plate 3). Due to the amount and large size of the cobbles present, both trenches were prepared by clearing the rocks from the bottom of the trenches to provide a relatively smooth surface for

scanning purposes. This enabled the antenna to stay directly coupled to the ground surface for the most part. The antenna occasionally encountered small cobbles protruding from the bottom of the trench causing the antenna to bump or stop, creating occasional artifacts in the data, as described further in this report. An estimated penetration of up to 20 to 25± feet below the bottom of the exploratory trenches was obtained, which resulted in imaging of the subsurface stratigraphy to an overall depth of approximately 40 to 45± feet below the existing ground surface.

The GPR survey lines (GPR-1 and GPR-2) performed for each exploratory trench are presented within Appendix B and consist of the processed profile images along with annotated images denoting both natural and anomalous features for visual and reference purposes. The distance stationing for both survey lines reflect the corresponding horizontal stationing for exploratory trenches FT-1 and FT-2. Both survey lines indicate typical fluvial sedimentation that would be expected within an alluvial fan such as sheet- and mud-flow deposits, scour and channeling, cross-bedding, etc. Some of the features discussed below have been annotated on the survey line images as presented within Appendix B.

➤ **Survey Line GPR-1**

Survey line GPR-1 consisted of scanning a total of 300-feet in length along the relatively flat bottom of your Exploratory Trench FT-1 (see GPR photograph on Plate 3), along a south to north direction. Due to the sloped ends of the trench, it was only possible to scan along the trench bottom between Stationing 0+50 to 3+50.

Survey Line GPR-1 appears to consist of very gently sloping bedding planes inclined overall towards the south, essentially mirroring the ground surface. These deposits most likely consist of interbedded sand, sand and gravel, and cobbly sand, such as observed along the exposed trench walls. Although somewhat discontinuous locally, at a depth of around 8- to 10±-feet there appears to be a potential lithologic change and/or a higher moisture layer where there is a noticeable change in the reflection amplitude (brighter color bands). This interface appears to be somewhat coincident with the V1/V2 velocity boundary as discussed for Seismic Line S-1.

Most notable is the anomalous feature that occurs between stationing 2+50 to 3+00, which has a northerly dip of around 15 to 20 degrees to the north. This very prominent feature may be related to low-angle thrust faulting which terminates at a depth of approximately 8-10± feet below the bottom of the trench (-30±' bgs). This anomalous feature does not appear to be indicative of other types of sedimentary processes and/or structures that would be found within a southerly dipping alluvial fan complex. Although not as prominent, there is another potential anomalous feature that may represent a fault structure found between stationing 3+13 to 3+50. This anomaly also dips towards the north at a low angle, generally mirroring the major anomaly to the south. This could also be interpreted as back-tilting of the sedimentary bedding caused by thrust faulting.

It should be noted that this survey traverse was collected using three 100-foot-long individual lines, 20± feet deep, that were post-processed and combined to create one continuous profile image for this report. Therefore, the slight vertical aberrations occurring at Stations 1+50 and 2+50 are caused by stopping and starting of the individual lines and the post-processing procedures used, and do not represent any geological features of interest. The vertical irregular features, such as imaged along Stations 0+56 and 1+90± for example, are artificial artifacts that are created when the antenna or survey wheel hits a rock, gets hung-up, and/or when the antenna slightly uncouples with the ground due to uneven terrain, causing multiple ringing high amplitude reflections from the trench bottom. The GPR-1 image presented within Appendix B includes an annotated model along with the original image for comparison of subsurface features.

➤ **Survey Line GPR-2**

Survey line GPR-2 consisted of scanning a total of 200-feet in length along the relatively flat bottom of Exploratory Trench FT-2 (see GPR photograph on Plate 3), along a south to north direction. This survey line was extended to a depth of 25± feet in order to see if deeper scanning would provide more information at depth, however, the radar returns were diminishing at depths greater than 20± feet. Due to the sloped ends of the trench, it was only possible to scan between Stations 0+50 to 2+50. Similar sedimentary features and structures are present within this image such as discussed for GPR-1.

However, most notable are the two prominent north dipping low-angle anomalies that occur between Stations 0+90 to 1+40 and 1+52 to 2+05. Both anomalies appear to terminate at approximately 10± feet below the bottom of the trench (corresponding to 30±' bgs) along an apparent lithologic boundary such as noted within GPR-1. The higher amplitude reflections noted along the northern anomaly (Stations 1+52 to 2+05) is suggestive of localized higher moisture content. Since the site is located along an existing golf course where the sediments are very permeable, it is possible that watering over the years has created localized areas of higher moisture. The GPR-2 image presented within Appendix B includes an annotated model along with the original image for comparison of subsurface features.

SUMMARY OF FINDINGS

The subject geophysical surveys, utilizing the seismic refraction and ground-penetrating radar methods for this project, proved to be a practical, non-destructive, and economical way to aid in evaluating if there are any anomalous features possibly associated with subsurface faulting. Based on the data obtained from the seismic refraction survey (see Appendix A) with respect to the Layer Velocity Model, there appears to be three distinct velocity layers, interpreted to be alluvial sedimentary units representing various ages and induration. These three units range from relatively recent deposits (late Holocene)

to possible Pleistocene age deposits at depth. The Refraction Tomographic Model revealed two localized low-angle velocity and structural differentials that are suggestive of thrust-type faulting. The deeper southerly anomaly appears to extrapolate upwards south of the subject property. The localized relatively higher seismic velocity zone found near the surface of the model between Stations 0+70 to 0+80 is believed to be caused by a relatively higher concentration of large boulders just beneath the trench bottom.

The GPR survey suggests that the subsurface below the bottom of the exploratory trench (corresponding to a beginning depth of $20\pm$ feet below the original ground surface) consists of relatively planar and slightly undulating stratigraphic alluvial sedimentation and fluvial morphology. Within your exploratory trench FT-1, both the seismic and GPR survey traverses (S-1 and GPR-1, respectively) indicate an anomalous feature suggestive of thrust-type faulting. Both the seismic and GPR models indicate this anomaly to extrapolate to the bottom of the exploratory trench at a station of around $2+30\pm$. The seismic model is not as high-resolution as the GPR data and therefore, is harder to trace and accurately denote. However, the GPR data has very high-resolution imaging and clearly the anomaly terminates around $8-10\pm$ feet below the bottom of the trench, which roughly coincides with the velocity layer boundary observed on the seismic Layer Velocity Model S-1. It is possible that there is another low-angle northerly dipping anomaly located between stationing $2+10$ to $3+00$ that is suggestive of a fault-related feature. This feature is not as well defined as the southern anomaly and may be related to back-tilting of the sediments.

Within your exploratory trench FT-2, the GPR-2 survey traverse indicates two anomalous features, both suggestive of thrust-type faulting, which were found to be generally parallel to each other with the same low-angle northerly dip, as expressed within GPR-1. These two features also appear to terminate within $8-10\pm$ feet of the bottom of the trench. Based on the correlation of the seismic and GPR data within exploratory trench FT-1 and the corroborating GPR data observed with exploratory trench FT-2, these anomalous features are believed to be related to a low-angle thrust-type fault and appear to be locally continuous.

CLOSURE

The field surveys were performed by the undersigned on April 5 and 9, 2022 using "state of the art" geophysical equipment and techniques along the selected locations of the seismic and GPR traverses. **Terra Geosciences** uses standard engineering geophysical practices and equipment.

The seismic data was evaluated using various seismic inversion computer programs, including using recently developed tomographic inversion techniques to provide a more thorough analysis and understanding of the subsurface structural conditions. It is important to understand that the fundamental limitation for seismic refraction surveys is

known as nonuniqueness, wherein a specific seismic refraction data set does not provide sufficient information to determine a single “true” earth model. Therefore, the interpretation of any seismic data set uses “best-fit” approximations along with the geologic models that appear to be most reasonable for the local area being surveyed. It should be noted that estimates of the layer velocity boundaries are generally considered to be within $10\pm$ percent of the total depth of the contact. The GPR data results reflect only the subsurface conditions that existed at the time of our field survey and could change with time.

Client should also understand that when using the theoretical geophysical principles and techniques discussed in this report for both survey methods, sources of error are possible in both the data obtained and, in the interpretation and that the results of this survey may not represent actual subsurface conditions. These are all factors beyond **Terra Geosciences** control and no guarantees as to the results of this survey can be made. We make no warranty, either expressed or implied. If the client does not understand the limitations of this geophysical survey, additional input should be sought from the consultant.

It is expected that the client understands that the subsurface geology, object size and composition, depth, and surface interference are all major factors regarding whether a target will be detected by surface geophysical methods. These are all factors beyond the control of **Terra Geosciences**, and no guarantees of the results of this survey can be made.

This opportunity to be of service is sincerely appreciated. If you should have any questions regarding this report or do not understand the limitations of this study or the data that is presented, please do not hesitate to contact our office at your earliest convenience.

Respectfully submitted,
TERRA GEOSCIENCES



Donn C. Schwartzkopf
Professional Geophysicist
PGP 1002



GOOGLE™ EARTH IMAGERY MAP



Base Map: Google™ Earth imagery (2022); Seismic survey line (S-1) shown as yellow line, GPR survey line (GPR-1 & GPR-2) shown as red lines.

GEOPHYSICAL SURVEY MAP



Base Map: Provided by client; Seismic survey line (S-1) shown as blue line, GPR survey lines GPR-1 & GPR-2 shown as red lines.

SURVEY LINE PHOTOGRAPHS



View looking northerly along Ground-Penetrating Radar survey line GPR-1.



View looking northerly along Ground Penetrating Radar Line GPR-2.

SURVEY LINE PHOTOGRAPHS



View looking southerly along Seismic Line S-1.



View looking northerly along Seismic Line S-1.

APPENDIX A

SEISMIC REFRACTION SURVEY



SEISMIC REFRACTION SURVEY

Methodology

The seismic refraction method is well suited to identify whether there is a distinct velocity change at depth which could represent a possible subsurface structural differential. The seismic refraction method consists of measuring (at known points along the surface of the ground) the travel times of compressional waves generated by an impulsive energy source and can be used to estimate the layering, structure, and seismic acoustic velocities of subsurface horizons. Seismic waves travel down and through the soils and rocks, and when the wave encounters a contact between two earth materials having different velocities, some of the wave's energy travels along the contact at the velocity of the lower layer.

The fundamental assumption is that each successively deeper layer has a velocity greater than the layer immediately above it. As the wave travels along the contact, some of the wave's energy is refracted toward the surface where it is detected by a series of motion-sensitive transducers (geophones). The arrival time of the seismic wave at each of the geophone locations can be related to the relative seismic velocities of the subsurface layers in feet per second (fps), which can then be used to aid in interpreting both the depth and type of materials encountered.

Field Procedures

One seismic refraction line was performed (Seismic Line S-1) along the bottom of Exploratory Trench FT-1, as shown on Plates 1 and 2, which was located by the client. Seismic Lines S-1 was 300 feet in length which consisted of a series of twenty-four, 40-Hertz geophones, that were spaced at regular 12-foot centers. The survey line length was based on the maximum available length along the bottom of the trench (see Survey Line Photographs, Plate 4) in order to maximize the subsurface imaging depth that was obtainable.

To produce the necessary seismic wave energy, a 16-pound sledge-hammer was used as the energy source to generate both the direct and refracted waves. Fourteen shot points were utilized using forward, reverse, and intermediate locations in order to obtain high resolution survey data for velocity analysis and depth modeling purposes. Each shot point used multiple hammer impacts to increase the signal to noise ratio, which provided clearer first "P"-Wave arrivals while canceling out the background noise.

The seismic wave arrivals were digitally recorded in SEG-2 format on a Geometrics StrataVisor™ NZXP model signal enhancement refraction seismograph. The data was acquired using a sampling rate of 0.0625 milliseconds having a record length of 0.10 seconds with no acquisition filters used in order to preserve the raw wave-forms. The data on the display screen were used to analyze the arrival time of the primary seismic "P"-Waves at each geophone station for quality control purposes in the field. Each geophone and seismic shot location were surveyed using a hand level and ruler for topographic correction, with "0" being the lowest point along the survey line.

Data Processing

The recorded seismic data was subsequently transferred to our office computer for processing and analyzing purposes, using the computer programs **SIPwin** (Seismic Refraction Interpretation Program for Windows) developed by Rimrock Geophysics, Inc. (2004); **Refractor** (Geogiga, 2001-2020); and **Rayfract**[™] (Intelligent Resources, Inc., 1996-2022). All of the computer programs perform their individual analyses using exactly the same input data, which includes the first-arrival times of the “P”-waves and the survey line geometry.

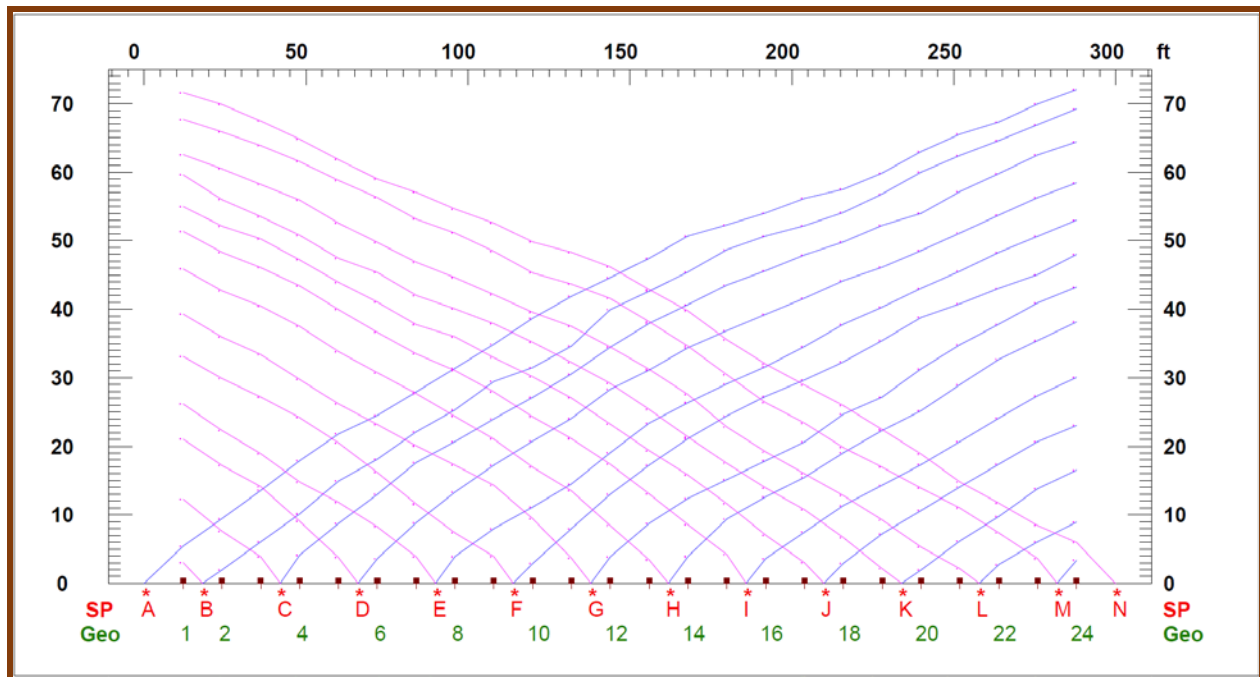
- **SIPwin** is a ray-trace modeling program that evaluates the subsurface using layer assignments based on time-distance curves and is better suited for layered media, using the “Seismic Refraction Modeling by Computer” method (Scott, 1973). The first step in the modeling procedure is to compute layer velocities by least-squares techniques. Then the program uses the delay-time method to estimate depths to the top of layer-2. A forward modeling routine traces rays from the shot points to each geophone that received a first-arrival ray refracted along the top of layer-2. The travel time of each such ray is compared with the travel time recorded in the field by the seismic system. The program then adjusts the layer-2 depths so as to minimize discrepancies between the computed ray-trace travel times and the first arrival times picked from the seismic waveform record. The process of ray tracing and model adjustment is repeated a total of six times to improve the accuracy of depths to the top of layer-2. This first-arrival picks were then used to generate the Layer Velocity Models using the **SIPwin** computer program, which presents the subsurface velocities as individual layers and are presented within Appendix A for reference. In addition, the associated Time-Distance Plot for the survey line, which shows the individual data picks of the first “P-wave” arrival times, also appears in Appendix A.
- **Refractor** is seismic refraction software that also evaluates the subsurface using layer assignments utilizing interactive and interchangeable analytical methods that include the Delay-Time method, the Plus-Minus method, and the Generalized Reciprocal Method (GRM). These methods are used for defining irregular non-planar refractors and are briefly described below.
 - The Delay-Time method will measure the delay time depth to a refractor beneath each geophone rather than at shot points. Delay-time is the time spent by a wave to travel up or down through the layer (slant path) compared to the time the wave would spend if traveling along the projection of the slant path on the refractor.
 - The Plus-Minus time analysis method includes a Plus time analysis for depth analysis and a Minus time analysis for velocity determination. The basis of the Plus-Minus time analysis method lies in the traveltimes reciprocity, i.e., the traveltimes of a seismic wave from source to receiver is equal to the traveltimes in the opposite direction if source and receiver are interchanged. It can be used to calculate the depth and velocity variations of an undulating layer boundary for slope angles less than $\sim 10^\circ$.

- The GRM method is a technique for delineating undulating refractors at any depth from in-line seismic refraction data consisting of forward and reverse travel-times and is capable of resolving dips of up to 20% and does not over-smooth or average the subsurface refracting layers. In addition, the technique provides an approach for recognizing and compensating for hidden layer conditions.
- **Rayfract™** is seismic refraction tomography software that models subsurface refraction, transmission, and diffraction of acoustic waves which generally indicates the relative structure and velocity distribution of the subsurface using first break energy propagation modeling. An initial 1D gradient model is created using the DeltatV method (Gebrande and Miller, 1985) which gives a good initial fit between modeled and picked first breaks. The DeltatV method is a turning-ray inversion method which delivers continuous depth vs. velocity profiles for all profile stations. These profiles consist of horizontal inline offset, depth, and velocity triples. The method handles real-life geological conditions such as velocity gradients, linear increasing of velocity with depth, velocity inversions, pinched-out layers and outcrops, and faults and local velocity anomalies. This initial model is then refined automatically with a true 2D WET (Wavepath Eikonal Traveltime) tomographic inversion (Schuster and Quintus-Bosz, 1993).

WET tomography models multiple signal propagation wave-paths contributing to one first break, whereas conventional ray tracing tomography is limited to the modeling of just one ray per first break. This computer program performs the analysis by using the same first-arrival P-wave times and survey line geometry that were generated during the layer velocity model analyses. The associated Refraction Tomographic Model, which display the subsurface earth material velocity structure, is represented by the velocity contours (isolines displayed in feet/second), supplemented with the color-coded velocity shading for visual reference, and is presented within this appendix. The data appeared to be of good quality which was verified by the Root Mean Square Error (RMS) that is displayed on the lower right-hand corner of the tomographic model. The RMS error (misfit between picked and modeled first break times) is automatically calculated during the processing routine, with a value of less than 5.0% being preferred, which was obtained on all of the seismic models. The resultant value was 2.6% (see lower right-hand corner of the model).

The combined use of these computer programs provided a more thorough and comprehensive analysis of the subsurface structure and velocity characteristics. Each computer program has a specific purpose based on the objective of the analysis being performed. **SIPwin** and **Refractor** were primarily used for detecting generalized subsurface velocity layers providing “weighted average velocities.” The processed seismic data of these two programs were compared and averaged to provide a final composite layer velocity model which provided a more thorough representation of the subsurface. **Rayfract™** provided tomographic velocity and structural imaging that is very conducive to detecting strong lateral velocity characteristics and other subsurface structural characteristics.

All of the computer programs performed their analysis using exactly the same input data which includes first-arrival "P"-waves and survey line geometry. The resultant travel-time curve (Time-Distance Plot) that was developed from picking of the primary seismic "P"-wave data is presented below for reference.

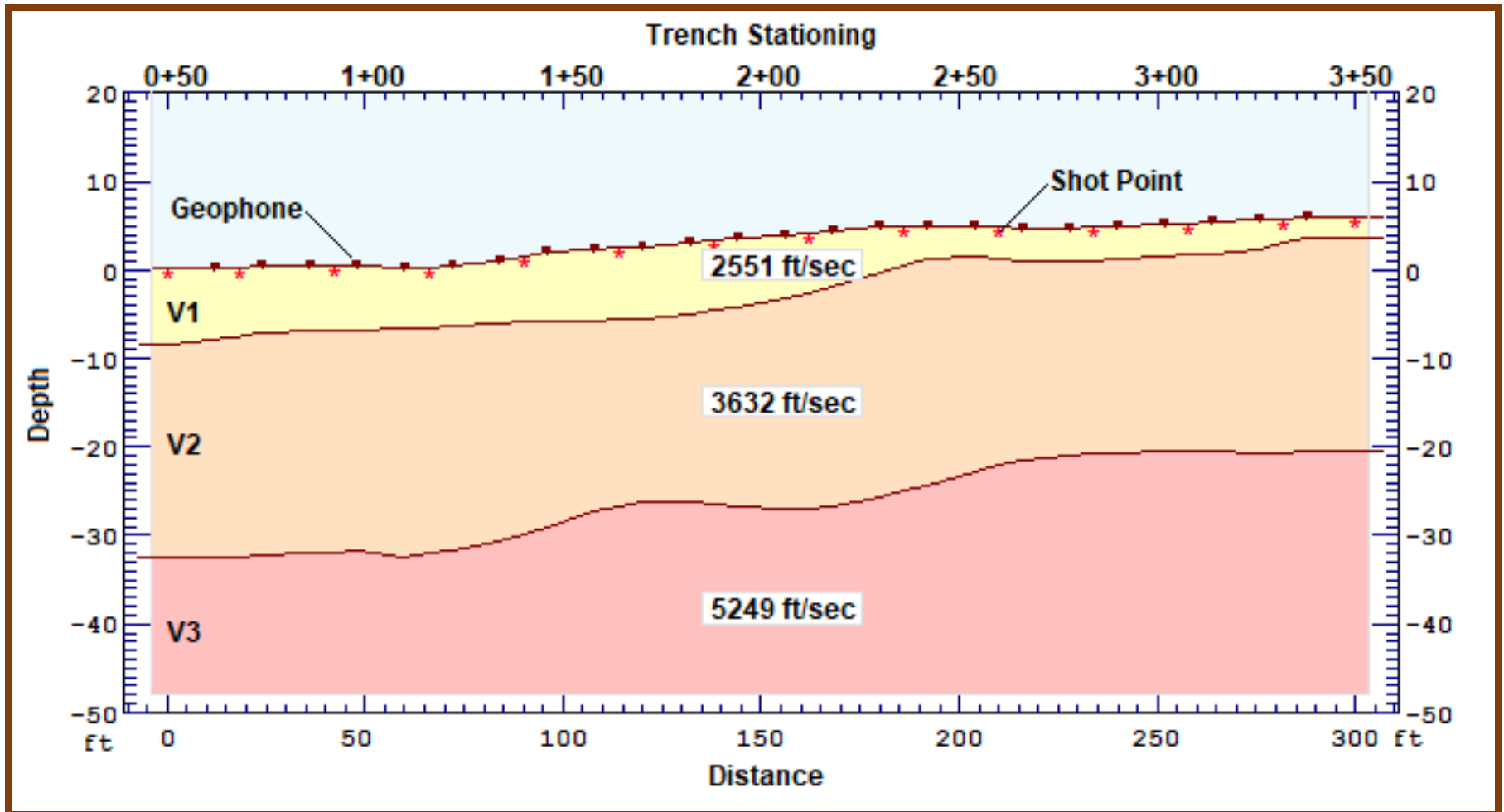


Time Distance Plot (Seismic Line S-1).

SEISMIC LINE S-1

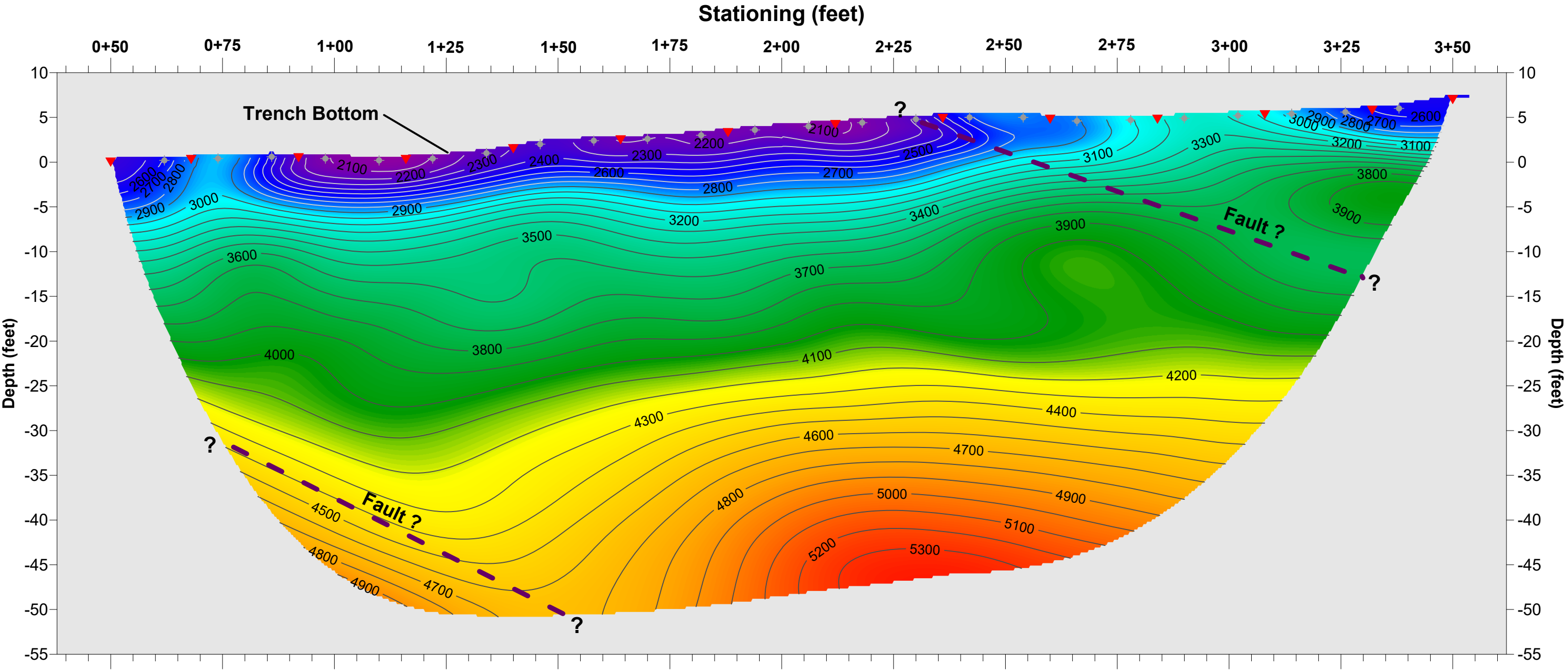
North 18° East >

LAYER VELOCITY MODEL

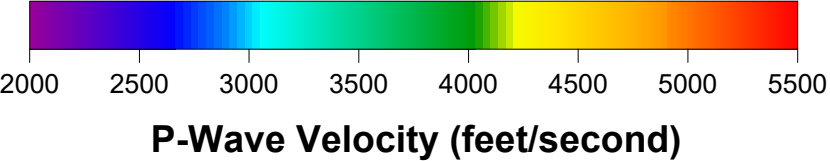


SEISMIC LINE S-1

North 18° East →



▼ Seismic Source
◆ Geophone Receiver



REFRACTION TOMOGRAPHIC MODEL
Warehouse Development Project
City of Azusa, California

APPENDIX B

GROUND-PENETRATING RADAR SURVEY



GROUND-PENETRATING RADAR SURVEY

Methodology:

GPR is an electromagnetic reflection technique that has a wide range of applications with respect to evaluating shallow subsurface features, which include sedimentology and structural geology, which were specifically targeted for this study (Baker and Jol, 2007). GPR detects changes in the physical character of the subsurface typically associated with geologic features associated with moisture variations, bedding structures, sediment particle size, etc. Evaluation of geologic structures is considered to be one of the uses for GPR, generally due to the contrasting electrical properties between earth materials, which generally creates strong radar reflections along this interface (Daniels, 2004). The general principle of the GPR method entails transmission of high-frequency electromagnetic radar pulses (within the general radio frequency spectrum) into the ground and measuring the time differential between wave transmission, reflection from a discontinuity or interface, and reception back at the surface.

The discontinuities where reflections originate usually occur along boundaries that are created by differing electromagnetic properties of the subsurface earth materials such as dielectric permittivity (capacity of a material to hold and pass and electromagnetic charge), electrical conductivity, magnetic permeability, changes in water content, bulk density, and stratigraphic interfaces. The greater the relative difference between these electric and other physical properties of adjacent earth materials (including sediment layer thickness), the stronger the reflected signal. GPR can provide high-quality data of near-surface conditions however it has some limitations. GPR is most effective in areas with resistive near-surface soil types, such as clay-poor gravel and sands. Clayey, silty, moist, or conductive soils often severely limit the depth of penetration by absorbing the energy and not transmitting it.

Instrumentation:

A GSSI SIR® SYSTEM-4000 Ground Penetrating Radar Digital Control Unit was used for this survey. Data were collected by transmitting electromagnetic waves from a mobile antenna into the subsurface, of which a center frequency 200 MHz (Megahertz) HyperStacking® antenna was utilized. This antenna is capable of imaging to a depth of 70± feet depending on the subsurface sediment electromagnetic properties. The advantage of the HyperStacking® antenna is that it records many samples from a single radar pulse, which allows the extra data to average, or stack, individual samples, which in turn helps to reduce the random noise present in the signal and results in cleaner and deeper data. The depth penetration and clarity of the GPR data were considered to be very good for this site.

For scanning purposes, the antenna, which is connected to the digital GPR unit by a control cable, was then slowly pulled along the trench bottom surface while maintaining direct coupling to the ground. A dedicated survey wheel was attached for accuracy. As the electromagnetic waves are transmitted into the scanned surface, a portion of the induced pulse is then reflected back to the antenna from various boundaries at depth.

These signals or reflection data are then received at the transducer and sent to the system control unit, where the returns are displayed in real-time on the digital control unit screen and stored in the in-board computer hard drive of the SIR-4000. The produced image is a continuous cross-sectional two-dimensional time profile of the shallow subsurface returns. The brightness (amplitude) of a single hyperbolic or layer reflection is stronger when the difference in dielectric properties of the two materials in contact is greater.

The GPR data was recorded using a setting of 24 scans per foot having a collection rate of 12 scans per second (to improve the HyperStacking® technology), with 1,024 samples per scan, and a dynamic range of 32 bits per sample, which better discriminates between two reflectors of small amplitude differences. A total two-way travel time window of 110 to 135 nanoseconds was used to record the reflection data to obtain an estimated depth of 20 to 25± feet, using a dielectric value of 7.0. The dielectric value of 7.0 was selected based on an average of the expected subsurface earth materials since calibration was not performed. Dielectric values for dry sandy soils are typically around 4.0 with wet sandy soils averaging around 15.0 (GSSI, 2019). Since the sediments were observed to be only slightly damp, the value of 7.0 seemed appropriate. The dielectric constant (unitless) represents the ratio of permittivity of a substance in a vacuum, which for GPR purposes describes how quickly GPR moves through materials.

Field Procedures:

The field survey consisted of performing two survey traverse lines (GPR-1 and GPR-2) along the bottom of the existing exploratory trench excavation (see survey photographs, Plate 3), as presented on Plates 1 and 2. Both traverses started at a distance of 50 feet from the beginning of each exploratory trench FT-1 and FT-2 at Station 0+50, due to the sloping nature of the trench ends. GPR-1 was extended a total of 300 feet along the bottom of Exploratory Trench FT-1 ending at Station 3+50 where the trench ramp began to slope steeply upwards. GPR-2 was extended a total of 200 feet along the bottom of Exploratory Trench FT-1 ending at Station 2+50 also where the trench ramp began to slope steeply upwards. Upon completion of these traverses, the images were reviewed in the field for quality control purposes.

Prior to recording these representative survey lines, numerous survey traverses were performed in order to determine the most suitable data collection parameters. During and after each radar scan, the GPR survey data was carefully reviewed in the field for the purpose of verifying if satisfactory data was collected, prior to recordation. If deemed unsatisfactory, the survey line data would be rescanned until acceptable data was obtained. The representative radar images that were recorded during our survey were stored on the internal SIR-4000 hard-drive and then subsequently downloaded into our office computer for further processing, analysis, and printing purposes. With respect to this project, a maximum depth of 25± feet appeared to be practical as deeper test scans showed diminishing results.

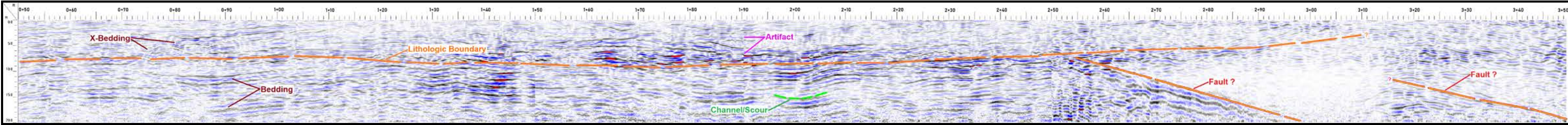
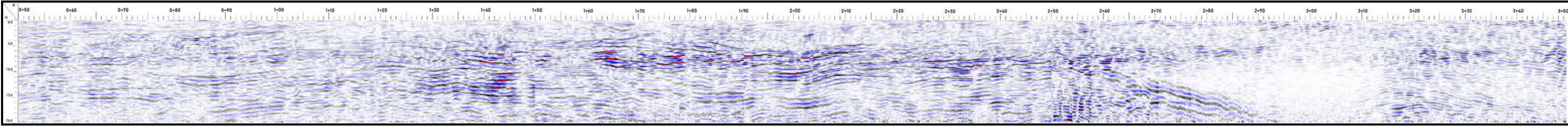
Data Processing:

The recorded data was then transferred from the digital control unit to our office computer for further analysis, processing, and printing purposes. The representative downloaded survey line was then processed and analyzed in our office using the computer program RADAN (**RA**dar **D**ata **AN**alyzer) for Windows Post Processing Software (Geophysical Survey Systems, Inc., 2019), in order to minimize the “noise” and interference and enhance reflection boundaries. The processing included using both vertical and horizontal finite-duration impulse response (FIR) filters. Additionally, a background removal filter was also applied to remove low frequency noise such as antenna ringing. These layers can obscure other “real” horizontal or point source reflectors. During the processing, the radar signal amplitude was somewhat reduced and therefore, range gain was applied to increase the gain to compensate for amplitude reduction.

The representative GPR images in this appendix are cross-sectional profiles that have been prepared at an approximate 1:1 (horizontal: vertical) scale in order to maintain a more accurate representation without vertical exaggeration. To maintain this equal ratio, the image size is variable due to the length of the survey scans.

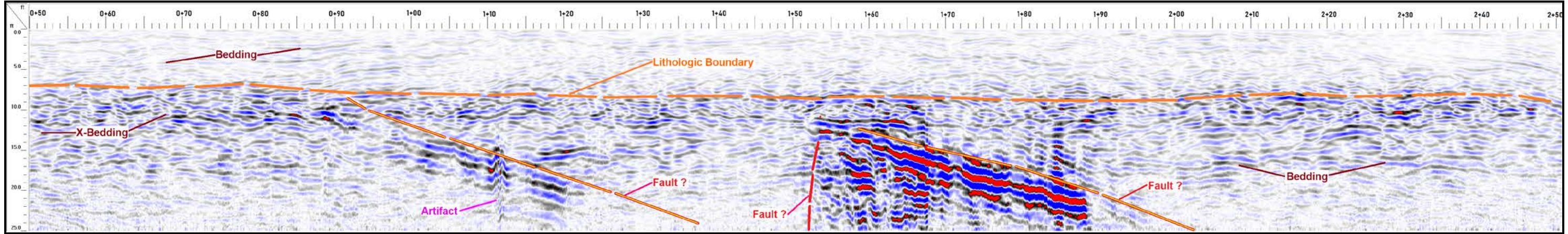
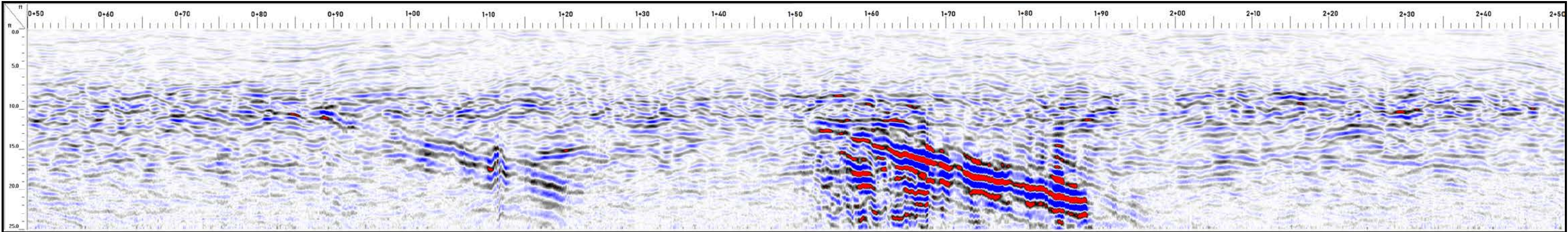
SURVEY LINE GPR-1

< South – North >



SURVEY LINE GPR-2

< South – North >



APPENDIX C

REFERENCES



REFERENCES

American Society for Testing and Materials, Intl. (ASTM), 1999, Standard Guide for Using the Subsurface Ground Penetrating Radar Method for Subsurface Investigation, ASTM Designation D 6432-99, 17 pp.

American Society for Testing and Materials, Intl. (ASTM), 2000, Standard Guide for Using the Seismic Refraction Method for Subsurface Investigation, ASTM Designation D 5777-00, 13 pp.

Baker, G.S., and Jol, H.M. (ed.), 2007, Stratigraphic Analysis using GPR, GSA Special Paper 432.

Bristow, C.S., and Jol, H.M. (ed.), 2003, Ground Penetrating Radar in Sediments, Geological Society London Special Publication No. 211, 330 pp.

California State Board for Geologists and Geophysicists, Department of Consumer Affairs, 1998, Guidelines for Geophysical Reports for Environmental and Engineering Geology, 5 pp.

Daniels, D.J., ed., 2004, Ground Penetrating Radar, 2nd Edition, The institution of Electrical Engineers IEE Radar, Sonar, Navigation and Avionics Series 15, 726 pp.

Geophysical Survey Systems, Inc., 1994-2012, RADAN 7 (RAdar Data ANalyzer for Windows) Post Processing Software, Version 7.4.16.11210.

Geophysical Survey Systems, Inc., 2015, RADAN 7 Manual, Version MN43-199 Rev F, Revised February 20, 2015, 265 pp.

Geophysical Survey Systems, Inc., 2019, SIR® System-4000 Operation Manual, MN72-574 Rev H, 172 pp.

Geogiga Technology Corp., 2001-2020, Geogiga Seismic Pro Refractor Software Program, Version 9.3, <http://www.geogiga.com/>.

Geometrics, Inc., 2012, StrataVisor™ NZXP Operation and Reference Manual, Revision M, Software Version 9.3, San Jose, California, 226 pp.

Google™ Earth, 2022, <http://earth.google.com/>, Version 7.3.4.8248 (64-bit).

Grau, Richard H., 1996, User's Guide: Ground-Penetrating Radar, U.S. Army Center for Public Works, Miscellaneous Paper FEAP-UG-96/03, 34 pp.

Intelligent Resources, Inc., 1991-2022, Rayfract™ Seismic Refraction Tomography Software, Version 4.02, (<http://rayfract.com/>).

Morton, D.M., 1973, Geology of Parts of the Azusa and Mount Wilson Quadrangles, San Gabriel Mountains, Los Angeles County, California, California Division of Mines and Geology Special Report 105, Scale 1: 24,000.

Redpath, Bruce B., 1973, Seismic Refraction Explorations for Engineering Site Investigation, Technical Report E-73-4, U.S. Army Waterways Experiment Station, Explosive Excavation Research Laboratory.

Rimrock Geophysics, Inc., 2004, **SIPwin, Seismic Refraction Interpretation Program for Windows**, Version 2.78, User Manual 78 pp.

Scott, James H., 1973, Seismic Refraction Modeling by Computer, in *Geophysics*, Volume 38, No. 2, pp. 271-284.

Schuster, G. T. and Quintus-Bosz, A., (1993), Wavepath Eikonal Traveltime Inversion: Theory, in, *Geophysics*, Vol. 58, No. 9, September, pp. 1314-1323.

Ulriksen, C. Peter F., 1982, Application of Impulse Radar to Civil Engineering, Lund University of Technology, Sweden, 179 pp.

APPENDIX



**Seismic Reflection Survey
N. Todd Avenue and W. 10th Street
Azusa, California**

GEOVision Project No. 22121

Prepared for

Southern California Geotechnical
22885 E. Savi Ranch Parkway, Suite E
Yorba Linda, California 92887

Prepared by

GEOVision Geophysical Services
1124 Olympic Drive
Corona, CA 92881
(951) 549-1234

Report 22121-01 rev0

May 23, 2022

TABLE OF CONTENTS

1	INTRODUCTION	1
2	SEISMIC REFLECTION BACKGROUND.....	1
3	PROCEDURES.....	3
4	DATA PROCESSING	3
5	RESULTS	4
6	CERTIFICATION	6
7	REFERENCES	7
8	APPENDIX TABLES & FIGURES	8

LIST OF TABLES

Table 1	Geophysical Survey Location (NAD83, California State Plane Zone 5).....	8
Table 2	Acquisition Parameters for P-Wave Survey	8
Table 3	Processing Sequence for P-Wave Data.....	9

LIST OF FIGURES

Appendix Figure 1 – Site Map.....	10
Appendix Figure 2 – Seismic Line Relative Trace Amplitude	11
Appendix Figure 3 – Seismic Line Signal Envelope	12
Appendix Figure 4 – Seismic Line Pseudo-Relief.....	13
Appendix Figure 5 – Seismic Line Interpreted Section.....	14
Appendix Figure 6 – Seismic Refraction Velocity Tomogram	15

Attachments:

Application Note Seismic Reflection Method
A200 P/S Hammer Cut Sheet

1 INTRODUCTION

A seismic reflection survey was conducted along a single line on the property northeast of North Todd Avenue and West 10th Street in Azusa, California on April 14, 2022. The purpose of the survey was to screen the area beneath the seismic line for a fault which may act as a groundwater barrier. The inferred location of the fault is based on geologic maps (Jennings, 1994; Treiman, 2000) and is mapped south of our line location. Groundwater data provided by Southern California Geotechnical during preparation of our proposal indicates an 80-foot vertical difference in water levels between two borings located adjacent to our seismic line (SCG 22P124 Proposed Exploration Plan).

Compressional-wave (P-wave) seismic reflection data were acquired during this investigation. The seismic line geometry is presented in Table 1. The location of the line is shown on Appendix Figure 1. An outside seismic data processing specialist processed the data and provided it to GEOVision for interpretation.

The following sections include a discussion of the seismic reflection technique, equipment and field procedures, data processing, interpretation of the seismic reflection data, and a summary of the investigation.

2 SEISMIC REFLECTION BACKGROUND

The seismic reflection technique is detailed in numerous geophysical texts (Dobrin and Savit, 1988; Telford, Geldart and Sheriff, 1990) and, therefore, only a brief synopsis of the technique is included in this report. The seismic reflection method involves projecting a wave down from the surface and then recording the returning wave back at the surface as it reflects off formations at depth. In accordance with Snell's Law, seismic energy will be reflected, refracted and diffracted at boundaries in the subsurface. The main design consideration for a successful seismic reflection survey is the ability to separate the reflected energy from other arrivals in processing.

A seismic reflection occurs when an acoustic wave front encounters an impedance boundary in the subsurface. Seismic impedance depends on both the velocity and density of a rock and impedance boundaries occur where these rock properties change abruptly, usually due to changes in lithology. The reflection coefficient, R , across an interface, is expressed by a function relating the acoustic impedance of adjacent layers. R determines the relative amplitude of the reflected wavelet.

$$R = \frac{\sigma_2 V_2 - \sigma_1 V_1}{\sigma_2 V_2 + \sigma_1 V_1}$$

where, R = reflection coefficient

σ_1 , σ_2 = mass density of the material on each side of the interface

V_1 , V_2 = seismic wave velocity on each side of the interface

The sign of the reflection coefficient determines the polarity of the reflected wave. The magnitude of the reflection coefficient is critical to obtaining usable data. The seismic reflection technique will not work if the acoustic contrast is not sufficient to produce a clear reflection, regardless of the survey parameters or processing techniques employed. The ability of the seismic reflection method to detect an individual sedimentary bed is not only a function of the acoustic impedance at the top and bottom of the bed, but also depends on the layer thickness. The minimum resolvable bed thickness (vertical resolution) is generally accepted as one quarter of the wavelength at the target depth.

$$VR = \frac{\lambda}{4} = \frac{V}{4f}$$

where, VR = vertical resolution

λ = dominant wavelength of the reflected energy

V = seismic wave velocity above the reflector

f = dominant frequency of the reflector

Geologic discontinuities such as faults are generally clearly discernable providing the offset is greater than the vertical resolution. A large utility or tunnel can often be interpreted as a hyperbolic diffraction centered on the strike plane, provided noise levels in the data are not too high.

When a reflecting boundary exists, it is important to optimize the field procedure and acquisition parameters to maximize the quality of the final processed data. Choosing the best field parameters involves determining the relative importance of several competing objectives, such as site constraints, equipment capabilities, and processing needs.

In all geophysical surveys, the objective is to extract the usable data (i.e., in this case, reflections from various lithologic boundaries) from the unwanted background information (source generated and ambient noise). In reflection seismology, it is desirable to record high frequency, high signal-to-noise ratio reflection events from the boundary of interest. The frequency of a reflection event is largely determined by the source output frequency and the filtering effect of the ground. Often, the target reflector frequency is similar to that commonly recorded for coherent noise (in particular, the noise from ground roll), making it difficult or impossible to selectively filter out the noise. Isolation of the reflection events requires careful design of field acquisition parameters (e.g., source/receiver geometry, source, and receiver types) and recording parameters (e.g., sampling rate, filter settings). With modern 24-bit A/D acquisition systems it is very unusual to apply acquisition filters (filtering before data is stored), except for automatic anti-alias filters.

Sufficient data redundancy, or fold, which is the number of individual source receiver pairs with a reflection occurring from the same midpoint (common midpoint or common depth point) on a geologic horizon, is also an important survey design parameter. Maximum fold is equal to the number of live channels divided by twice the shot station spacing. Therefore, for example, shot locations at every station (geophone spacing) with 72 channel recording capability results in a maximum fold of 36 (maximum fold for this survey). Data quality always degrades at the ends of a seismic line because the fold on the first trace of a processed seismic section is one (i.e., only 1 source receiver pair used to generate the trace), with fold increasing incrementally with

increasing station numbers until maximum fold is reached, after which fold decreases again toward the last trace.

The frequency content of seismic reflection data is a function of both the energy source and the medium through which the energy travels. Vibratory sources have control of the frequency input to the ground, unlike impulsive sources such as a hammer or explosives. With a vibratory source, the frequency input into the ground is a function of the beginning and ending frequencies of the sweep, the length of the sweep, and ground coupling. The second factor is the transmission and attenuation of various frequency components in the subsurface, often termed the “earth response.” The frequency bandwidth of the recorded data was primarily in the 20-40 Hz range for this project.

3 PROCEDURES

The seismic line was marked at the appropriate station interval (geophone spacing) using a fiberglass measuring tape. A 5 ft station interval was used for this investigation.

Geospace 28 Hz vertical geophones planted via a 2-3-inch spike at the appropriate station interval and cabled into a Geometrics Geode distributed recording system. Each Geode seismograph records signals from 24 live geophone receivers. Three Geodes were used to meet the 355-foot line length.

A US Alliance 200-lb nitrogen spring accelerated weight drop was the seismic energy source used for this investigation. Ten individual hammer blows were recorded at each shot location for stacking during the data processing phase. Source locations included 10 and 25 feet southwest of the first geophone, and 25, 75, and 100 feet northeast of the last geophone. Shot points were also located at every geophone station along the line with the exception of stations 7-12 where the weight drop could not access the line. A 2s record length and 0.25ms sample rate with no acquisition filters were the recording parameters. Acquisition parameters are summarized in Table 2.

4 DATA PROCESSING

The seismic reflection data were processed by Castillo Geophysical Ltd, a dedicated seismic processor based in Reno, NV. The processing flow for the data is based on a standard common midpoint (CMP) reflection processing sequence with modifications for specific conditions at the survey site. Table 3 shows the processing sequence leading to the final stacks used for interpretation.

After receipt of the digital data from Castillo, the data were loaded into a seismic workstation: Kingdom Software from IHS Markit for assistance in interpretation. The processed output SEG-Y data were loaded into a SQL database along with the line geometry. The common midpoint gathers were plotted along the X-axis and time on the Y-axis. The signal envelope, Hilbert transform, and several display filters were evaluated as possible aids for seismic interpretation.

5 RESULTS

The purpose of this investigation was to identify any distinct seismic anomalies which may be interpreted as caused by faults that may intersect our survey profile.

The processed P-wave sections for Line 1 are presented as Appendix Figures 2-5. These figures include the following:

- Uninterpreted, P-wave migrated, enhanced trace amplitude seismic sections with post-stack processing (spectral balancing and trace equalization). Referred to as Relative Amplitude section in Figure 2. This is a common presentation of seismic reflection data.
- Uninterpreted, P-wave migrated, enhanced amplitude envelope seismic sections with post-stack processing (spectral balancing and FX predictive deconvolution). Referred to as Signal Envelope section in Figure 3. Amplitude Envelope generally depicts the energy level of the seismic signal. It is the “signal” where the seismic wave is the carrier. Many faults or discontinuities show a change in this attribute from one side to the other.
- Uninterpreted, P-wave migrated, enhanced trace amplitude seismic sections with post-stack processing (spectral balancing and FX predictive deconvolution). Referred to as pseudo relief section in Figure 4. Pseudo relief attributes are used to promote easier interpretation of structural features – in particular, faults and horizons. The RMS amplitude of the trace signal is calculated, and an inverse Hilbert transform is applied across a user-defined window of samples (3 was used for this project, a smoothing scalar less than half the period of the wavelet at a reflector). The pseudo-relief attribute is popular for adding apparent texture to a flat 2D cross-section of often overloading polarity reversals and signal characters.
- The Relative Amplitude section described above but with interpreted seismic events highlighted (Figure 5).

All seismic sections are presented using distance along the line as the X-axis and two-way travel time for the Y-axis. As is typical with seismic reflection data, data quality decreases on the edges of the section due to a decrease in data redundancy (fold), with the midpoint of the line the location of maximum fold.

Data quality along Line 1 were of fair quality. Traffic noise was mitigated partially by signal stacking but was still present and at times significant. Shear-wave conversion of the P-wave impulse created destructive interference. The upper 100 milliseconds of the data did not show coherent events, which is unfortunately common for P-wave reflection, and thus unused (the “shadow zone”). Borehole velocity data would be required to convert travel time data to depth below the ground surface and this was unavailable at the time of data processing. An extremely simplistic seismic refraction model (Figure 6) indicates that the soils may be 2,000 - 4,000 ft/s above the water table. Using this velocity range as a gross estimate, our “shallow” cutoff of the P-wave reflection data would be approximately 100-200 feet BGS and we are not likely imaging the best reflector possible within the alluvium (the water table itself) to inspect it for vertical offset. Any offset in the groundwater table is within the 100 millisecond shadow zone where we

do not have coherent data. Longer lines would be needed to better constrain the near-surface structure (increased source-receiver offset).

Seismic reflection data is interpreted by identifying continuous events (reflectors) across the section. Vertical discontinuities, as imaged in these sections, may be the result of channels, discontinuous geologic units, man-made structures, or potential faulting. A fault with 80+ feet of vertical displacement would be characterized by disruptions in continuous reflectors. This is most obvious when discontinuities cross rock, not soil, boundaries. Soil layers are difficult to image with seismic reflection due to their (general) lack of strong impedance contrast, non-homogenous makeup and often irregular structure.

Figures 2, 4 and 5 show seismic events in the travel time data interpreted as being caused by lithologic interfaces with significant impedance contrast (reflectors). There is some ~20 millisecond anticlinal displacement in some of the events at the southern end of the line, projecting to the surface at our profile distance of ~50-75 feet, but this feature does not clearly extend through the shallower reflection events. As this feature is not imaged in the shallow time-section, it could be caused by a structure out of plane or oblique to the survey line and we cannot determine this attitude of the feature without parallel survey lines.

Very shallow displacement is inferred at profile distance 88 feet (near the mapped Possible Northern Limit of Faulting” and “Possible Fault Setback” boundaries are identified on the SCG Exploration Plan). However, the projection of this feature crosses deeper reflectors without displacement, as should be expected for a fault. If this feature is caused by geologic structure perpendicular to our line, it is not interpreted as a fault. If the feature is oblique to the line, this could be the effect of 3D geologic structure being imaged in only two dimensions. There is a similar feature around our profile distance 260 feet.

The displacement feature at profile distance 22 feet is near our southern end of line where our resolution is poor (low fold), and we do not typically interpret features this close to the end of a line. In order to better image beneath the southern end of the line, we would have had to extend the line toward the south (crossing W 10th Street, and possibly N. Todd Avenue), which was not accessible. There is a similar feature beneath profile distance 300-350, also in a low fold region, and also apparently not crossing shallow reflection events.

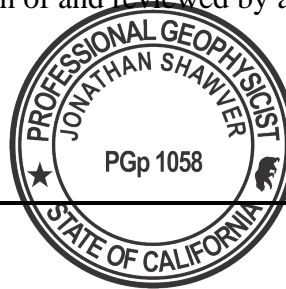
There is some indication of deeper dipping layers beneath the northern end of the line, but this is not expected to be caused by a fault, given the apparent low angle.

Unfortunately, due to (A) the relatively short line length, particularly limited to the southern end (B) noise conditions and (C) unknown attitude of potential faulting from your trenching results and how 3D geology impacts 2D reflection imaging, we cannot definitively interpret any features observed in this data set as being caused by a shallow fault.

6 CERTIFICATION

All geophysical data, analysis, interpretations, conclusions, and recommendations in this document have been prepared under the supervision of and reviewed by a **GEOVision** California Professional Geophysicist.

JB Shawver



May 23, 2022

Date

California Professional Geophysicist, P.Gp. 1058
GEOVision Geophysical Services

- * This geophysical investigation was conducted under the supervision of a California Professional Geophysicist using industry standard methods and equipment. A high degree of professionalism was maintained during all aspects of the project from the field investigation and data acquisition, through data processing interpretation and reporting. All original field data files, field notes, and observations, and other pertinent information are maintained in the project files and are available for the client to review for a period of at least one year.

A professional geophysicist's certification of interpreted geophysical conditions comprises a declaration of his/her professional judgment. It does not constitute a warranty or guarantee, expressed or implied, nor does it relieve any other party of its responsibility to abide by contract documents, applicable codes, standards, regulations, or ordinances.

7 REFERENCES

- Dobrin, M.S., and Savit, J., 1988, Introduction to Geophysical Prospecting, McGraw-Hill Co., New York.
- Jennings, C.W., 1994, Fault activity map of California and adjacent areas, with locations of recent volcanic eruptions: California Division of Mines and Geology Geologic Data Map 6, 92 p., 2 pls., scale 1:750,000.
- Southern California Geotechnical, 2022, Exploration Plan SEC Todd Avenue / Sierra Madre Avenue Azusa California, Scale 1"=100, SCG Project 22P124-1, Plate X
- Telford, W. M., Geldart, L.P., Sheriff, R.E., 1990, Applied Geophysics, Second Edition, Cambridge University Press.
- Treiman, J.A., compiler, 2000, Fault number 105f, Sierra Madre fault zone, Sierra Madre D section, in Quaternary fault and fold database of the United States: U.S. Geological Survey website, <https://earthquakes.usgs.gov/hazards/qfaults>, accessed 05/09/2022 09:31 PM.

8 APPENDIX TABLES & FIGURES

Table 1 Geophysical Survey Location (NAD83, California State Plane Zone 5)

Name	Location (ft)	Station	Northing (US Feet)	Easting (US Feet)
Line 1	0	1	1873341.9	6584448.1
	355	72	1873691.6	6584502.1

Table 2 Acquisition Parameters for P-Wave Survey

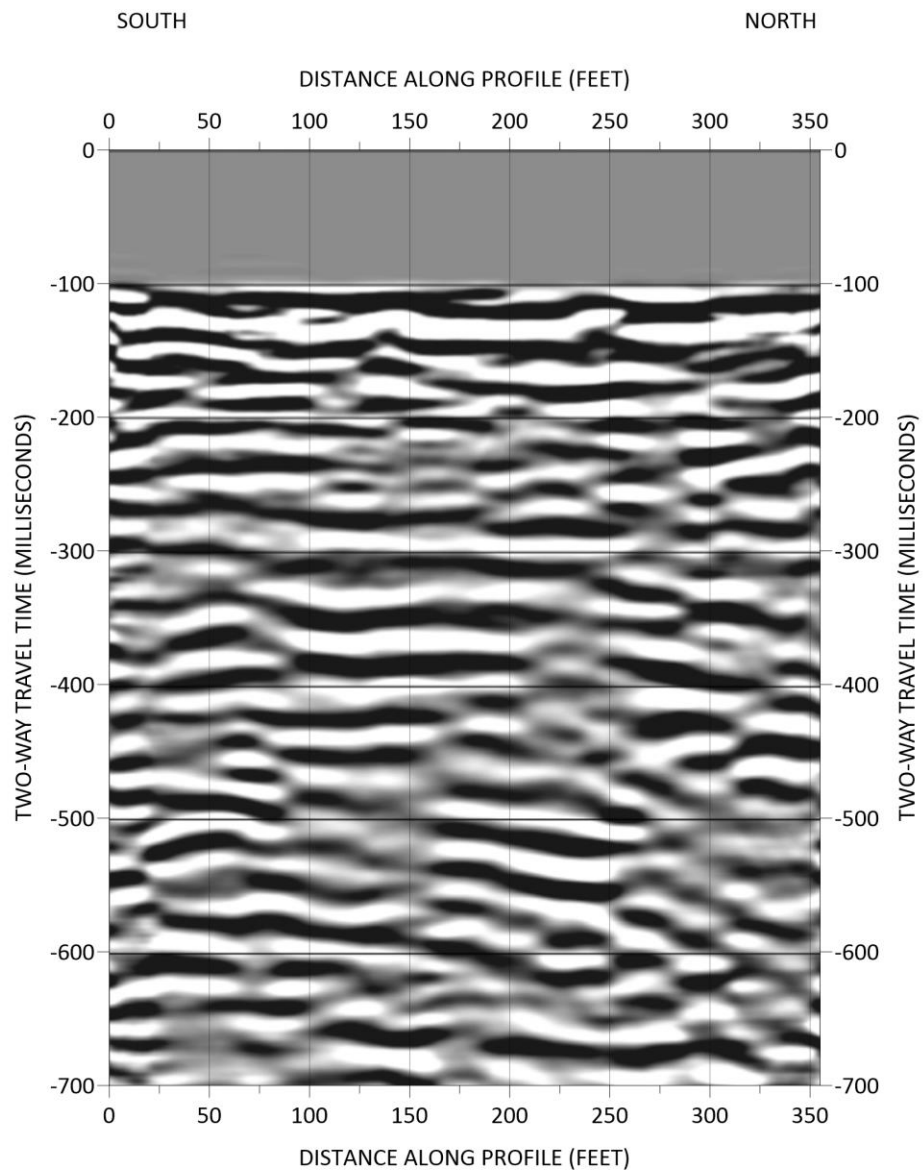
Type of survey	P-Wave reflection
Station interval	5 feet
Source	Impulse source
Source interval	5 feet
Record length	Impact + 2 second listen
Taper	To be determined
Recording instrument	Geometrics Geodes (3)
Low Cut Filter	Out
High Cut filter	Out
Notch Filters	Out
Data redundancy	36-fold maximum
Geophones	Sunfull 28Hz vertical single
Number of channels	72
Sample interval	0.25 millisecond
Spread Configuration	No gap
Source Position	on station


Table 3 Processing Sequence for P-Wave Data

Sequence #	Description
1	SEGY TO INTERNAL FORMAT CONVERSION
2	FIELD GEOMETRY AND LAND SURVEY IMPORT
3	TRACE EDITING
4	TRUE AMPLITUDE GAIN RECOVERY
5	REFRACTION / FLOATING DATUM STATICS APPLIED
6	SURFACE CONSISTENT AMPLITUDE ANALYSIS AND COMPENSATION
7	SURFACE CONSISTENT DECONVOLUTION 200 MSEC OPERATOR
8	SPECTRAL BALANCING
9	COMMON DEPTH POINT GATHERS: PASS 1: NORMAL MOVEOUT VELOCITY AND MUTE ANALYSIS PASS 1: SURFACE CONSISTENT RESIDUAL STATICS APPLICATION PASS 2: NORMAL MOVEOUT VELOCITY AND MUTE ANALYSIS PASS 2: SURFACE CONSISTENT RESIDUAL STATICS APPLICATION
10	TV EQUALIZATION / AGC
11	COMMON DEPTH POINT STACK

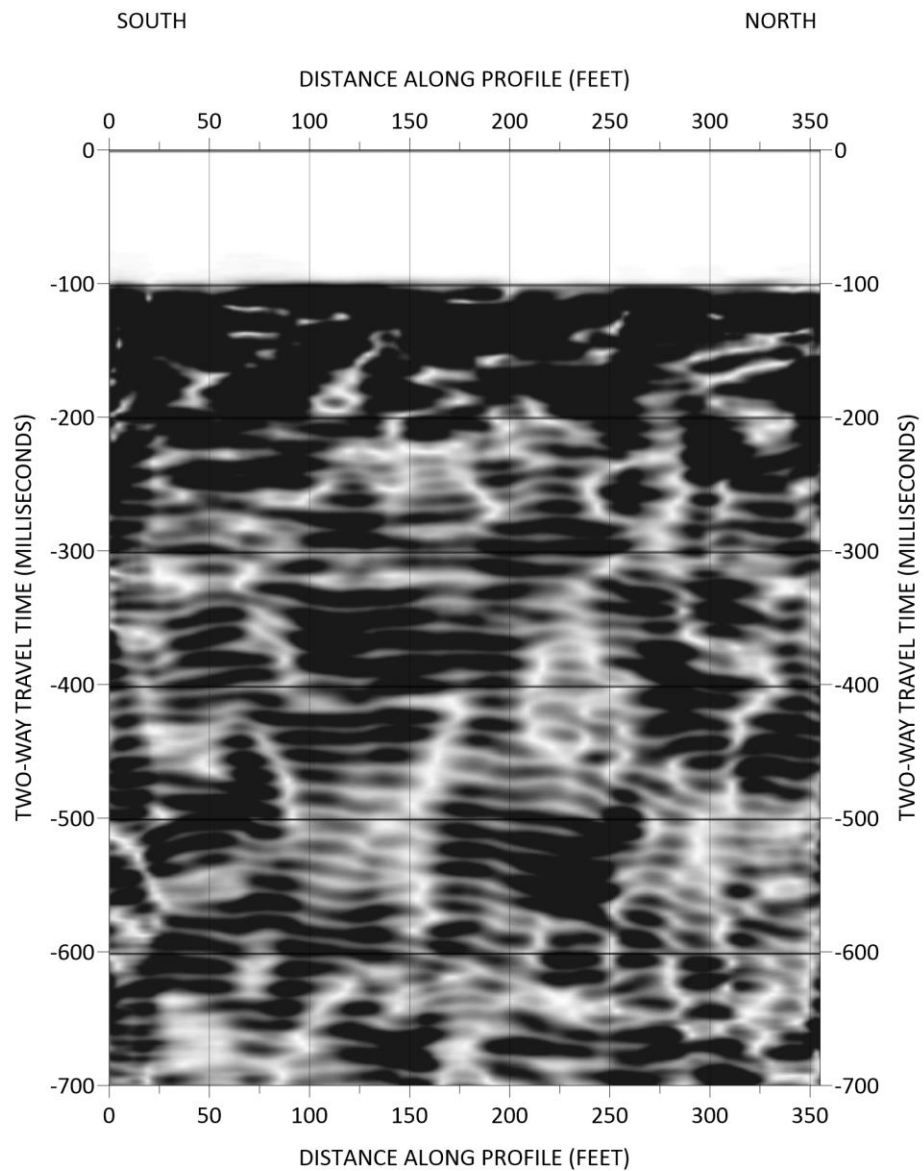



Appendix Figure 1 – Site Map



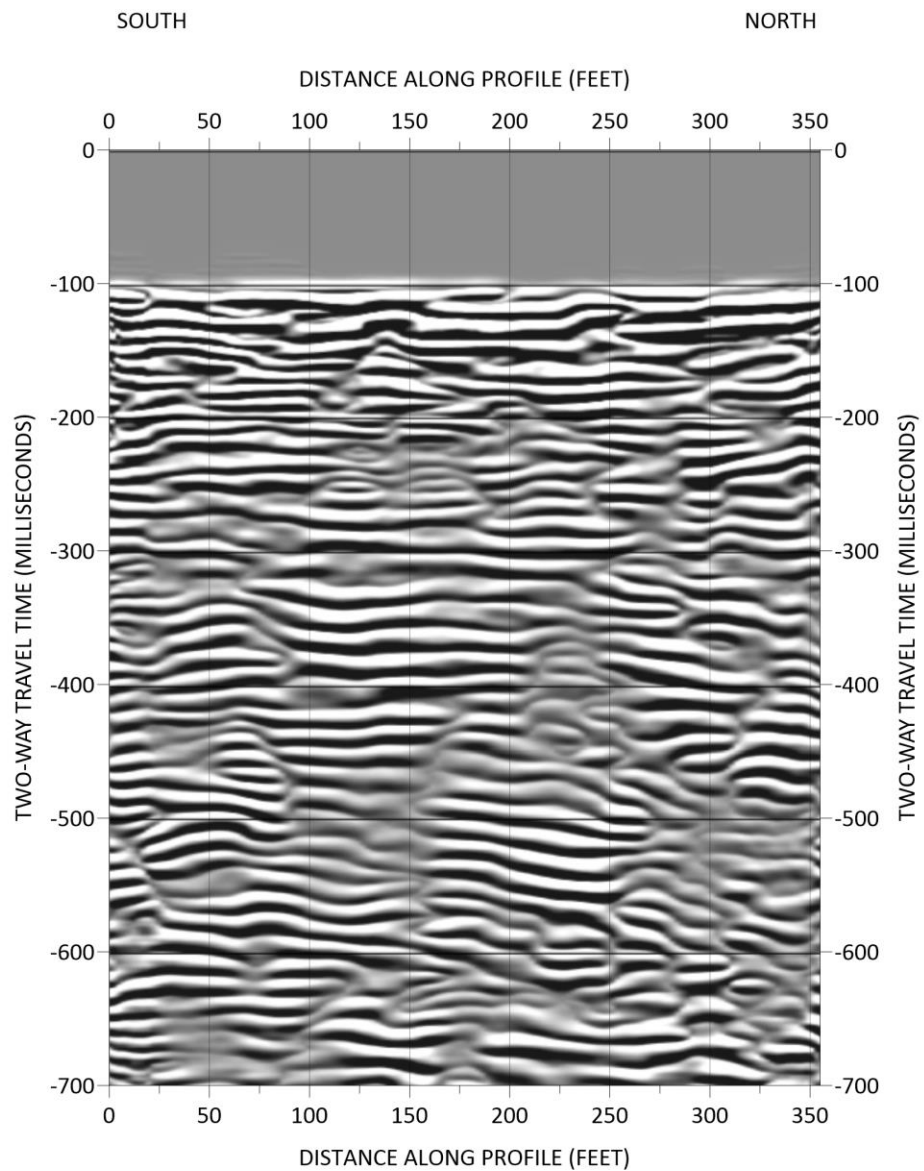
	FIGURE 2
	SEISMIC REFLECTION LINE AMPLITUDE SECTION
	PREPARED FOR SCG


Appendix Figure 2 – Seismic Line Relative Trace Amplitude



	FIGURE 3
	SEISMIC REFLECTION LINE SIGNAL ENVELOPE
	PREPARED FOR SCG

Appendix Figure 3 – Seismic Line Signal Envelope



	FIGURE 4
	SEISMIC REFLECTION LINE PSEUDO-RELIEF
	PREPARED FOR SCG

Appendix Figure 4 – Seismic Line Pseudo-Relief

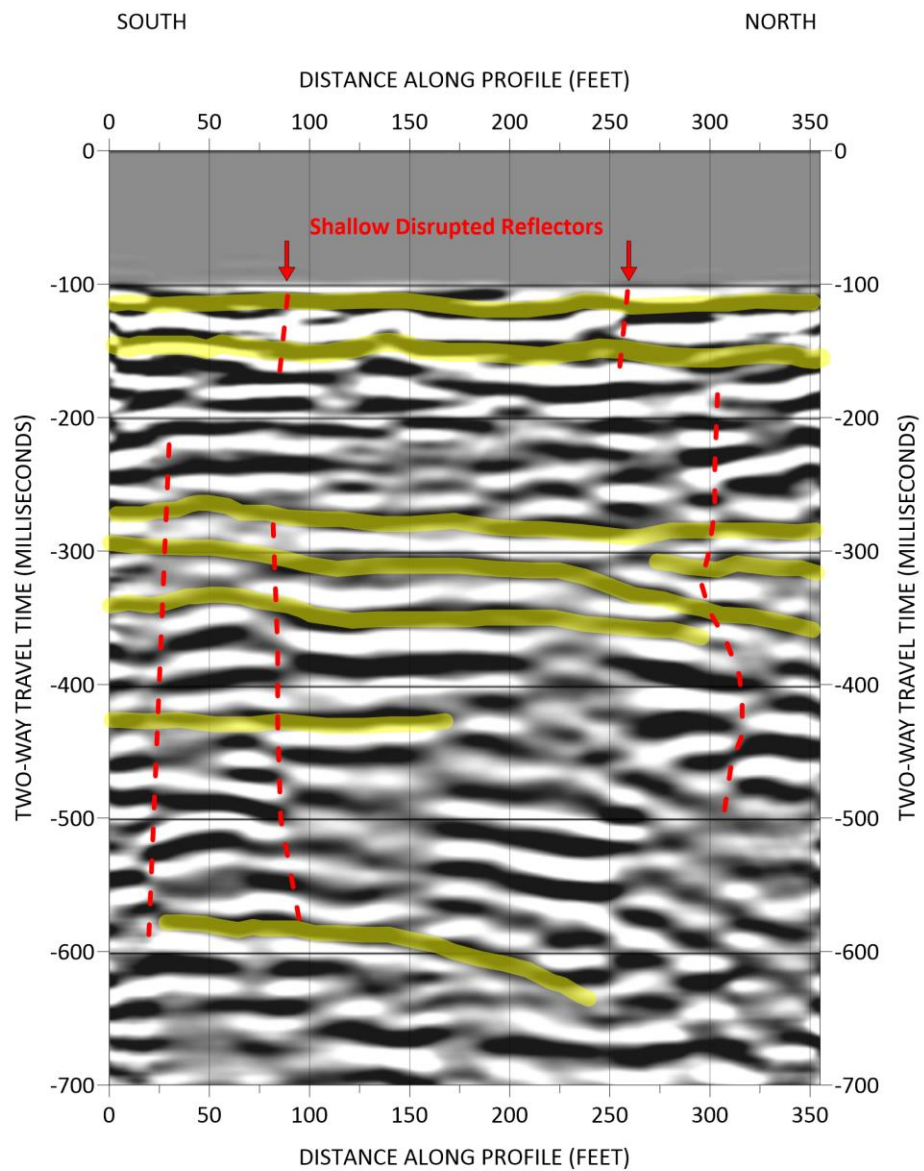
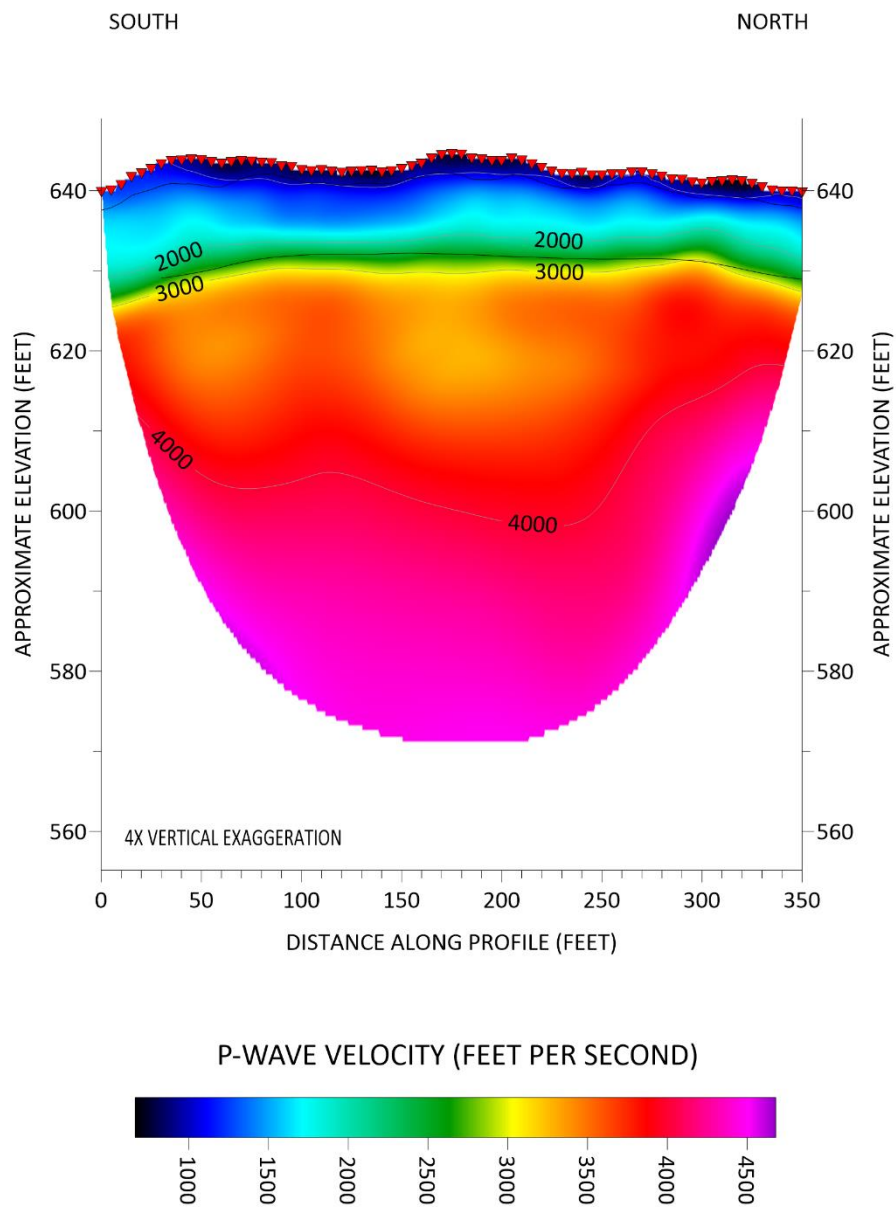



FIGURE 5

SEISMIC REFLECTION LINE
SEISMIC INTERPRETATION

PREPARED FOR
SCG

Appendix Figure 5 – Seismic Line Interpreted Section



	FIGURE 6
	SEISMIC REFRACTION MODEL VELOCITY TOMOGRAM
	PREPARED FOR SCG

Appendix Figure 6 – Seismic Refraction Velocity Tomogram